EVALUATION OF CALCIUM HANDLING AND DWARF OPEN READING FRAME AAV GENE THERAPY IN DUCHENNE MUSCULAR DYSTROPHY

A Dissertation

presented to

the Faculty of the Graduate School

at the University of Missouri-Columbia

In Partial Fulfillment

of the Requirements for the Degree

Doctor of Philosophy

---

by

EMILY D. MORALES

Dr. Dongsheng Duan, Dissertation Supervisor

JULY 2022

The undersigned, appointed by the dean of the Graduate School, have examined the dissertation entitled

EVALUATION OF CALCIUM HANDLING AND DWARF OPEN READING FRAME AAV GENE THERAPY IN DUCHENNE MUSCULAR DYSTROPHY

presented by Emily Morales,

a candidate for the degree of Doctor of Philosophy,

and hereby certify that, in their opinion, it is worthy of acceptance.

_____

Dr. Dongsheng Duan

_____

Dr. Chris Lorson

_____

Dr. Dawn Cornelison

_____

Dr. Kerry McDonald

_____

Dr. Timothy Domeier

DEDICATION

I dedicate this dissertation to my best friend and husband, Alejandro, who has been my rock and my source of encouragement throughout graduate school and our life together. I also dedicate this dissertation to all the lives affected by Duchenne muscular dystrophy.

ACKNOWLEDGEMENTS

First, I would like to thank my mentor, Dr. Dongsheng Duan, for supporting me through every stage of my research career. I first met Dr. Duan in 2012, when he allowed me to do a high school internship in his lab. This is where I first learned about gene therapy and becoming a scientist. Five years later, he generously welcomed me back as a graduate student and invested many hours shaping me into the researcher I am today. His love of research and genuine care for patients with DMD are inspiring. Thank you, Dr. Duan, for your mentorship!

I also want to thank all the members of the Duan lab, past and present, who have helped me with my research. I want to give special thanks to Ping, Thais, and Jin for helping me perform muscle function studies while I was pregnant and on maternity leave. It meant the world to me to be able to care for my family while pursuing my degree, knowing that someone was there to help. I also want to thank Chady, Xiufang, Keqing, Junling, and Nalinda for teaching me many of the techniques used to complete my studies. To all the other Duan lab members, thank you! I recognize each and every person assisted me in some way, and I truly appreciate your support.

Thanks also to Dr. Mark Hannink and Deborah Allen for their continuous support through the Life Sciences Fellowship. Mark gave me great advice on how to become a better presenter, and Debbie was a constant source of encouragement.

Thank you to my committee members: Dr. Chris Lorson, Dr. Dawn Cornelison, Dr. Kerry McDonald, and Dr. Timothy Domeier for their time and support. Thank you for teaching me to think like a scientist and for helping me troubleshoot along the way.

Lastly, thank you to all others who have assisted me in my career. Dr. Brian Bostick and Dr. Xiao Heng, thank you for helping me jumpstart my research career. To the office, IT, and janitorial staff, thank you for solving every small problem and for making the workplace fun.

Thank you all!

TABLE OF CONTENTS

LIST OF TABLES

LIST OF FIGURES

LIST OF ABBREVIATIONS

DMD	Duchenne muscular dystrophy
DGC	Dystrophin-glycoprotein complex
WT	Wild-type
SR	Sarcoplasmic reticulum
Ca_v	L-type calcium channels
RyR	Ryanodine receptor
CICR	Calcium-induced calcium release
SERCA	Sarcoendoplasmic reticulum calcium ATPase
MCU	Mitochondrial uniporter
NCX	Sodium-calcium exchanger
PMCA	Plasma membrane calcium ATPase
TRPML1	Transient receptor potential mucolipin 1
SOCC	Store-operated calcium channel
STIM	Stromal interaction molecule
CSQ	Calsequestrin
$iPLA_2$	Calcium-independent phospholipase A_2
TRPC	Transient receptor potential canonical channel
TRPV2	Transient receptor potential vanilloid type 2
Cx	Connexins
CLP	Calsequestrin-like protein

HRCBP	Histidine-rich calcium-binding protein
CaM	Calmodulin
SLM	Sarcalumenin
PLN	Phospholamban
SLN	Sarcolipin
MLN	Myoregulin
DWORF	Dwarf open reading frame
AAV	Adeno-associated virus
ddPCR	Droplet digital PCR
dP	Change in pressure
dt	Change in time
ECG	Electrocardiography
EGFP	Enhanced green fluorescent protein
H&E	Hematoxylin and eosin
IRES	Internal ribosomal entry site
MTC	Masson trichrome
V_{max}	Maximum rate of calcium uptake
vg	Vector genome copy
Tg	Transgenic
GFP	Green fluorescent protein

ECU	Extensor carpi ulnaris
cDNA	Complementary DNA

EVALUATION OF CALCIUM HANDLING AND DWARF OPEN READING FRAME AAV GENE THERAPY IN DUCHENNE MUSCULAR DYSTROPHY

Emily D. Morales

Dr. Dongsheng Duan, Dissertation Supervisor

ABSTRACT

Duchenne muscular dystrophy (DMD) is a progressive muscle wasting disease. Increased concentrations of cytosolic calcium in dystrophic muscle cells has been implicated in DMD pathogenesis. In healthy muscle, calcium from within the sarcoplasmic reticulum (SR) is released to the cytosol to initiate muscle contraction and is returned to the SR by the sarcoendoplasmic reticulum calcium ATPase (SERCA) during relaxation. In DMD, SR calcium release is elevated, while calcium uptake by SERCA is reduced. Strategies that improve SERCA function hold promise to reduce cytosolic calcium levels and treat DMD. In the present work, we explored the role of a small peptide SERCA enhancer, dwarf open reading frame (DWORF), in dystrophic muscle. We found DWORF was significantly reduced in the heart and diaphragm of the mdx mouse model of DMD. Following this discovery, we delivered 6×10^{12} vg particles/mouse of an AAV9.DWORF vector to 6-week-old mdx mice by tail vein injection. Because SERCA over-activation has been reported to reduce muscle function, we also injected wild-type (WT) mice, whose DWORF levels are already significantly higher than in mdx mice. We found that AAV DWORF gene therapy (1) improved SERCA uptake, heart function, and fibrosis in mdx hearts, (2) reduced SERCA uptake, worsened heart function, and induced expression of the SERCA inhibitor sarcolipin in

WT hearts, and (3) did not improve muscle force production but slowed maximum rates of contraction and relaxation in mdx diaphragm. Additionally, we assessed the transcript levels of several calcium handling proteins in the canine model of DMD. We found transcriptional differences between normal and dystrophic muscles and between male and female muscles. Our findings are the first to show DWORF downregulation plays a role in SERCA dysfunction in dystrophic muscle and that AAV DWORF gene therapy is a promising technique to treat DMD, especially DMD cardiomyopathy. Our findings also highlight the importance of considering animal age and sex in dystrophic canine studies.

Chapter 1. An introduction to calcium mishandling in Duchenne muscular dystrophy

Emily D. Morales[1]

[1], Department of Molecular Microbiology and Immunology, School of Medicine, The University of Missouri, Columbia, MO 65212

Introduction

Duchenne muscular dystrophy (DMD) is the most common form of muscular dystrophy, affecting approximately 1 in 5,000 male births worldwide(D. Duan et al., 2021; Mendell & Lloyd-Puryear, 2013). Patients with this disease harbor a mutation in the X chromosome-linked dystrophin gene. Dystrophin protein plays an important role in muscle cell integrity and function. This rod-shaped protein is responsible for connecting the intracellular cytoskeleton network directly to the plasma membrane and to the extracellular matrix through interactions with the dystrophin-glycoprotein complex (DGC)(Allen et al., 2016; Gao & McNally, 2015). When functional dystrophin protein is absent, patients experience progressive muscle degeneration and loss of muscle function. Most patients become wheelchair bound at 10-12 years of age, require assisted ventilation by approximately 20 years of age, and die prematurely of cardiac and/or respiratory failure by 20-40 years of age(Mercuri et al., 2019). Currently, there is no cure for DMD. Advancements in gene therapy techniques make dystrophin gene editing and delivery promising therapeutic options. These methods are being actively pursued. Another approach to treating DMD is to identify alternative disease pathways for therapeutic targeting.

One such approach is to target intracellular calcium pathways within dystrophic muscle cells. Multiple studies document dysregulated intracellular calcium pathways in DMD(Burr & Molkentin, 2015; Mareedu, Million, et al., 2021). These dysregulations result in increased calcium concentrations within the cytosol of muscle fibers(Hopf et al., 1996a; Turner et al., 1988). Increased cytosolic calcium activates calcium-dependent

proteases and phospholipases, which degrade cellular proteins and lipids, leading to damage in dystrophic muscle cells(Hussain, 2000; Lindahl, Bäckman, et al., 1995; Shanmuga Sundaram et al., 2006; Spencer & Mellgren, 2002; Voit et al., 2017).

In the present review, we elaborate on calcium mishandling in DMD, focusing on two sources of aberrant cytosolic calcium: (1) extracellular calcium and (2) sarcoplasmic reticulum (SR) calcium stores. We then discuss the approach to resolving calcium mishandling outlined in this dissertation, including the research questions being addressed and the significance of the overall work with respect to the field.

Calcium handling in normal muscle

In healthy muscle cells, calcium plays a vital role in the contraction and relaxation cycle. In order to understand this cycle, it is important to first understand where calcium resides and at what concentrations. At rest, extracellular calcium concentrations are ~2-4 mM, cytosolic calcium concentrations are ~50-250 nM, and SR calcium concentrations are ~0.4-0.5 mM(Gehlert et al., 2015; Kuo & Ehrlich, 2015; MacLennan & Kranias, 2003). In cardiac muscle, diastolic (resting) cytosolic calcium levels are ~100 nM, and systolic cytosolic calcium levels increase to ~1 μM(MacLennan & Kranias, 2003).

In both cardiac and skeletal muscle, an action potential signals for contraction by activating voltage-gated L-type calcium channels (Ca_v; $Ca_v1.1$ in skeletal muscles and $Ca_v1.2$ in cardiac muscle) in the plasma membrane. This signal leads to the opening of the ryanodine receptor (RyR; RyR1 in skeletal muscles and RyR2 in cardiac muscle) in the SR membrane. In cardiac muscle, opening of L-type calcium channels allows extracellular calcium to enter the cell and activate RyR opening through a process known as calcium-induced calcium release (CICR)(MacLennan & Kranias, 2003; Ríos, 2018). In skeletal muscle, RyR opening is primarily independent of extracellular calcium influx and occurs as L-type calcium channels physically interact with and open RyR(Franzini-Armstrong, 2018; Protasi, 2002). Opening of RyR allows SR calcium to enter the cytosol, where it initiates contraction by interacting with contractile proteins. Relaxation is initiated as calcium is removed from the cytosol. ~70-90% of cytosolic calcium is returned to the SR by the sarcoendoplasmic reticulum calcium ATPase (SERCA; SERCA1 and SERCA2a in skeletal muscle and SERCA2a in cardiac muscle), a calcium

pump residing in the SR membrane. A very small amount of calcium is taken up by the mitochondrial uniporter (MCU). The remaining calcium is removed from the cell by pumps residing in the plasma membrane, including the sodium-calcium exchanger (NCX) and plasma membrane calcium ATPase (PMCA). Throughout this cycle, calcium-sequestering proteins in the SR lumen are responsible for isolating calcium ions and regulating their uptake and release.

Calcium mishandling in dystrophic muscle: Mechanisms of extracellular calcium influx

Increased plasma membrane permeability is an early feature of dystrophin-deficient muscle, allowing an excess of enzymes such as creatine kinase to exit skeletal muscle fibers and ions such as calcium to enter. Early on, this phenomenon was solely attributed to microtears in the plasma membrane during mechanical stress, which were believed to occur because the lack of dystrophin created membrane instability. However, evidence for such membrane tears did not rule out alternative possibilities, such as calcium influx due to opening ion channels. It appears that disorganization of the cytoskeleton and disruption of the DGC have contributed to increased calcium entry through ion channels(Allen & Whitehead, 2011). Here we describe various pathways for extracellular calcium influx in skeletal and cardiac muscle cells and present evidence for dysfunction of these pathways in DMD.

Membrane tearing and repair

The primary function of dystrophin is to support the plasma membrane during muscle use by anchoring it to the cytoskeleton and to the extracellular matrix through interactions with the DGC(Chakkalakal et al., 2005; Ervasti & Campbell, 1993; Gao & McNally, 2015; Koenig et al., 1988; Petrof et al., 1993). Several studies provide evidence that the absence of dystrophin destabilizes the plasma membrane, making it more susceptible to microtears during mechanical stress(Danialou et al., 2001; Petrof et

al., 1993). However, one study found mdx muscle fibers are capable of repairing the plasma membrane just as efficiently as wildtype (WT) muscle fibers, suggesting microtears in dystrophic cells are not the primary cause of calcium entry and muscle cell death(Cooper & Head, 2015).

This membrane repair relies on calcium signaling. Increased cytosolic calcium levels activate calcium-dependent repair mechanisms(Andrews et al., 2014; Cooper & Head, 2015). These repair mechanisms operate by patching plasma membrane tears with exocytic vesicles. Several studies implicate the lysosomal calcium release channel transient receptor potential mucolipin 1 (TRPML1) is involved in the lysosomal exocytosis needed for membrane repair in DMD(Cheng et al., 2014; Yu et al., 2020). Ablation of TRPML1 in mice impaired plasma membrane repair in skeletal muscle and led to a DMD-like phenotype(Cheng et al., 2014). Activation or overexpression of TRPML1 alleviated dystrophic phenotypes in mdx mouse skeletal and cardiac muscle(Yu et al., 2020).

Voltage-gated L-type channels

In cardiac muscle cells, $Ca_v1.2$ is responsible for sustaining calcium entry during the plateau phase of the action potential. Its activation in significantly increased in mdx cardiac muscle cells, which may cause arrhythmias in dystrophic hearts(Koenig et al., 2014).

In skeletal muscle, the involvement of $Ca_v1.1$ in abnormal calcium entry is unclear. A study performed in dystrophic hamsters lacking delta-sarcoglycan (a

component of the DGC) showed administration of an L-type calcium channel antagonist reduced cytosolic calcium content(Bhattacharya et al., 1982). This suggests calcium entry through $Ca_v1.1$ may contribute to aberrant cytosolic calcium. However, a second study found $Ca_v1.1$ activity is already reduced in the fast-twitch muscle cells of mdx mice(Friedrich et al., 2004).

Store-operated calcium channels

Store-operated calcium channels (SOCCs) are channels residing at the plasma membrane that open in response to depleted SR calcium stores. Two proteins have been identified as the necessary players involved in store-operated calcium entry: Stromal interaction molecule (STIM) and Orai(Derler et al., 2016). STIM acts as a calcium sensor residing in the SR membrane and dimerizes upon decreased SR calcium stores. Simultaneously, Orai oligomerizes at the sarcolemmal membrane to form calcium channels. STIM1 and Orai1 bind to one another directly, forming puncta that allow extracellular calcium to enter the muscle fiber. In skeletal muscle, STIM1 is regulated by calsequestrin (CSQ), a protein responsible for calcium buffering in the SR lumen. When CSQ is low, store-operated calcium entry is increased(Cho et al., 2017).

Store-operated calcium entry is increased in dystrophin-deficient muscle cells due to increased expression of SOCC proteins(Edwards et al., 2010). CSQ is also decreased in multiple mdx muscle types, which may contribute to increased calcium entry through SOCCs(Pertille et al., 2010). Lastly, SOCC activity may be increased by a calcium-independent pathway. Calcium-independent phospholipase A_2 ($iPLA_2$) acts as a

messenger to trigger calcium entry through SOCCs and is elevated in dystrophic muscles(Boittin et al., 2010; Smani et al., 2004; Smani et al., 2003).

Transient receptor potential canonical channels

Transient receptor potential canonical channels (TRPCs) are a family of plasma membrane cation channels. These channels are opened in response to either SR calcium store depletion or membrane stretch. Several lines of evidence suggest TRPCs are a major contributor to increased cytosolic calcium in DMD. First, stretch-activated channel blockers ameliorated force reduction in mdx muscle fibers(Yeung et al., 2005). Second, TRPC1, TRPC3, and TRPC6 are all elevated in mdx mouse muscle(Gervásio et al., 2008; Matsumura et al., 2011; Vandebrouck et al., 2007). The most well-understood of these is TRPC1, which interacts with dystrophin and α1-syntrophin, a member of the DGC. In one model, the DGC acts as a scaffold for signaling molecules responsible for regulating TRPC1 activity(Sabourin et al., 2009). When dystrophin is absent, this scaffolding is lost and TRPC1 activity is increased(Vandebrouck et al., 2007). Supporting this theory, Matsumura and colleagues showed TRPC1 expression levels correlated with disease severity in mdx mice(Matsumura et al., 2011).

A related channel type, the transient receptor potential vanilloid type 2 (TRPV2) channel, may also play a role in increased calcium influx in DMD. In healthy muscle, TRPV2 is localized on intracellular organs. However, TRPV2 translocates to the plasma membrane in dystrophin-deficient muscle(Iwata et al., 2009). Inhibition of TRPV2 in mdx mice ameliorated phenotypes of the disease(Iwata et al., 2009).

Sodium regulators

In addition to an increase in intracellular calcium levels, dystrophic muscle also exhibits an increase in intracellular sodium levels(Burr et al., 2014; Hirn et al., 2008; Iwata et al., 2007). In normal muscle, sodium influx is important for plasma membrane depolarization and for regulating the import and export of other ions, including calcium, through ion exchangers. Sodium homeostasis is controlled by several plasma membrane exchangers, including the sodium calcium exchanger (NCX). NCX is a major source of calcium efflux from the cell. However, under high cytosolic sodium levels, as occurs in DMD, NCX may operate in reverse and instead allow sodium to exit the cell and calcium to enter(Deval et al., 2002).

ATP-gated ion channels

It has been suggested that ATP-gated ion channels also play a role in elevated cytosolic calcium levels in DMD muscle. One such channel is the P2X receptor. Evidence suggests either large amounts of extracellular ATP and/or inflammatory mediators in dystrophic muscles activate P2X7(Górecki, 2019; Young et al., 2012; Young et al., 2018). In addition, an upregulation of P2X receptors was observed in mdx muscle and myoblasts(Yeung et al., 2006; Young et al., 2012). Targeting of P2X7 via genetic or pharmacological methods reduced dystrophic inflammation and increased muscle repair(Górecki, 2019).

Connexins

Connexins (Cx) are proteins responsible for forming gap junction channels and hemichannels that coordinate depolarization and ion movement between cells(Cea et al., 2012). Cx hemichannels formed by Cx39, Cx43, and Cx45 are observed in dystrophic muscle but are absent in normal muscle(Cea et al., 2016). Ablation of Cx43/Cx45 in mdx mice reduced cytosolic calcium levels and necrotic phenotype(Cea et al., 2016). In addition, Cx43 is increased and mislocalized in dystrophic mouse cardiomyocytes(Gonzalez et al., 2018; Himelman et al., 2020).

Calcium mishandling in dystrophic muscle: Mechanisms of sarcoplasmic reticulum dysregulation

A main function of the SR is to alter and maintain calcium levels within itself and the cytoplasm through calcium storage, release, and reuptake. This is accomplished by the RyR, SR luminal calcium-sequestering proteins, and SERCA. As discussed earlier, regulation of cytosolic calcium levels is important for controlling muscle contraction and relaxation(Mareedu, Million, et al., 2021). Muscle contraction occurs when calcium is released from the SR and binds to myofilament regulatory proteins within the cytosol. Muscle relaxation occurs as calcium shuttled back into the SR. In DMD, the functions of several SR proteins are dysregulated, resulting in increased calcium release and slowed calcium reuptake. This contributes to the increased cytosolic calcium levels observed in dystrophin-deficient muscle.

Ryanodine receptor

RyR is a calcium channel residing in the SR membrane that is responsible for calcium release into the cytosol during muscle contraction. Three isoforms exist: RyR1 (skeletal muscle), RyR2 (cardiac muscle), and RyR3 (brain and skeletal muscle). RyR regulation occurs through phosphorylation or nitrosylation of the channels and through interaction of RyR with its stabilizing protein calstabin. Calcium is excessively leaked from the SR when RyR is hyperphosphorylated or hypernitrosylated or when the RyR-calstabin interaction is lost.

Studies performed in skinned EDL and soleus muscle fibers show SR calcium release via RyR is more pronounced in mdx muscle fibers(Divet & Huchet-Cadiou, 2002). In support of this finding, Robin and colleagues showed an increase in passive SR calcium leak in myofibers from the mdx5cv mouse model of DMD(Robin et al., 2012). Contrary to these findings, Plant and Lynch showed SR calcium leak was unaltered in skinned mdx muscle fibers(Plant & Lynch, 2003). Several additional studies elucidate possible mechanisms for RyR leak in dystrophic muscles. Two studies show progressive S-nitrosylation of RyR and depletion of calstabin are responsible for RyR leak in dystrophic skeletal and cardiac muscle(Bellinger et al., 2009; Fauconnier et al., 2010). In addition, it has been shown that RyR2 phosphorylation and oxidation increases calcium leak in dystrophic cardiac muscle, and inhibition of this phosphorylation can reduce RyR2 oxidation as well(Prosser et al., 2011; Shannon, 2009; Wang et al., 2015; Williams & Allen, 2007).

SR luminal calcium-sequestering proteins

Several proteins reside within the SR lumen that are responsible for buffering calcium concentrations and regulating SR calcium uptake and release. These proteins include calsequestrin (CSQ), CSQ-like proteins (CLPs), histidine-rich calcium-binding protein (HRCBP), calreticulin, calmodulin (CaM), and sarcalumenin (SLM)(Arvanitis et al., 2011; Beard et al., 2004; Jiao et al., 2012). Among these, CSQ is the major calcium-buffering protein (CSQ1 in skeletal muscle, CSQ2 in cardiac and slow-twitch muscle).

In all, calcium-sequestering proteins show a trend of downregulation in dystrophic muscle. CSQ is reduced in mdx diaphragm, soleus, and sternomastoid muscles, while CaM is reduced in mdx diaphragm and tibialis anterior(Pertille et al., 2010). Interestingly, these two proteins are increased in the extraocular and intrinsic laryngeal muscles, two spared muscles in mdx mice(Pertille et al., 2010). One study shows CSQ is also downregulated in dystrophic cardiac muscle(Lohan & Ohlendieck, 2004). However, multiple later studies conducted by others show CSQ is unaltered in mouse models of DMD(Mareedu, Pachon, et al., 2021; Pertille et al., 2010; Voit et al., 2017). Surprisingly, CSQ is upregulated in fast-twitch muscles of two mouse models of DMD(Schneider et al., 2013a; Voit et al., 2017). The reason for this is currently unknown. CLPs and SLM are also reduced in mdx muscle, while HRCBP is increased in mdx heart(Culligan et al., 2002; Lohan & Ohlendieck, 2004). Overall, these findings show SR calcium-sequestering proteins play a role in altered calcium cycling in DMD.

SERCA and SERCA regulators

SERCA plays a vital role in initiating muscle relaxation by returning cytosolic calcium to the SR. Several isoforms exist, including SERCA1 (fast-twitch muscle), SERCA2a (heart and slow-twitch muscle), and SERCA3 (non-muscle tissues). SERCA function is modulated by several micro-peptides, including phospholamban (PLN), sarcolipin (SLN), myoregulin (MLN), and dwarf open reading frame (DWORF)(Anderson et al., 2015; Bhupathy et al., 2007; Nelson et al., 2016; Shaikh et al., 2016). PLN, SLN, and MLN are inhibitors of SERCA function, while DWORF is an enhancer of SERCA function. PLN is highly expressed in the ventricles. SLN is

expressed the atria of the heart, in slow-twitch rodent muscle, and in all skeletal muscle in large mammals. MLN is expressed in skeletal muscle. DWORF is expressed in slow-twitch and heart muscle.

It is well-established that SERCA function is reduced in dystrophic muscle(Mareedu, Pachon, et al., 2021; Schneider et al., 2013a; Voit et al., 2017; Wasala et al., 2020). Previous research indicates that SLN upregulation is to blame in dystrophic mouse and canine models(Mareedu, Pachon, et al., 2021; Voit et al., 2017). In addition, it is possible that posttranslational modifications of SERCA under oxidative stress contribute to SERCA dysfunction in DMD(Kim et al., 2013).

Present approach

Currently, there is no cure for DMD. One approach to treating DMD is to target dysregulated calcium pathways. Evidence suggests reducing cytosolic calcium in DMD muscle fibers will improve muscle survival and function by diminishing calcium-dependent activation of proteases and phospholipases that degrade cellular components.

One method for reducing cytosolic calcium in DMD is to improve SERCA function. Previous studies have achieved this through SERCA overexpression or knockdown of the SERCA inhibitor SLN(Balakrishnan et al., 2022; Goonasekera et al., 2011; Mareedu, Pachon, et al., 2021; Morine et al., 2010; J. H. Shin et al., 2011; Voit et al., 2017; Wasala et al., 2020). DWORF is a positive enhancer of SERCA function(Nelson et al., 2016). Makarewich and colleagues showed DWORF overexpression ameliorated cardiomyopathy in a mouse model of ischemic heart failure and a LIM protein deficiency mouse model of cardiomyopathy(Makarewich et al., 2020; Makarewich et al., 2018). However, when considering SERCA-activating therapies for DMD, it is important to consider the implications of SERCA overactivation, as several recent studies suggest it could worsen phenotypes of DMD(Fajardo et al., 2017; Law et al., 2018; Sato et al., 2021).

The following research is conducted in response to the need for methods aimed at reducing cytosolic calcium in dystrophic muscle. Due to the recent discovery of DWORF and its implications in cardiac health, we hypothesize that adeno-associated virus (AAV)-mediated DWORF overexpression can improve SERCA function and

mitigate phenotypes of DMD. In Chapter 2, we assess the effects of AAV DWORF gene therapy on mdx mouse cardiomyopathy. In Chapter 3, we explore the effects of DWORF overexpression in WT mice and hypothesize SERCA overactivation will have negative consequences in healthy hearts. In Chapter 4, we assess the effects of AAV DWORF gene therapy on mdx skeletal muscle. Lastly, we measure the transcript levels of various calcium handling proteins in normal and dystrophic canines, including assessments made in different age groups and in male vs female animals. This data is intended to elucidate part of the mechanisms behind calcium dysregulation in an animal model that more closely resembles human patients. This data is presented in Chapter 5.

Chapter 2. Dwarf open reading frame (DWORF) gene therapy ameliorated Duchenne muscular dystrophy cardiomyopathy in aged mdx mice

Emily D. Morales[1], Yongping Yue[1], Thais B. Watkins[1], Jin Han[1], Xiufang Pan[1], Aaron M. Gibson[2], Gang Yao[3], Catherine A. Makarewich[2, 4], Gopal J. Babu[5], Dongsheng Duan[1, 3, 6, 7 *]

[1], Department of Molecular Microbiology and Immunology, School of Medicine, The University of Missouri, Columbia, MO 65212

[2], The Heart Institute, Division of Molecular Cardiovascular Biology, Cincinnati Children's Hospital Medical Center, Cincinnati, OH, 45229

[3], Department of Biomedical, Biological & Chemical Engineering, College of Engineering, The University of Missouri, Columbia, MO 65212

[4], Department of Pediatrics, The University of Cincinnati College of Medicine, Cincinnati, OH 45229

[5], Department of Cell Biology and Molecular Medicine, Rutgers, New Jersey Medical School, Newark, NJ 07103

[6], Department of Neurology, School of Medicine, The University of Missouri, Columbia, MO 65212

[7], Department of Biomedical Sciences, College of Veterinary Medicine, The University of Missouri, Columbia, MO 65212

Abstract

Cardiomyopathy is a leading health threat in Duchenne muscular dystrophy (DMD), a dystrophin-deficient muscle wasting disease. Upregulation of cytosolic calcium has been implicated in the pathogenesis of DMD cardiomyopathy. Cytosolic calcium is mainly removed by the sarcoendoplasmic reticulum calcium ATPase (SERCA). SERCA activity is reduced in DMD. Strategies that improve SERCA function hold promise to treat Duchenne cardiomyopathy. Dwarf open reading frame (DWORF) is a recently discovered positive regulator for SERCA. Transgenic or adeno-associated virus (AAV)-mediated DWORF overexpression significantly improved cardiac function in other types of cardiomyopathies. We found DWORF expression was significantly reduced in the mdx model of DMD. To test whether AAV DWORF gene therapy can mitigate Duchenne cardiomyopathy, we delivered 6×10^{12} vg particles/mouse of the AAV9.DWORF vector to 6-week-old mdx mice by tail vein injection. Mice were examined at 18 months of age. We observed significant improvement in myocardial histology and multiple parameters of electrocardiography and heart hemodynamics. Uphill treadmill running was also significantly improved. Our data suggest that DWORF deficiency contributes to SERCA dysfunction in mdx mice and that DWORF gene therapy holds promise to treat Duchenne cardiomyopathy.

Introduction

Duchenne muscular dystrophy (DMD) is a rare muscle-wasting disease caused by mutations in the dystrophin gene(D Duan et al., 2021). Dystrophin offers structural support to the muscle cell membrane during contraction and relaxation. When dystrophin is absent, muscles undergo degeneration, resulting in muscle weakness and eventual heart and/or respiratory failure. Restoration of dystrophin expression by genetic editing or gene replacement is being actively pursued to treat DMD. An alternative gene therapy approach is to upregulate cellular genes that may mitigate the pathogenic mechanisms of DMD.

It is well-documented that muscle cell death in DMD is partly due to dysregulated intracellular calcium pathways(Burr & Molkentin, 2015; Mareedu, Million, et al., 2021). These dysregulations create an increased concentration of cytosolic calcium, which activates calcium-dependent proteases and phospholipases that digest cellular proteins and lipids, respectively(Hopf et al., 1996b; Lindahl, Backman, et al., 1995; Turner et al., 1988). Therefore, strategies aimed at normalizing cytosolic calcium levels in dystrophic cells are expected to reduce muscle disease in DMD.

A major source of cytosolic calcium is the sarcoplasmic reticulum (SR), which acts as a calcium store and plays a large role in the contraction-relaxation cycle(Rossi & Dirksen, 2006). In a healthy muscle cell, contraction is initiated as calcium from the SR is released into the cytosol via the opening of the ryanodine receptor (RyR). Once in the cytosol, calcium binds to myofilament regulatory proteins to initiate contraction. During relaxation, calcium is pumped back into the SR by the sarcoendoplasmic reticulum

calcium ATPase (SERCA), leading to its release from contractile proteins(Periasamy & Kalyanasundaram, 2007; Xu & Van Remmen, 2021). In DMD, however, calcium release from the SR is increased while calcium reuptake into the SR via SERCA is decreased(Bellinger et al., 2009; Fauconnier et al., 2010; Kargacin & Kargacin, 1996; Schneider et al., 2013b). This contributes to increased resting cytosolic calcium concentrations.

One method of reducing cytosolic calcium overload in dystrophic muscle is to enhance SERCA function. This has been achieved by SERCA overexpression or knockdown of sarcolipin (SLN), a negative regulator of the SERCA pump(Balakrishnan et al., 2022; Goonasekera et al., 2011; Mareedu, Pachon, et al., 2021; Morine et al., 2010; J.-H. Shin et al., 2011; Voit et al., 2017; Wasala et al., 2020). The micro-peptide dwarf open reading frame (DWORF) is a positive regulator of the SERCA pump(Nelson et al., 2016). It has been shown that DWORF overexpression ameliorates ischemic heart failure and muscle-specific LIM protein deficiency cardiomyopathy(Makarewich et al., 2020; Makarewich et al., 2018). We hypothesize that adeno-associated virus (AAV)-mediated DWORF upregulation can improve SERCA function and mitigate DMD cardiomyopathy.

To test our hypothesis, we quantified DWORF expression in the hearts of normal and dystrophin-null mdx mice. We found DWORF expression was significantly decreased in mdx mice. We then delivered a DWORF expression cassette with AAV serotype 9 (AAV9) to 6-week-old mdx mice via tail vein injection. DWORF expression, calcium uptake, myocardial fibrosis, electrocardiography (ECG), uphill treadmill running, and left ventricular hemodynamics were examined. In support of our hypothesis, AAV9 DWORF gene transfer significantly enhanced cardiac SR calcium

uptake and improved myocardial histology and heart function. Our results support further development of DWORF gene therapy to treat DMD cardiomyopathy.

Results

DWORF expression was decreased in the hearts of mdx mice. Previous research shows SERCA function is reduced in DMD(Kargacin & Kargacin, 1996; Schneider et al., 2013b; Voit et al., 2017; Wasala et al., 2020). To determine whether DWORF plays a role, we compared DWORF cDNA and protein levels in the hearts of 6-month-old mdx and wild-type BL10 (WT) mice **(Figure 2.1)**. cDNA levels were detected using droplet digital PCR (ddPCR) methods. DWORF cDNA levels were significantly decreased in mdx hearts compared to that of WT hearts **(Figure 2.1A)**. Consistent with the cDNA data, western blot analysis showed an ~50% decrease in DWORF protein expression in the mdx heart **(Figure 2.1B)**.

AAV.DWORF delivery increased DWORF expression and enhanced SR calcium uptake in the mdx mouse heart. As a prelude to evaluating DWORF gene therapy, we engineered an AAV9.DWORF vector **(Figure 2.2A)**. In this vector, a codon-optimized mouse DWORF cDNA was expressed from the ubiquitous CAG promoter. To facilitate the detection of AAV transduction, we also introduced the enhanced green fluorescence protein (EGFP) cDNA under the control of an internal ribosomal entry site (IRES). The AAV genome was packaged in myocardial-tropic AAV9 capsids(Bostick et al., 2007). We injected the AAV9.DWORF vector to 6-week-old mdx mice at the dose of 6×10^{12} vector genome particles (vg)/mouse via the tail vein and examined DWORF expression in the heart when mice reached 6 months of age **(Figure 2.2B)**. Supra-physiological levels of DWORF expression were detected in the AAV-injected mdx mouse hearts (~

50-fold higher than those of un-injected mdx mouse hearts). For reasons yet unknown, we failed to detect GFP expression (data not shown). Despite the dramatic increase in DWORF expression, no remarkable changes were detected in the protein levels of SERCA2a (SERCA isoform expressed in the heart), calsequestrin, sarcolipin (SLN), or phospholamban (PLN) **(Figure 2.2C)**.

Next, we analyzed SR calcium uptake **(Figure 2.2D-E)**. As expected, SR calcium uptake was reduced in mdx hearts. AAV9.DWORF delivery significantly enhanced SR calcium uptake **(Figure 2.2D)**. The maximum velocity of calcium uptake was also significantly increased **(Figure 2.2E)**. Nonetheless, improvements did not reach the levels of WT mouse hearts.

AAV.DWORF delivery did not change heart anatomy but reduced myocardial fibrosis in aged mdx mice. After validation of the DWORF vector, we evaluated its therapeutic effects (6×10^{12} vg/mouse, tail vein injection at 6 weeks of age, examination at 18 months of age). We opted to study 18-month-old mice because this is the age at which mdx mice display dilated cardiomyopathy(Bostick et al., 2008). On anatomic examination, we did not detect significant differences in heart weight, ventricular weight, and weight ratios between DWORF-treated and untreated mdx mice **(Table 2.1)**. On histology examination, we performed Masson trichrome staining and quantified fibrosis **(Figure 2.3)**. DWORF gene therapy significantly reduced myocardial fibrosis.

AAV.DWORF delivery ameliorated mdx ECG defects. To determine whether DWORF gene therapy can improve cardiac electrophysiology, we performed ECG **(Figure 2.4)**.

All parameters showed expected changes in mdx mice compared to WT mice **(Figure 2.4)**. DWORF therapy normalized heart rate, QTc interval, and cardiomyopathic index. Other ECG parameters (PR interval, QRS duration, and Q amplitude) showed a trend of improvement, though not statistically significant.

AAV.DWORF delivery improved uphill treadmill running. Uphill treadmill running is frequently used to evaluate mouse heart function(Bernstein, 2003; Bostick et al., 2009; Wasala et al., 2020). Following 5 days of acclimation, we quantified mouse running distance on a 7° uphill treadmill. Mdx mice ran an average of 3.3 meters/g body weight (m/g). WT mice ran an average of 20.9 m/g **(Figure 2.5)**. DWORF gene therapy significantly increased treadmill performance. Treated mice reached an average of 8.0 m/g **(Figure 2.5)**.

AAV.DWORF delivery enhanced left ventricular hemodynamic function in mdx mice. Cardiac pump function was evaluated using a closed-chest catheterization assay as we previously reported(Bostick et al., 2011). Consistent with our previous publications(Bostick et al., 2010; Bostick et al., 2008; Wasala et al., 2020), untreated mdx mice showed a classic profile of dilated cardiomyopathy **(Figure 2.6)**. Specifically, end-systolic and end-diastolic chamber volumes were significantly enlarged while the ejection fraction, maximum pressure, and rates of pressure change during contraction (dP/dt max) and relaxation (dP/dt min) were significantly decreased. DWORF gene therapy normalized maximum pressure and ejection fraction. A trend of improvement was also detected in dP/dt max and dP/dt min. Intriguingly, end-systolic and end-diastolic

volumes of the treated mdx mice were smaller than those of WT mice, though statistical significance between WT mice and DWORF-treated mdx mice was only observed for the end-diastolic volume. The only parameter that showed no improvement was tau, the time constant of left ventricular relaxation.

Discussion

In this study, we evaluated DWORF expression in normal and dystrophic mouse hearts and explored AAV DWORF gene therapy for Duchenne cardiomyopathy in the mdx mouse model of DMD. We found that endogenous DWORF expression was significantly reduced at both the transcript and protein levels in mdx hearts **(Figure 2.1)**. Intravenous delivery of an AAV9.DWORF vector resulted in supraphysiological levels of DWORF expression in the mdx heart and significantly improved cardiac SR calcium uptake **(Figure 2.2)**. Importantly, a single AAV DWORF gene therapy in 6-week-old mdx mice resulted in significant improvements in myocardial histology, uphill running, ECG, and left ventricular hemodynamics at 18 months of age **(Figures 2.3 to 2.6)**. Our results suggest (1) decreased DWORF expression may contribute to SERCA dysfunction in dystrophic cardiac tissue and (2) DWORF gene therapy at a young age holds promise to significantly prevent dilated cardiomyopathy in DMD.

DWORF was discovered in 2016 as a small peptide encoded in a long noncoding RNA(Nelson et al., 2016). It is the only known endogenous SERCA activator. DWORF is expressed in ventricular and slow-twitch skeletal muscle fibers. Initial studies suggest DWORF enhances SERCA function through competition with inhibitory peptides SLN and PLN for SERCA binding(Makarewich et al., 2018; Nelson et al., 2016; Singh, Dalton, Cho, Pribadi, Zak, Seflova, et al., 2019). More recent studies suggest DWORF may also directly activate SERCA(Fisher et al., 2021; Reddy et al., 2022a). It is possible both mechanisms are in play(Li et al., 2021). More studies are needed to clarify this.

Recently, DWORF has received attention for playing a large role in the development and treatment of cardiomyopathy. DWORF expression was reduced in two independent mouse models of heart failure, including myocardial infarct and a genetic model of dilated cardiomyopathy caused by the loss of the muscle-specific LIM protein(Makarewich et al., 2020; Makarewich et al., 2018). Expression of DWORF via a transgenic approach or AAV9.DWORF gene delivery enhanced SERCA activity and improved heart function in these models(Makarewich et al., 2020; Makarewich et al., 2018).

It is well established that SERCA activity reduction contributes to DMD pathogenesis(Burr & Molkentin, 2015; Law et al., 2020; Mareedu, Million, et al., 2021). Previous studies have connected SERCA dysfunction with SLN overexpression(Niranjan et al., 2019; Schneider et al., 2013b; Voit et al., 2017). Indeed, SLN knockdown ameliorated dystrophic phenotypes in murine DMD models(Balakrishnan et al., 2022; Mareedu, Pachon, et al., 2021; Voit et al., 2017). The discovery of DWORF as a positive SERCA regulator raises the possibility of DWORF downregulation as an alternative mechanism for SERCA activity reduction in DMD. Given the established involvement of DWORF in other types of cardiomyopathy, we focused the current study on DMD heart disease.

In the mouse myocardial infarct model, DWORF expression was reduced by ~ 60% (Makarewich et al., 2020). In the muscle-specific LIM protein-deficient cardiomyopathy model, DWORF expression was reduced by ~ 70% (Makarewich et al., 2018). Consistent with these results, we found DWORF expression was reduced by ~50% in the mdx heart **(Figure 2.1)**. These results suggest low-level DWORF

expression (30-50% of the wild-type level) is likely insufficient for normal mouse heart function.

To establish a causal relationship between DWORF downregulation and SERCA dysfunction, we delivered an AAV9.DWORF vector (6×10^{12} vg/mouse) to the heart of mdx mice via tail vein injection. Compared with untreated mdx hearts, AAV injected mdx hearts exhibited an approximately 50-fold increase in DWORF levels **(Figure 2.2B)**. This is ~25-fold higher than that of WT hearts. Despite supraphysiological DWORF expression, myocardial SR calcium uptake was only partially restored (**Figure 2.2D and E)**. This suggests DWORF downregulation may have contributed to SERCA activity reduction in the mdx heart, but it is unlikely the sole cause. Previous literature shows DWORF has a higher SERCA binding affinity than PLN(Makarewich et al., 2018; Nelson et al., 2016), but there is no literature covering the dynamics of DWORF versus SLN competition in the heart. Our results suggest either DWORF is weaker than SLN in binding with SERCA (hence cannot fully compete away SLN from SERCA) or there may exist additional yet unknown SERCA inhibition mechanism(s) in the mdx heart that cannot be revoked by DWORF overexpression.

We also examined the expression of several other SR calcium-regulating proteins and did not see significant alterations **(Figure 2.2C)**. This is consistent with what has been shown in DWORF transgenic mice, where proteins involved in calcium handling are largely unaffected(Nelson et al., 2016).

To explore DWORF as a potential target for treating cardiomyopathy in mdx mice, we followed AAV9.DWORF injected mice until they reached 18 months of age **(Figures 2.3-2.6)**. This is necessary because young adult mdx mice display minimal

heart disease (Duan, 2006). On anatomical examination, no statistically significant improvement was detected **(Table 2.1)**. Nevertheless, cardiac fibrosis, ECG, closed-chest cardiac catheter assay, and uphill treadmill running showed significant improvements in many, though not all, parameters **(Figures 2.3-2.6)**. This is expected given that SR calcium uptake was only partially restored in treated mice **(Figure 2.2D, E)**.

We have previously conducted a similar long-term study in mdx mice using the AAV9.SERCA2a vector(Wasala et al., 2020). Systemic injection of the same dose (6 x 10^{12} vg/mouse) of SERCA2a vector completely corrected cardiac SR calcium uptake, prevented myocardial fibrosis, and normalized most parameters in physiology assays (ECG, heart hemodynamics, and uphill treadmill running). The difference in the therapeutic outcome between DWORF and SERCA2a gene therapy suggests that there is room to further improve DWORF gene therapy. This can be accomplished by several approaches. One is to further increase DWORF expression. Makarewich and colleagues found that ~60-fold DWORF overexpression resulted in better cardioprotection than ~17-fold DWORF overexpression in a dilated cardiomyopathy mouse model caused by genetic knockout of the gene encoding the muscle-specific LIM protein(Makarewich et al., 2020; Makarewich et al., 2018). We are not in favor of this approach because (a) increasing the AAV dose may lead to severe adverse consequences, even death(Srivastava, 2020); (b) an *ex vivo* study in isolated rat hearts suggests that exogenous administration of high-dose DWORF peptide may induce coronary vasoconstriction(Mbikou et al., 2020).

Another approach is to combine SLN knockdown and DWORF overexpression. This is tempting. On one hand, SERCA inhibition will be reduced (by lowering SLN expression and/or by enhancing SERCA function through DWORF binding)(Fisher et al., 2021; Reddy et al., 2022a). On the other hand, a potential caveat of this approach is SERCA overactivation. Law et al ablated PLN from mdx mice(Law et al., 2018). These mice showed enhanced calcium handling and myocardial contractility, but heart function was worsened, and cardiac fibrosis was aggravated. Similarly, genetic deletion of SLN from mdx mice resulted in more severe skeletal muscle disease(Fajardo et al., 2018). It is possible that enhanced contractility from untuned calcium cycling may have made the dystrophic sarcolemma more fragile, hence causing more damage.

A third approach is to combine DWORF overexpression with micro-dystrophin gene therapy. Systemic AAV micro-dystrophin gene therapy is currently being tested in DMD patients(Duan, 2018). Micro-dystrophin re-establishes the linkage between the cytoskeleton and the extracellular matrix to maintain sarcolemmal integrity during contraction. Despite encouraging data in murine models, micro-dystrophin only resulted in limited force improvement in the canine DMD model(Shin et al., 2013). A recent phase II trial also failed to yield significant functional improvements in all patients(Mullard, 2021). Multiple strategies have been proposed to enhance micro-dystrophin gene therapy. One possibility is to combine micro-dystrophin with therapies that can improve calcium homeostasis in muscle cells. In this regard, DWORF has a unique advantage. The small size of the DWORF cDNA (102 bp) makes it possible to fit into existing micro-dystrophin vectors. Future side-by-side comparisons of the micro-

dystrophin vector, the DWORF vector, and the micro-dystrophin/DWORF vector will show whether the combined approach is indeed superior.

In summary, our study demonstrates for the first time that DWORF expression is reduced in mdx hearts and AAV DWORF gene therapy prevented the deterioration of mdx mouse heart function. Future studies will shed light on whether AAV DWORF therapy can ameliorate dystrophic skeletal muscle disease in mice, and more importantly, whether positive findings seen in our study can be translated to canine models and eventually benefit human patients.

Materials and Methods

Mice. All animal experiments were approved by the institutional animal care and use committee. All mice were maintained in a specific pathogen-free animal care facility on a 12-hour light (25 lux):12-hour dark cycle with access to food and water *ad libitum*. Dystrophin-deficient mdx mice (C57BL/10ScSn-*Dmd*^{mdx}/J, stock number 001801) and normal control BL10 (C57BL/10ScSnJ, stock number 000476) mice were originally purchased from The Jackson Laboratory (Bar Harbor, ME). Experimental mice were generated in-house in a barrier facility using breeders purchased from The Jackson Laboratory. We have previously shown that female mdx mice display a more severe cardiomyopathy (Bostick et al., 2010), hence, only female mice were used in the current study.

AAV production and administration. The *cis*-plasmid for AAV packaging (also called pEM1) consisted of (from 5'-end to 3'-end) the ubiquitous CAG promoter, a codon-optimized mouse DWORF cDNA, the encephalomyocarditis virus IRES (Clontech, Mountain View, CA), the EGFP gene, and an SV40 virus polyadenylation signal. The codon-optimized mouse DWORF cDNA was synthesized by GenScript (Piscataway, NJ). The vector genome was packaged in the capsid of AAV9 and purified through two rounds of isopycnic ultracentrifugation according to our previously published method (J.-H. Shin et al., 2012). AAV was delivered to 6-week-old mice via tail vein injection at a concentration of 6 x 10^{12} vg/mouse.

Western blot. For DWORF western blots, freshly isolated heart tissue was snap-frozen in liquid nitrogen and homogenized in radioimmunoprecipitation assay buffer (150 mM NaCl; 1% v/v igepal CA-630; 50 mM Tris-Cl, pH 8.3; 0.5% w/v sodium deoxycholate; 0.1% w/v sodium dodecyl sulfate) with added protease inhibitors (cOmplete ULTRA mini-tablet, Roche, Indianapolis, IN). 40 μg of the heart lysate was run on 15% bis/acrylamide gels made by standard preparation, and proteins were transferred to PVDF membranes (Millipore, Immoblion-P) by wet transfer technique. Membranes were incubated with a previously validated custom rabbit polyclonal antibody against mouse DWORF (New England Peptide) at a concentration of 1:1,000 (Nelson et al., 2016). Blots were incubated with a goat anti-rabbit IgG-HRP secondary antibody and developed using ClarityTM Western ECL chemiluminescent substrate (Bio-Rad, Hercules, CA) and a digital Bio-Rad ChemiDocTM MP Imaging System.

For all other western blots, tissues were homogenized in lysis buffer (50 mM Tris, pH 7.4, 150 mM NaCl, 1 mM EDTA, and 0.5% NP-40) with added 1 mmole PMSF, 5 mmole NaVO3, 10 nmole Okadaic Acid, 1 mmole NaF, and 1 mmole benzamidine. Heart lysates were run on sodium dodecyl sulfate-polyacrylamide gels. Proteins were then electroblotted onto PVDF membranes and incubated with antibodies specific for SLN (anti-rabbit, 1:3000)(Babu et al., 2007), SERCA2a (anti-rabbit, 1:5000, custom made)(Babu et al., 2007), PLN (anti-rabbit, 1:3000, custom made)(Babu et al., 2007), CSQ (anti-rabbit, 1:5000, Affinity BioReagents, Golden, CO), or GAPDH (anti-mouse, 1:10,000, Sigma, St. Louis, MO). Quantification was completed using ImageJ/Fiji Software (ImageJ 1.48b) and then normalized to GAPDH levels.

DWORF and GFP transcript quantification. Transcript quantification was completed using ddPCR methods. Tissue samples were collected and stored in RNAlater stabilization solution (Thermo Fisher Scientific, Waltham, MA; Cat No: AM7021) until RNA was extracted using the RNeasy Fibrous Tissue Mini kit (Qiagen, Hilden, Germany; Cat No: 74704). Reverse transcription was performed using the SuperScript IV VILO Master Mix with ezDNase Enzyme (Thermo Fisher Scientific, Cat No: 11766050), and the resulting cDNA concentrations were detected using the Qubit ssDNA assay kit (Thermo Fisher Scientific, Cat No: Q10212). Primer and probe sets were designed as follows: Forward primer: 5'-TTCTTCTCCTGGTTGGATGG-3', Reverse primer: 5'-TCTTCTAAATGGTGTCAGATTGAAGT-3', and Probe 5'-TTTACATTGTCTTCTTCTAGAAAAGGAAGAAG-3'. Probes were labeled with a 5' 6-carboxyfluorescein, an internal ZEN quencher, and a 3' Iowa Black quencher. ddPCR was completed on the QX200 ddPCR system (Bio-Rad) using ddPCR supermix for probes (no dUTP) (Bio-Rad, Cat No: 186-3024). Results were presented as the number of transcript copies per ng of cDNA used in the ddPCR reaction.

SR calcium uptake. SR calcium uptake was measured using a previously described Millipore filtration technique (Voit et al., 2017). Approximately 150 μg of protein extract was incubated at 37° C in 1.5 ml of calcium uptake medium (40 mM imidazole, pH 7.0, 100 mM KCl, 5 mM MgCl2, 5 mM NaN3, 5 mM potassium oxalate, and 0.5 mM EGTA) and various concentrations of $CaCl_2$ to yield 0.03–3 μM free calcium. Ruthenium red was added to a final concentration of 1 μmole immediately before adding substrates to begin calcium uptake. A final concentration of 5 mmole ATP was added to

initiate the reaction. The reaction was terminated at 1 minute by filtration. The rate of SR calcium uptake and the calcium concentration required for EC50 were determined by non-linear curve fitting analysis using GraphPad Prism v6.01 software (GraphPad, San Diego, CA).

ECG and hemodynamic assay. 12-lead ECG was performed using a commercial system from AD Instruments (Colorado Springs, CO, USA). Results were evaluated using our previously published standard operating protocol in "Cardiac protocols for Duchenne animal models" (http://www.parentprojectmd.org/site/PageServer?pagename=Advance_researchers_sops) (Duan et al., 2016). All ECG parameters but Q wave amplitude were analyzed using the lead II tracing. Q wave amplitude was determined using the lead I tracing. QTc interval was calculated by correcting the QT interval with the heart rate as described by Mitchell et al (Mitchell et al., 1998b). Cardiomyopathy index was calculated by dividing the QT interval by the PQ segment(Bostick et al., 2011). Left ventricular hemodynamics was performed using our previously described closed chest approach with the Millar catheter, which can also be found in the "Cardiac protocols for Duchenne animal models" (Duan et al., 2016). Resulting pressure-volume loops were analyzed using the PVAN software (Millar Instruments, Houston, TX, USA). Cardiac relaxation time constant (Tau) was calculated according to Weiss et al (Weiss et al., 1976). Body surface area was calculated as described by Cheung et al (Cheung et al., 2009).

Treadmill running. The treadmill endurance assay was performed according to previous protocols but with minor modifications (Bostick et al., 2009; Wasala et al., 2020). Mice were subjected to 5 days of treadmill acclimation and training on a 7° uphill treadmill (Columbus Instruments, Columbus, OH, USA). During training, mice were encouraged to run by gently nudging mice from behind with a ruler. Each training day began with acclimating mice to a flat, unmoving treadmill surface for 2 minutes. The rest of the protocol was conducted at a 7° incline. Training days were conducted as follows: (1) mouse acclimated to an unmoving treadmill surface for 5 minutes, mouse run for 15 minutes at 5 m/min, mouse run for 5 minutes at 10 m/min, (2) mouse run for 5 minutes at 5 m/min, mouse run for 15 minutes at 10 m/min, mouse run for 5 min at 12 m/min, (3) mouse run for 5 minutes at 5 m/min, mouse run for 15 minutes at 10 m/min, mouse run for 10 min at 12 m/min, (4) mouse run for 5 minutes at 5 m/min, mouse run for 20 minutes at 10 m/min, mouse run for 5 min at 12 m/min, mouse run for 5 minutes at 15 m/min, (5) mouse run for 5 minutes at 5 m/min, mouse run for 20 minutes at 10 m/min, mouse run for 5 min at 12 m/min, mouse run for 5 minutes at 15 m/min. On day 6, mice were again acclimated to a flat, unmoving treadmill surface for 2 minutes. Following, mice were run at a 7° incline. Mice were run for 5 minutes at 5 m/min. The speed of running was then increased by 1 m/min every 5 minutes until mice were exhausted. Exhaustion was diagnosed when a mouse exited the treadmill and refused to reenter, despite gentle nudging, for 3 seconds. At this point, total running distance was recorded. Results were recorded as distance run/mouse body weight.

Morphological studies. 10 μm cryosections were sectioned from OCT-embedded heart samples. General histology was examined by hematoxylin and eosin (H&E) staining. Fibrosis was examined by Masson trichrome staining, which was conducted using the Masson Trichrome Stain Kit (Epredia, Kalamazoo, MI). Percent fibrotic area of entire heart sections was quantified by dividing the area of blue staining by the total area using ImageJ/Fiji Software (ImageJ 1.48b).

Statistical analysis. Data are presented as mean ± stand error of mean. One-way ANOVA with Holm-Sidak's multiple comparisons was performed on more than two group comparisons including one independent variable. Unpaired t-test was used for two-group comparisons. All statistical analyses were performed using GraphPad PRISM software version 9.1.2 (GraphPad Software, La Jolla, California). A $p < 0.05$ was considered statistically significant.

Acknowledgments

Conceived and designed experiments: EM, XP, and DD. Performed the experiments: EM, YY, TL, JH, XP, AG, CM, and GB. Wrote the paper: EM and DD.

Figures

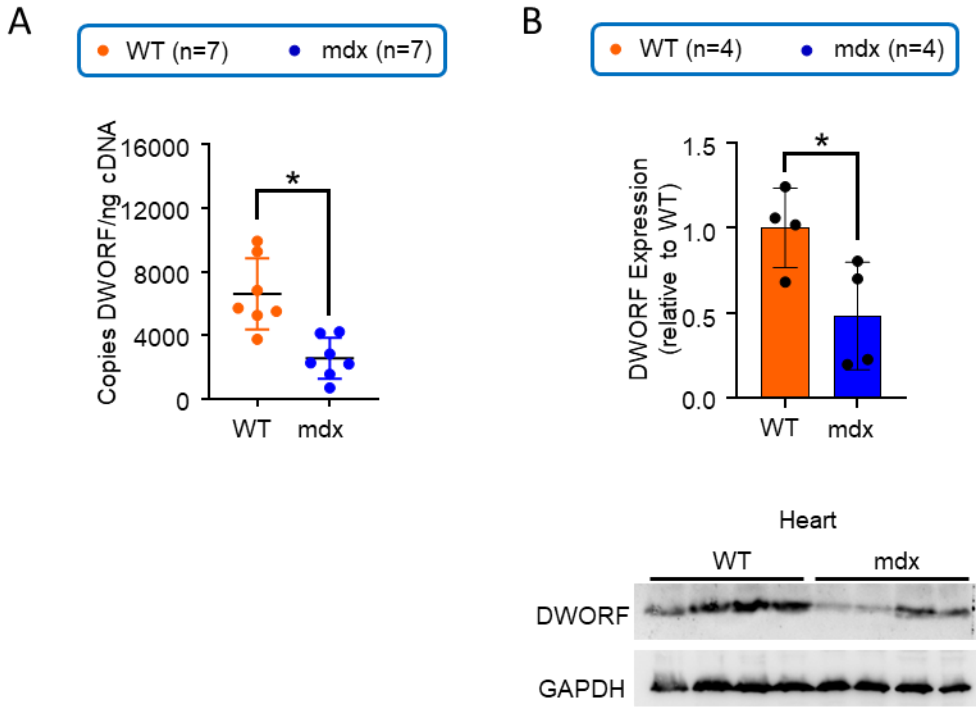

Figure 2.1. DWORF expression was decreased in mdx mouse hearts. A, Quantification of DWORF transcript in wild type BL10 (WT) and mdx hearts. **B,** Quantification of DWORF protein expression by western blot. The bottom panel shows western blot images, and the top panel shows densitometry results. *$p<0.05$.

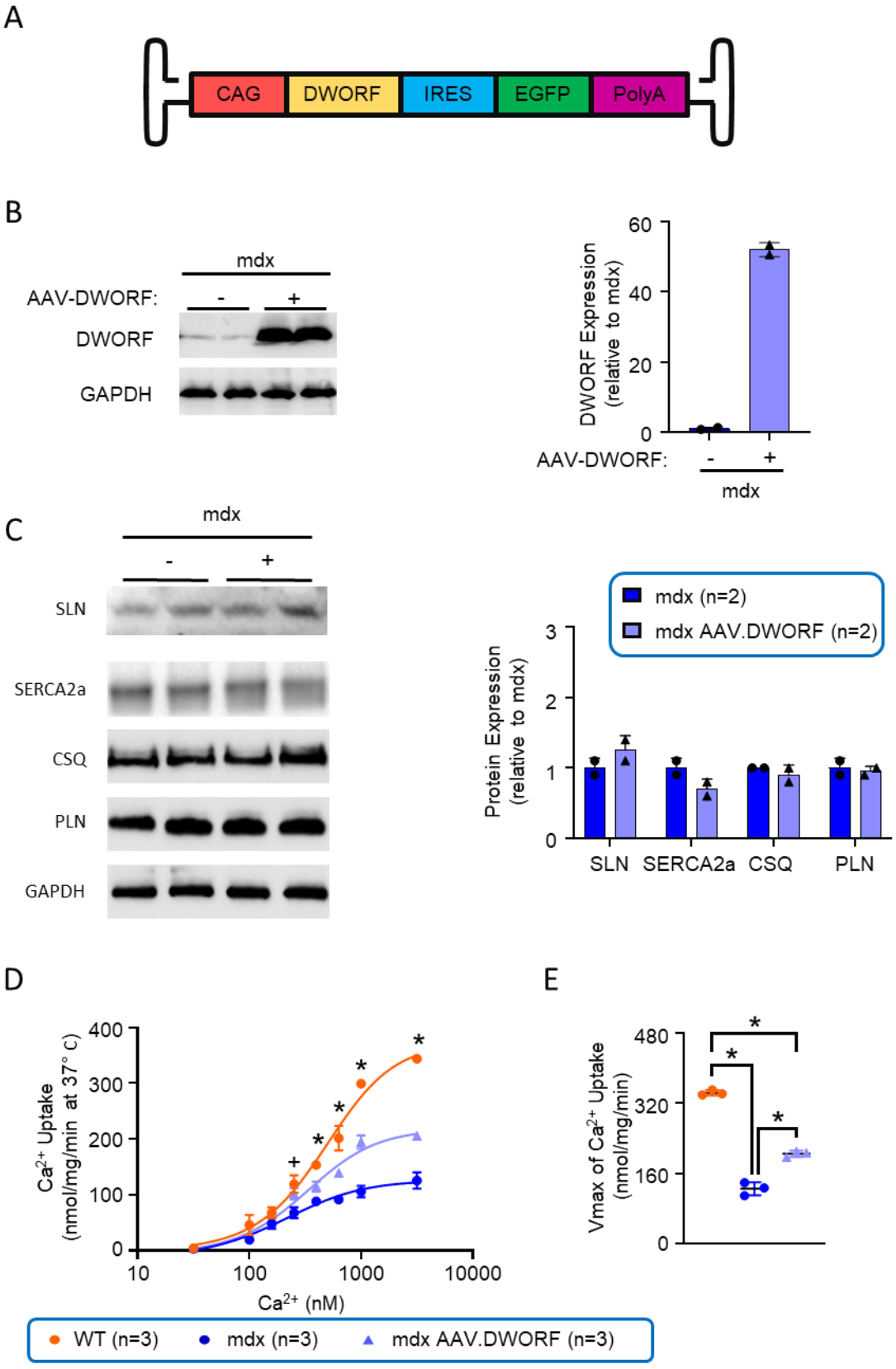
A
CAG
DWORF
IRES
EGFP
PolyA
B
mdx
AAV-DWORF:
-
+
DWORF
GAPDH
DWORF Expression (relative to mdx)
60
40
20
0
AAV-DWORF:
-
+
mdx
C
mdx
-
+
SLN
SERCA2a
CSQ
PLN
GAPDH
mdx (n=2)
mdx AAV.DWORF (n=2)
Protein Expression (relative to mdx)
3
2
1
0
SLN
SERCA2a
CSQ
PLN
D
Ca2+ Uptake (nmol/mg/min at 37° C)
400
300
200
100
0
10
100
1000
10000
Ca2+ (nM)
WT (n=3)
mdx (n=3)
mdx AAV.DWORF (n=3)
E
Vmax of Ca2+ Uptake (nmol/mg/min)
480
320
160
0

Figure 2.2. AAV.DWORF delivery increased DWORF expression and sarcoendoplasmic reticulum (SR) calcium uptake in mdx hearts. A, Schematic drawing of the AAV.DWORF vector. **B,** Quantification of DWORF protein expression by western blot. The left panel shows western blot images, and the right panel shows densitometry results. **C,** Quantification of the expression of various calcium-handling proteins. The left panel shows western blot images, and the right panel shows densitometry results. Please note SERCA2a and sarcolipin (SLN) blots were run with one set of lysates while calsequestrin (CSQ) and phospholamban (PLN) were run with another. **D,** Heart SR calcium uptake curve. **E,** Maximum rate of calcium uptake in the heart (V_{max}). *$p<0.05$ between all compared groups, +$p<0.05$ between mdx and all other groups but there is no statistically significant difference between wild type BL10 (WT) and AAV.DWORF-treated mdx mice.

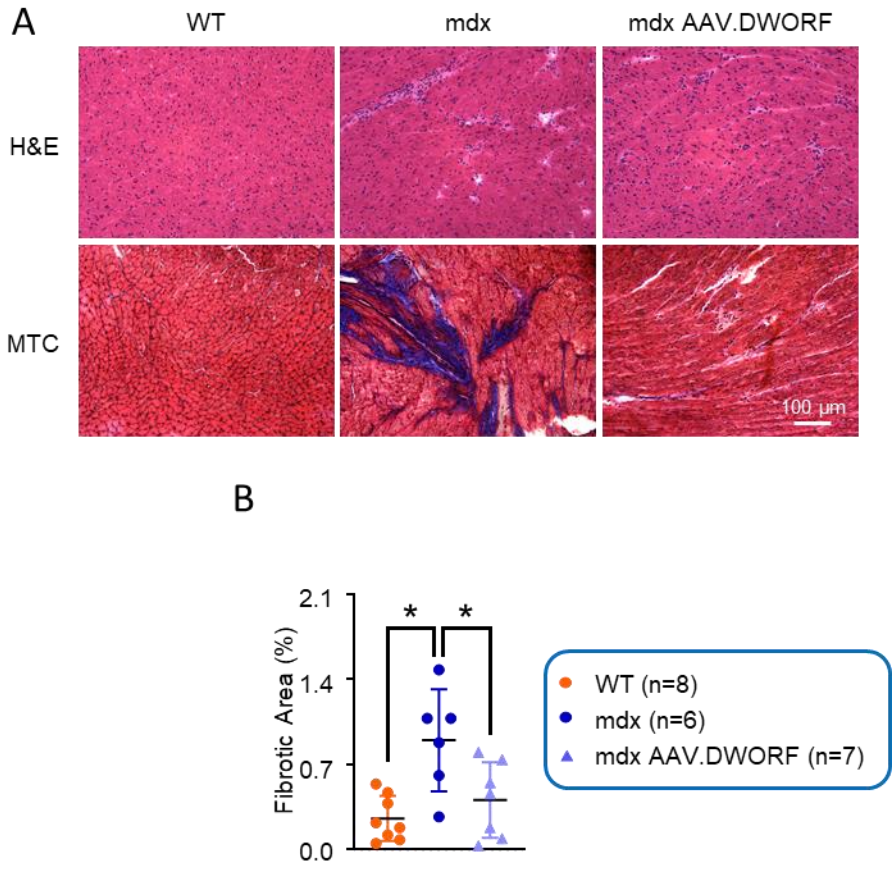

Figure 2.3. AAV.DWORF delivery ameliorated fibrosis in treated mdx mice. A, Representative photomicrographs of hematoxylin (H&E) and Masson's trichrome (MTC) staining from wild type BL10 (WT), mdx, and AAV.DWORF-treated mdx mouse ventricles. **B,** Quantification of the fibrotic area in the ventricles. *$p<0.05$.

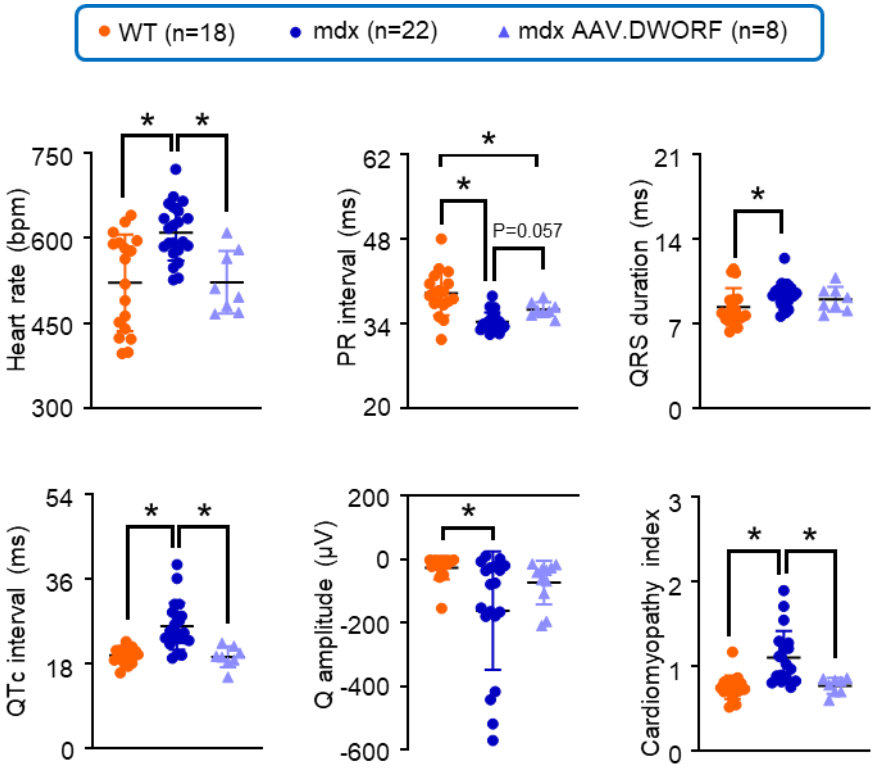

Figure 2.4. AAV.DWORF delivery improved ECG. ECG evaluation of heart rate, PR interval, QRS duration, QTc interval, Q amplitude, and cardiomyopathy index. *p<0.05.

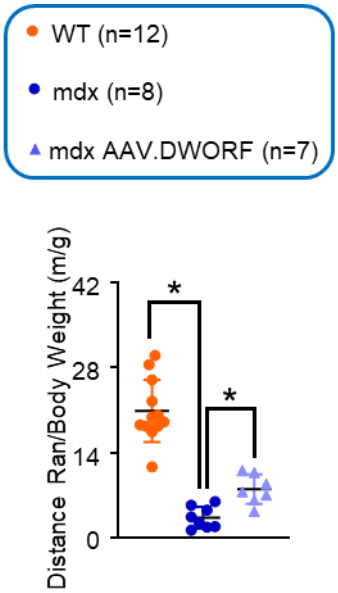

Figure 2.5. AAV.DWORF delivery improved uphill treadmill running. Total distance ran on a 7° uphill treadmill normalized by mouse body weight. *p<0.05.

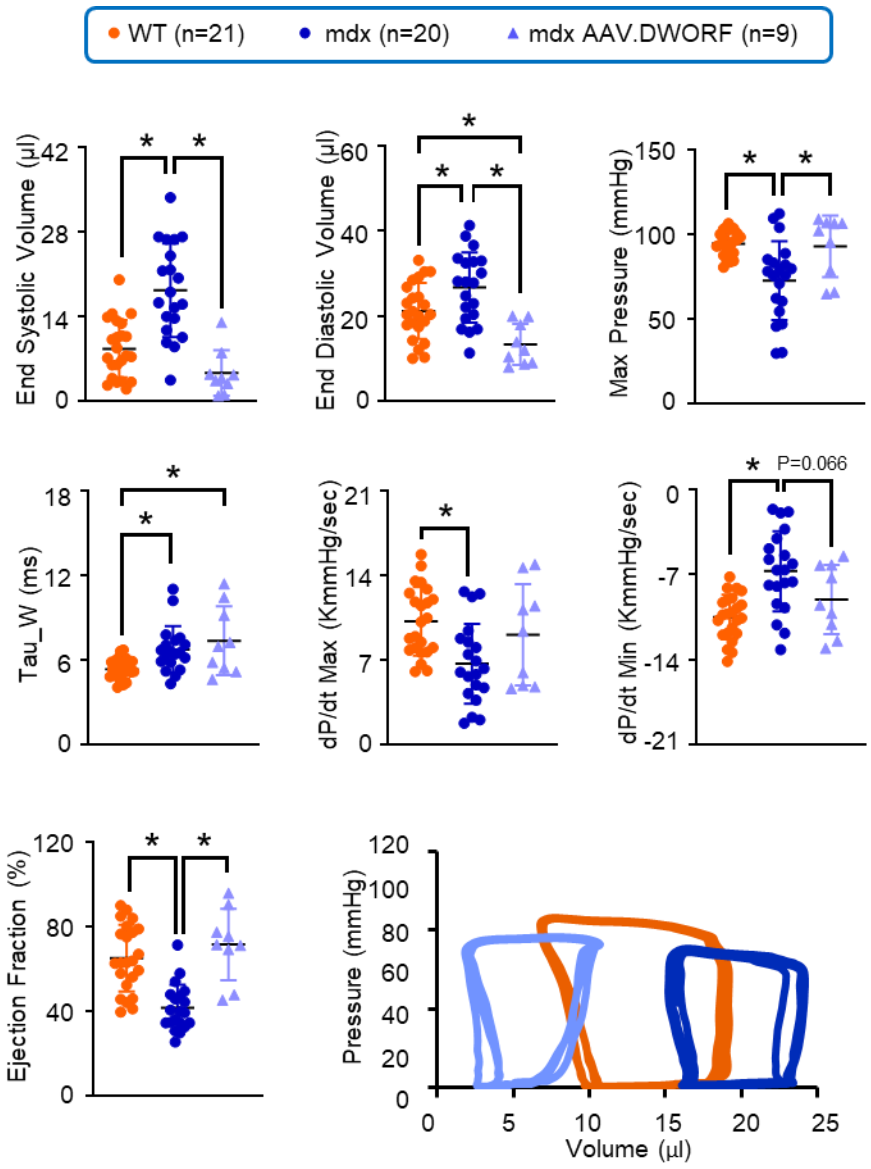

Figure 2.6. AAV.DWORF delivery improved left ventricular hemodynamics.

Evaluation of left ventricular hemodynamics, including the end-systolic volume, end-diastolic volume, maximum pressure, ejection fraction, time constant of left ventricular relaxation (Tau), dP/dt max, and dP/dt min. Representative pressure-volume loops from wild type BL10 (WT), mdx, and AAV.DWORF-treated mdx mice (bottom right panel). *p<0.05.

Tables

Table 2.1. Weights and weight ratios

	Wildtype	mdx	mdx AAV.DWORF
Sample Size (N)	15	15	11
BW (g)	28.24 ± 4.64	23.17 ± 3.07*	22.67 ± 4.81*
HW (mg)	98.87 ± 14.43	104.8 ± 18.6	104.6 ± 27.6
VW (mg)	94.11 ± 14.79	100.8 ± 18.3	101.2 ± 27.9
Tibia Length (mm)	18.17 ± 0.47	18.72 ± 0.53*	18.57 ± 0.55*
TW (mg)	33.07 ± 5.62	28.57 ± 7.47*	27.29 ± 8.04*
HW/BW (mg/g)	3.52 ± 0.74	4.53 ± 0.68*	4.61 ± 0.60*
HW/ Tibia Length	5.44 ± 0.91	5.58 ± 1.06	5.63 ± 1.39
TW/BW (mg/g)	1.18 ± 0.28	1.23 ± 0.31	1.21 ± 0.23
HW/TW (mg/g)	3.00 ± 0.44	3.72 ± 0.95*	3.85 ± 0.83*
VW/BW (mg/g)	3.35 ± 0.72	4.36 ± 0.68*	4.46 ± 0.55*
VW/ Tibia Length	5.18 ± 0.93	5.38 ± 1.05	5.44 ± 1.41
VW/TW (mg/g)	2.86 ± 0.42	3.58 ± 0.91*	3.73 ± 0.78*

*, significantly different from WT

Abbreviations: ***BW****, body weight;* ***HW****, heart weight;* ***TL****, tibia length;* ***TW****, tibialis muscle weight;* ***VW****, ventricle weight.*

Chapter 3. DWORF overexpression using AAV gene therapy induces ventricular sarcolipin expression and cardiac defects in mice

Emily D. Morales[1], Yongping Yue[1], Thais B. Watkins[1], Jin Han[1], Xiufang Pan[1], Aaron M. Gibson[2], Catherine A. Makarewich[2, 3], Gopal J. Babu[4], Dongsheng Duan[1, 5, 6, 7 *]

[1], Department of Molecular Microbiology and Immunology, School of Medicine, The University of Missouri, Columbia, MO 65212

[2], The Heart Institute, Division of Molecular Cardiovascular Biology, Cincinnati Children's Hospital Medical Center, Cincinnati, OH, 45229

[3], Department of Pediatrics, The University of Cincinnati College of Medicine, Cincinnati, OH 45229

[4], Department of Cell Biology and Molecular Medicine, Rutgers, New Jersey Medical School, Newark, NJ 07103

[5], Department of Biomedical, Biological & Chemical Engineering, College of Engineering, The University of Missouri, Columbia, MO 65212

[6], Department of Neurology, School of Medicine, The University of Missouri, Columbia, MO 65212

[7], Department of Biomedical Sciences, College of Veterinary Medicine, The University of Missouri, Columbia, MO 65212

Abstract

Heart disease remains a leading cause of death worldwide. It is becoming more apparent that improper calcium handling in cardiac muscle cells plays a role. The sarcoendoplasmic reticulum calcium ATPase (SERCA) is a calcium pump responsible for moving calcium from the cytosol to the sarcoplasmic reticulum (SR) during muscle relaxation. Reduced SERCA activity has been implicated in multiple models of heart failure and muscle disease. Dwarf open reading frame (DWORF) is a newly discovered micro-peptide activator of SERCA. Studies show DWORF therapy can mitigate the effects of heart disease in several mouse models of cardiomyopathy. Despite these promising results, recent studies have also shown over-activation of SERCA can cause increased SR calcium leak and cardiac arrhythmias. To test whether DWORF overexpression using AAV gene therapy can cause cardiac defects, we delivered 6×10^{12} vg particles/mouse of the AAV9.DWORF vector to 6-week-old wildtype mice by tail vein injection. Wildtype mice naturally express higher levels of DWORF than the cardiomyopathy models where DWORF therapy was studied. Mice were examined at 18 months of age. We found several ECG and left ventricular hemodynamic parameters were worsened following treatment. To our surprise, AAV DWORF gene therapy induced expression of the SERCA inhibitor sarcolipin in the ventricles, leading to a reduction in SR calcium uptake in the presence of high calcium concentrations. Our results suggest supraphysiological levels of DWORF expression can lead to cardiac defects, and DWORF and sarcolipin are co-regulated in healthy hearts. These findings

emphasize the importance of balancing SERCA activation and inhibition as the number of studies testing DWORF therapy for heart disease continues to rise.

Introduction

Dwarf open reading frame (DWORF) is a small peptide activator of the sarcoendoplasmic reticulum calcium ATPase (SERCA), a pump that resides in muscle cells and is responsible for moving cytosolic calcium to the sarcoplasmic reticulum (SR) during muscle relaxation(Nelson et al., 2016). DWORF is naturally expressed in cardiac and slow-twitch skeletal muscle and is the only known endogenous peptide activator of SERCA. Early studies suggest DWORF enhances SERCA function indirectly by attaching to the pump and preventing the binding of other small peptide SERCA inhibitors such as phospholamban (PLN) and sarcolipin (SLN)(Makarewich et al., 2018; Nelson et al., 2016; Singh, Dalton, Cho, Pribadi, Zak, Šeflová, et al., 2019). More recent studies have contested this idea and show DWORF directly enhances SERCA function(Fisher et al., 2021; Reddy et al., 2022b). It is possible DWORF functions via multiple mechanisms.

It is becoming more apparent that reduced SERCA activity contributes to heart failure and muscle diseases such as Duchenne muscular dystrophy (DMD)(Denniss et al., 2020; Mareedu, Million, et al., 2021; Zhihao et al., 2020). Recent studies show increasing DWORF expression, and thus enhancing SERCA function, improves cardiac function in multiple mouse models of heart failure and one mouse model of DMD **(Chapter 2)**(Makarewich et al., 2020; Makarewich et al., 2018). In these studies, DWORF was expressed through a transgenic approach or by using adeno-associated virus (AAV) gene delivery and improved cardiac function and left ventricular dilation and fibrosis.

Despite the recent advances in our knowledge of the SERCA-DWORF interaction and its role in heart disease, concerns remain about the safety of DWORF delivery and SERCA over-activation. Although enhanced SERCA function increases SR calcium load and improves cardiac function, over-activation may also lead to increased SR calcium leak and cardiac arrhythmias(Sato et al., 2021). In addition, increasing SERCA function through total ablation of individual SERCA inhibitors worsened muscle function in the mdx mouse model of DMD(Fajardo et al., 2017; Law et al., 2018). Ablation of PLN improved calcium handling and myocardial contractility but worsened overall cardiac function and fibrosis, while ablation of SLN worsened disease parameters in the skeletal muscle. We hypothesize delivery of supraphysiological levels of DWORF will produce a similar decline in cardiac function and histology.

To test the effects of exceedingly high levels of DWORF, we delivered our previously tested DWORF expression cassette with AAV serotype 9 (AAV9) to 6-week-old wild-type (WT) mice, whose DWORF levels are already high compared with previously studied cardiac failure models. Injections were delivered intravenously through the tail vein. By 6 months, DWORF expression was ~10-fold higher in treated mice compared with untreated WT mice. At 18 months of age, we analyzed electrocardiography (ECG), uphill treadmill running, left ventricular hemodynamics, and cardiac fibrosis in WT and treated WT mice. In support of our hypothesis, AAV9 DWORF delivery worsened several ECG and hemodynamic parameters. To our surprise, DWORF delivery induced SLN expression in the ventricles, despite SLN being known as an atrial chamber-specific protein in healthy mouse hearts(Babu et al., 2007; Minamisawa et al., 2003). Supporting this finding, DWORF delivery also reduced SR

calcium uptake in the presence of high levels of calcium. No notable differences were detected in uphill treadmill running capability, heart anatomy, or fibrosis. Our results confirm supraphysiological levels of DWORF expression can cause cardiac defects and are the first to show a feedback mechanism in non-diseased hearts, where increased expression of DWORF is countered with an upregulation of SLN. These findings bring to light the importance of treatment dose and design to avoid SERCA over-activation during the use of future DWORF therapies for cardiac failure.

Results

AAV.DWORF delivery increased DWORF expression but decreased SR calcium uptake in WT mice. Before evaluating the effects of DWORF gene therapy, we performed western blot analysis and SR calcium uptake measurements of heart tissue to ensure successful DWORF expression **(Figure 3.1)**. The gene therapy vector was packaged into AAV.9 and contained codon-optimized mouse DWORF cDNA under the control of a ubiquitous CAG promoter **(Figure 3.1A)**. To monitor AAV transduction, enhanced green fluorescent protein (EGFP) was also included under the control of an internal ribosomal entry site (IRES). Mice were injected at 6 weeks of age at a dose of 6 x 10^{12} vector genome particles (vg)/mouse via the tail vein. As discussed in Chapter 2, EGFP was not expressed due to unknown reasons (data not shown). At 6 months of age, injected mice exhibited an ~10-fold increase in DWORF expression compared with un-injected WT control mice **(Figure 3.1B)**.

Surprisingly, SR calcium uptake was significantly reduced in treated mice at high calcium concentrations **(Figure 3.1C).** The maximum velocity of calcium uptake was also significantly decreased **(Figure 3.1D)**.

AAV.DWORF delivery induced endogenous SLN expression in the ventricles. Next, we performed western blot analysis to assess whether DWORF gene therapy altered expression of other calcium handling proteins. No significant changes were detected in protein levels of the SERCA isoform found in the heart (SERCA2a), calsequestrin

(CSQ), or phospholamban (PLN) **(Figure 3.2A)**. Although SLN is believed to be an atria chamber-specific protein, DWORF gene therapy induced expression of SLN in the ventricles **(Figure 3.2B)**.

AAV.DWORF increased heart weight ratios but did not change myocardial fibrosis. After confirming vector delivery in treated mice, we evaluated the effects of DWORF gene therapy on cardiac tissue at 18 months of age. 18 months was selected because of the additional pressure placed on mouse hearts at old age. No differences were detected in heart weight or ventricular weight between WT and treated WT mice **(Table 3.1)**. However, significant differences were detected when heart weight and ventricular weight were normalized by body weight or weight of the tibialis anterior skeletal muscle (TA). Histological examination performed by Masson trichrome staining revealed no differences in quantified fibrosis between WT and treated groups **(Figure 3.3)**.

DWORF therapy in WT mice does not affect uphill treadmill running capability. To test the effects of DWORF overexpression on cardiac function, we first performed uphill treadmill running. This method is commonly used to evaluate heart function(Bernstein, 2003; Bostick et al., 2009; Wasala et al., 2020). To begin, we acclimated and trained mice within the treadmill for 5 days. On day 6, we quantified mouse running distance on a 7° uphill incline normalized by body weight (meters/g body weight) **(Figure 3.4)**. Both WT control and treated WT mice ran an average of ~21 m/g.

AAV.DWORF therapy in WT mice leads to abnormalities in ECG. Next, we tested the effects of DWORF gene therapy on ECG. DWORF-injected mice exhibited worsening of several ECG parameters including PR interval, QRS duration, and cardiomyopathy index **(Figure 3.5)**. QTc interval was also worsened in injected mice but did not reach statistical significance (p=0.084).

DWORF therapy in WT mice leads to dysfunction in left ventricular hemodynamics. Following ECG analysis, we tested the effects of DWORF overexpression on left ventricular hemodynamics using a catheter to record pressure and volume data **(Figure 3.6)**. End systolic volume, ejection fraction, and dP/dt maximum were all worsened in DWORF-injected mice.

Discussion

In the present study, we examined the effects of delivering supraphysiological levels of AAV9.DWORF gene therapy to healthy WT mice, whose DWORF levels are already elevated compared with several models of heart failure(Makarewich et al., 2020; Makarewich et al., 2018). This study was designed in response to the increased use of DWORF overexpression in mouse heart failure models and the emerging evidence suggesting SERCA over-activation may lead to SR calcium leak, cardiac arrhythmias, and/or worsened muscle function(Fajardo et al., 2017; Law et al., 2018; Sato et al., 2021). In support of this evidence, we found that DWORF overexpression in WT mice led to a decline in multiple ECG and left ventricular hemodynamic parameters **(Figures 3.5 to 3.6)**. To our surprise, DWORF gene therapy induced SLN expression in the ventricles, despite SLN being known as an atrial chamber-specific protein in healthy mouse hearts(Babu et al., 2007; Minamisawa et al., 2003)**(Figure 3.2B)**. To back this finding, our measurements show a reduction in SERCA calcium uptake at high calcium concentrations **(Figure 3.1C)**. No differences were found in uphill treadmill running distance, heart anatomy, or heart fibrosis. Our results suggest (1) delivery of supraphysiological levels of DWORF may lead to cardiac defects in mouse hearts and (2) a feedback mechanism exists within mouse ventricles to induce SLN expression in the presence of an overabundance of DWORF. As the number of studies utilizing DWORF gene therapy in cardiac failure models continues to rise, these findings highlight the importance of balancing SERCA activation/inhibition when designing DWORF or other SERCA-targeting therapies.

Proper intracellular calcium cycling is critical to striated muscle function. To initiate muscle contraction, calcium is released from the SR and enters the cytosol via the ryanodine receptor. Once in the cytosol, calcium binds to contractile proteins and a contraction ensues. Calcium is then returned to the SR by SERCA to initiate relaxation. Reduced SERCA function has been implicated in many muscle diseases. DWORF down-regulation is evident in several mouse models of heart disease, including a model of myocardial infarct, a genetic model of dilated cardiomyopathy caused by a loss of muscle-specific LIM protein, and the mdx mouse model of Duchenne muscular dystrophy (DMD)(Makarewich et al., 2020; Makarewich et al., 2018). DWORF mRNA is also downregulated in ischemic failing human hearts(Nelson et al., 2016).

The emerging knowledge of DWORF's role in various muscle diseases makes DWORF delivery a promising therapeutic option for multiple conditions. However, data suggesting SERCA overactivation is damaging to muscle mechanics is also surfacing. The present study is the first to show decreased SR calcium uptake and damaging cardiac effects following the delivery of AAV DWORF to cardiac tissues. This is at first glance contradictory to the findings of Nelson et al., who show transgenic (Tg) mice overexpressing DWORF have increased SR calcium uptake compared to WT mice in the presence of low calcium concentrations in the heart(Nelson et al., 2016). However, SLN expression and the degree of DWORF overexpression in these Tg mice is unknown. In the present study, DWORF protein was increased by ~10-fold in mice treated with AAV DWORF gene therapy. It is possible that either (1) DWORF expression in Tg mice is low enough to increase SR calcium uptake without prompting SLN expression or (2) DWORF expression in Tg mice is high enough to overcome SLN expression through

increased DWORF competition. Future studies are needed to assess the outcomes of different DWORF dosages, as this may affect the balance of SERCA activation/inhibition.

The upregulation of SLN following AAV DWORF delivery indicates for the first time that DWORF and SLN expression are by some means co-regulated. Some sources have suggested that although SLN upregulation can negatively affect muscle function, it can also serve as a beneficial response to calcium overload and disease. It does so by allowing calcium signals to stimulate adaptive mitochondrial biogenesis, skeletal muscle fiber type switching, and muscle hypertrophy(Chambers et al., 2022). At what point and why SLN expression occurred in response to DWORF upregulation is difficult to pinpoint. More work needs to be done to determine the mechanisms by which SERCA inhibitors and DWORF are regulated and to elucidate an optimal degree of SERCA activation.

It is likely that the unknown factors controlling the expression of SERCA inhibitors and DWORF are altered in diseases such as DMD. In Chapter 2, where we delivered the same AAV DWORF construct at the same dose (6×10^{12} vs/mouse) to the mdx mouse model of DMD, SLN upregulation was not observed. This suggests that the feedback mechanism between DWORF and SLN is altered in this disease state. Further elucidating the mechanisms behind the expression and regulation of SERCA inhibitors and DWORF may help identify future therapeutic targets.

In summary, our study demonstrates for the first time that supraphysiological expression of DWORF using AAV gene therapy can cause cardiac defects and induce SLN expression in the ventricles of WT mice. These findings highlight the importance of

balancing SERCA activation and inhibition through therapy design and dose during the use of DWORF and other SERCA-regulating therapies for heart failure.

Materials and Methods

Mice. Due to the differences in male and female cardiac function, female mice were used in all studies. All experiments were approved by the institutional animal care and use committee. Mice were contained in a specific pathogen-free animal care facility with continuous access to food and water. Lights in this facility were on a 12-hour light, 12-hour dark schedule (25 lux). WT control (C57BL/10ScSnJ, stock number 000476) mice were purchased from The Jackson Laboratory (Bar Harbor, ME).

AAV production and administration. AAV9 preparation was completed and purified through two rounds of isopycnic ultracentrifugation according to previously published methods(J. H. Shin et al., 2012). The *cis*-plasmid for AAV packaging contained codon-optimized mouse DWORF cDNA under the control of a CAG ubiquitous promoter followed by the EGFP gene under the control of the encephalomyocarditis virus IRES (Clontech, Mountain View, CA). The DWORF gene was synthesized by GenScript (Piscataway, NJ). Virus was delivered intravenously to the tail vein at 6 weeks of age at a concentration of 6×10^{12} vg/mouse.

Western blot. For DWORF western blots, fresh mouse hearts were snap-frozen in liquid nitrogen prior to homogenization in assay buffer (150 mM NaCl; 1% v/v igepal CA-630; 50 mM Tris-Cl, pH 8.3; 0.5% w/v sodium deoxycholate; 0.1% w/v sodium dodecyl sulfate) with added protease inhibitors (cOmplete ULTRA mini-tablet, Roche,

Indianapolis, IN). 40 μg of lysate was run on standard 15% bis/acrylamide gels and then transferred by wet transfer technique to PVDF membranes (Millipore, Immoblion-P). A previously used, custom polyclonal DWORF antibody (New England Peptide) was used to incubate membranes at a concentration of 1:1000(Nelson et al., 2016). Membranes were then incubated in a goat anti-rabbit IgG-HRP secondary antibody and developed using ClarityTM Western ECL chemiluminescent substrate (Bio-Rad, Hercules, CA) and a digital Bio-Rad ChemiDocTM MP Imaging System.

For other western blots, snap-frozen hearts were homogenized in lysis buffer (50 mM Tris, pH 7.4, 150 mM NaCl, 1 mM EDTA, and 0.5% NP-40) with added 1 mmole PMSF, 5 mmole NaVO3, 10 nmole Okadaic Acid, 1 mmole NaF, and 1 mmole benzamidine. Lysates were run on sodium dodecyl sulfate-polyacrylamide gels, electroblotted onto PVDF membranes, and incubated with antibodies for SLN (anti-rabbit, 1:3000), SERCA2a (anti-rabbit, 1:5000, custom made)(Babu et al., 2007), PLN (anti-rabbit, 1:3000, custom made)(Babu et al., 2007), CSQ (anti-rabbit, 1:5000, Affinity BioReagents, Golden, CO)(Babu et al., 2007), or GAPDH (anti-mouse, 1:10,000, Sigma, St. Louis, MO).

All densitometry quantification was completed using ImageJ/Fiji Software (ImageJ 1.48b) and normalized to levels of GAPDH.

SR calcium uptake. A previously described Millipore filtration technique was used to measure SR calcium uptake(Voit et al., 2017). Snap-frozen heart tissue was used for protein extraction. Approximately 150 μg was incubated at 37° C in 1.5 ml of calcium

uptake medium (40 mM imidazole, pH 7.0, 100 mM KCl, 5 mM MgCl2, 5 mM NaN3, 5 mM potassium oxalate, and 0.5 mM EGTA) and various concentrations of CaCl2 to yield 0.03–3 μM free calcium. Ruthenium red was added to a final concentration of 1 μmole immediately before adding substrates to begin calcium uptake, and a final concentration of 5 mmole ATP was added to initiate the reaction. At 1 minute, the reaction was terminated by filtration. Non-linear curve fitting analysis was used to determine the rate of SR calcium uptake and the calcium concentration required for EC50 using GraphPad Prism v6.01 software (GraphPad, San Diego, CA).

ECG and hemodynamic assay. ECG was performed using a 12-lead ECG approach. The commercial system used was acquired from AD Instruments (Colorado Springs, CO). All parameters except for Q wave amplitude were analyzed using lead II data. Q wave amplitude was determined from lead I data. Results were evaluated using the standard operating protocol outlined in "Cardiac protocols for Duchenne animal models" (http://www.parentprojectmd.org/site/PageServer?pagename=Advance_researchers_sops) (Duan et al., 2016). QTc interval was calculated according to methods described by Mitchell et al (Mitchell et al., 1998a), where QT interval is corrected for heart rate. Cardiomyopathy index was calculated by dividing the QT interval by the PQ segment(Bostick et al., 2011).

Hemodynamics was also performed using a previous protocol described in "Cardiac protocols for Duchenne animal models"(Duan et al., 2016). A Millar catheter was inserted to the left ventricle and used to record pressure-volume loops. Loops were analyzed using PVAN software (Millar Instruments, Houston, TX). Cardiac relaxation

time constant (Tau) was calculated according to Weiss et al(Weiss et al., 1976), and body surface area was calculated as described by Cheung et al(Cheung et al., 2009).

Treadmill running. Uphill treadmill running was conducted according to the protocol presented in Chapter 2. Mice were trained for five days to run on a 7° uphill treadmill (Columbus Instruments, Columbus, OH, USA). Throughout training, mice were encouraged to run by gentle nudging with a ruler. On day 6, mice were run until the point of exhaustion, and results were recorded as the distance ran/mouse body weight. On the day of recording, mice ran for 5 minutes at a speed of 5 m/min. The speed of the treadmill was then increased by 5 m/min every 5 minutes until the point of exhaustion. Exhaustion was determined as the point when a mouse exited the treadmill and did not re-enter for three seconds, even with gentle nudging.

Morphological studies. OCT-embedded heart tissues were used to create 10 μm cryosection samples. Fibrosis was examined and quantified from Masson trichrome stained slides, which were stained using the Masson Trichrome Stain Kit (Epredia, Kalamazoo, MI). Percent fibrotic area of entire heart sections was determined by dividing the area of blue staining by the total tissue area using ImageJ/Fiji Software (ImageJ 1.48b). General heart histology was examined by hematoxylin and eosin (H&E) staining.

Statistical analysis. Data are presented as mean ± stand error of mean. Unpaired t-test was used for all two-group comparisons. Statistical analyses were performed using GraphPad PRISM software version 9.1.2 (GraphPad Software, La Jolla, California). A $p < 0.05$ was considered statistically significant.

Acknowledgements

Conceived and designed experiments: EM, XP, and DD. Performed the experiments: EM, YY, TL, JH, AG, CM, and GB. Wrote the paper: EM.

Figures

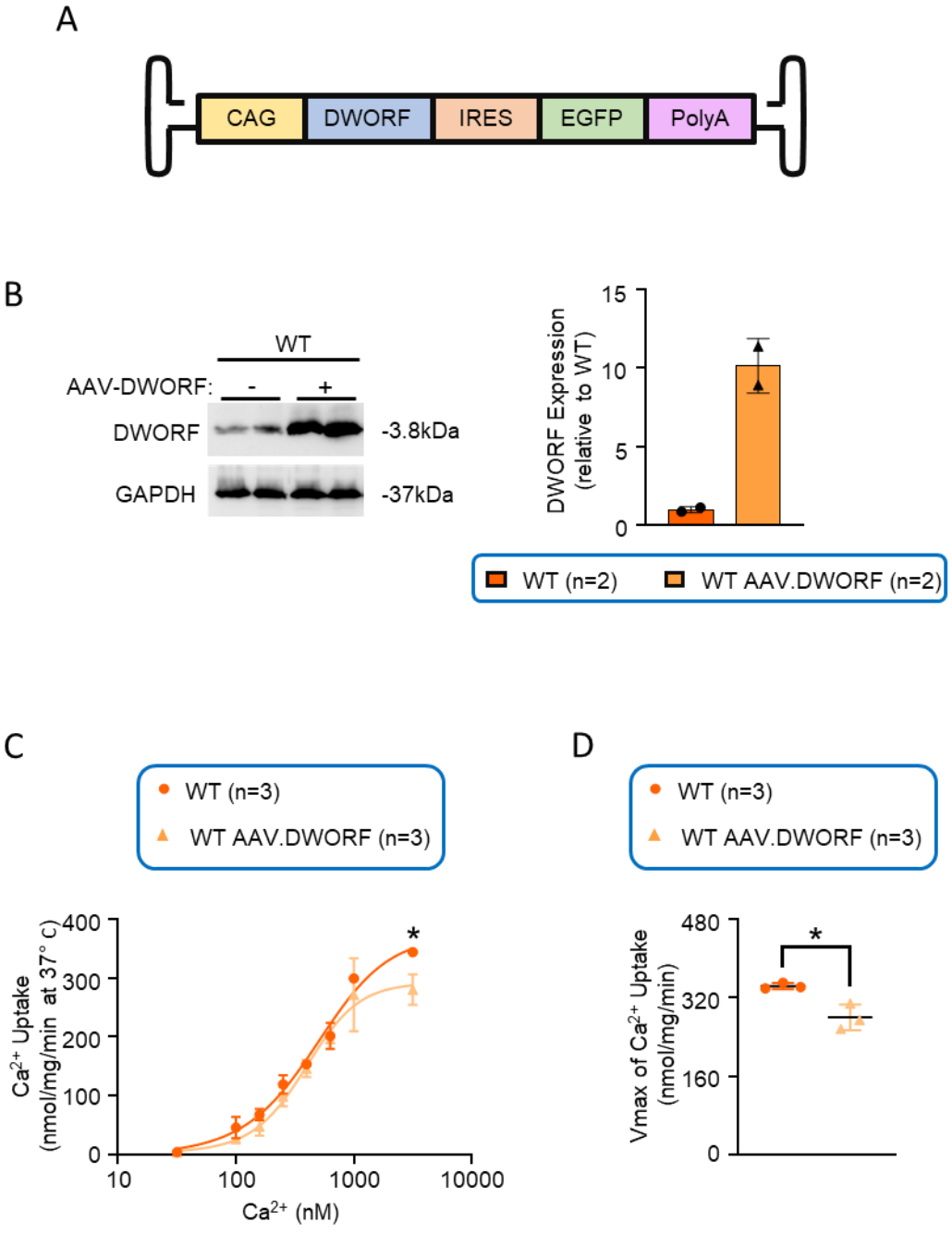

Figure 3.1. AAV.DWORF delivery increased DWORF expression and decreased sarcoendoplasmic reticulum (SR) calcium uptake in WT hearts. A, Schematic

drawing of the AAV.DWORF vector. **B,** Quantification of DWORF protein expression by western blot. The left panel shows western blot images, and the right panel shows densitometry results. **C,** Heart SR calcium uptake curve. **D,** Maximum rate of calcium uptake in the heart (V_{max}). *$p<0.05$ between all compared groups.

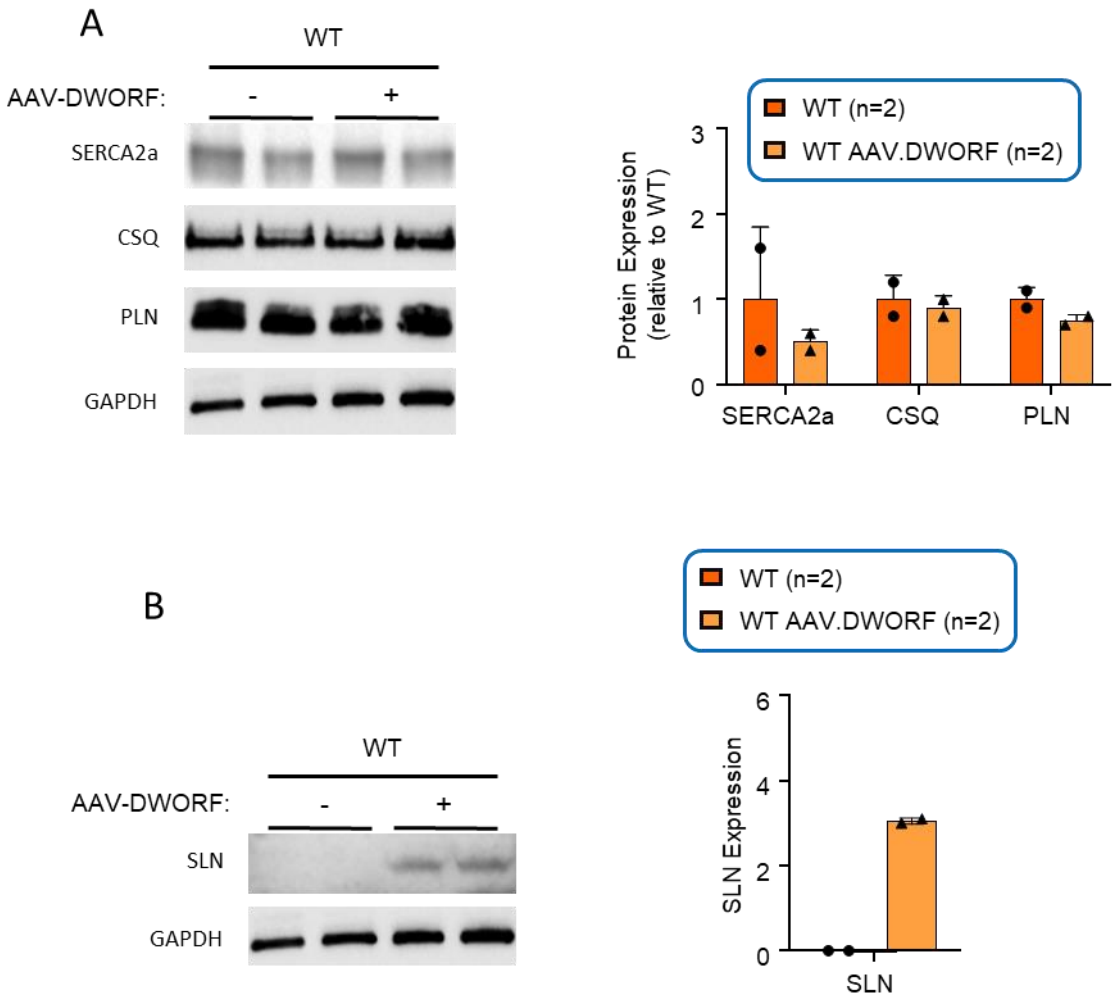

Figure 3.2. AAV.DWORF delivery induced sarcolipin expression in the ventricles. **A,** Quantification of the expression of various calcium-handling proteins. The left panel shows western blot images, and the right panel shows densitometry results. Please note SERCA2a and sarcolipin (SLN) (see Figure 3.2B) blots were run with one set of lysates while calsequestrin (CSQ) and phospholamban (PLN) were run with another. **B,** Quantification of SLN expression. The left panel shows the western blot image, and the right panel shows densitometry results. Please note SLN results are not relative to untreated WT, as no SLN was detected in these samples.

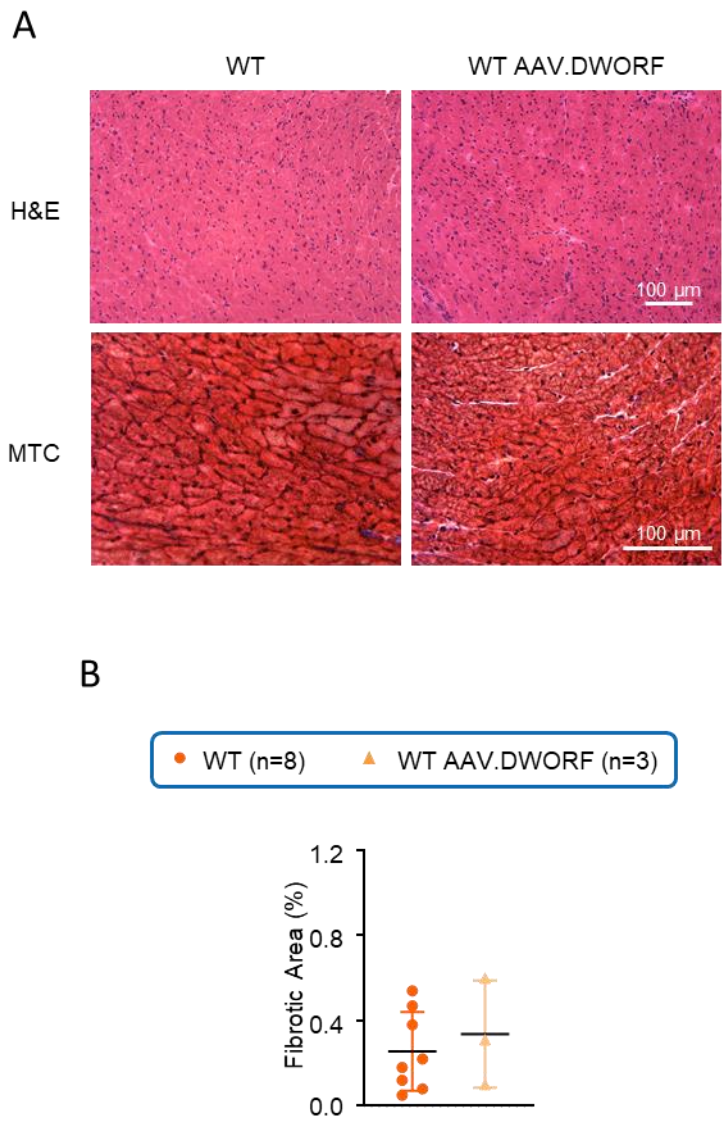

Figure 3.3. AAV.DWORF delivery had no effect on fibrosis in treated WT mice. A, Representative photomicrographs of hematoxylin (H&E) and Masson's trichrome (MTC) staining from WT and AAV.DWORF-treated WT mouse ventricles. **B,** Quantification of the fibrotic area in the ventricles. *$p<0.05$.

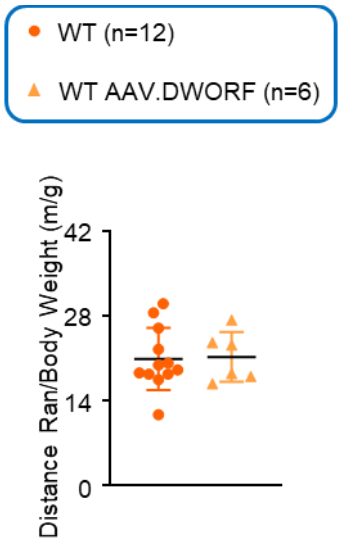

Figure 3.4. AAV.DWORF delivery did not affect uphill treadmill running. Total distance ran on a 7° uphill treadmill normalized by mouse body weight. *p<0.05.

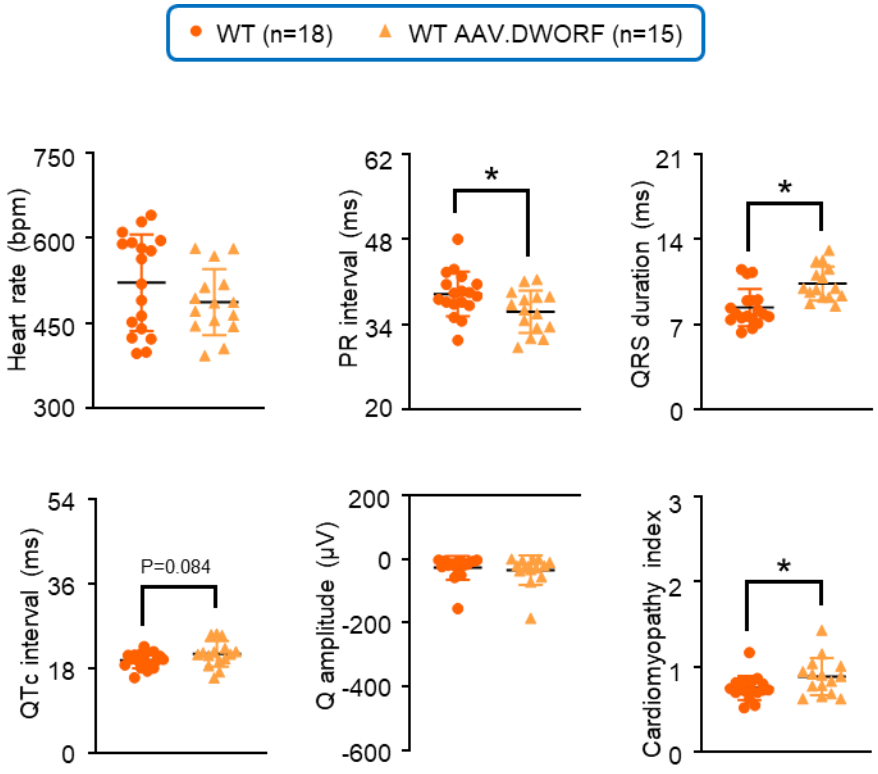

Figure 3.5. AAV.DWORF delivery worsened ECG. ECG evaluation of heart rate, PR interval, QRS duration, QTc interval, Q amplitude, and cardiomyopathy index. *p<0.05.

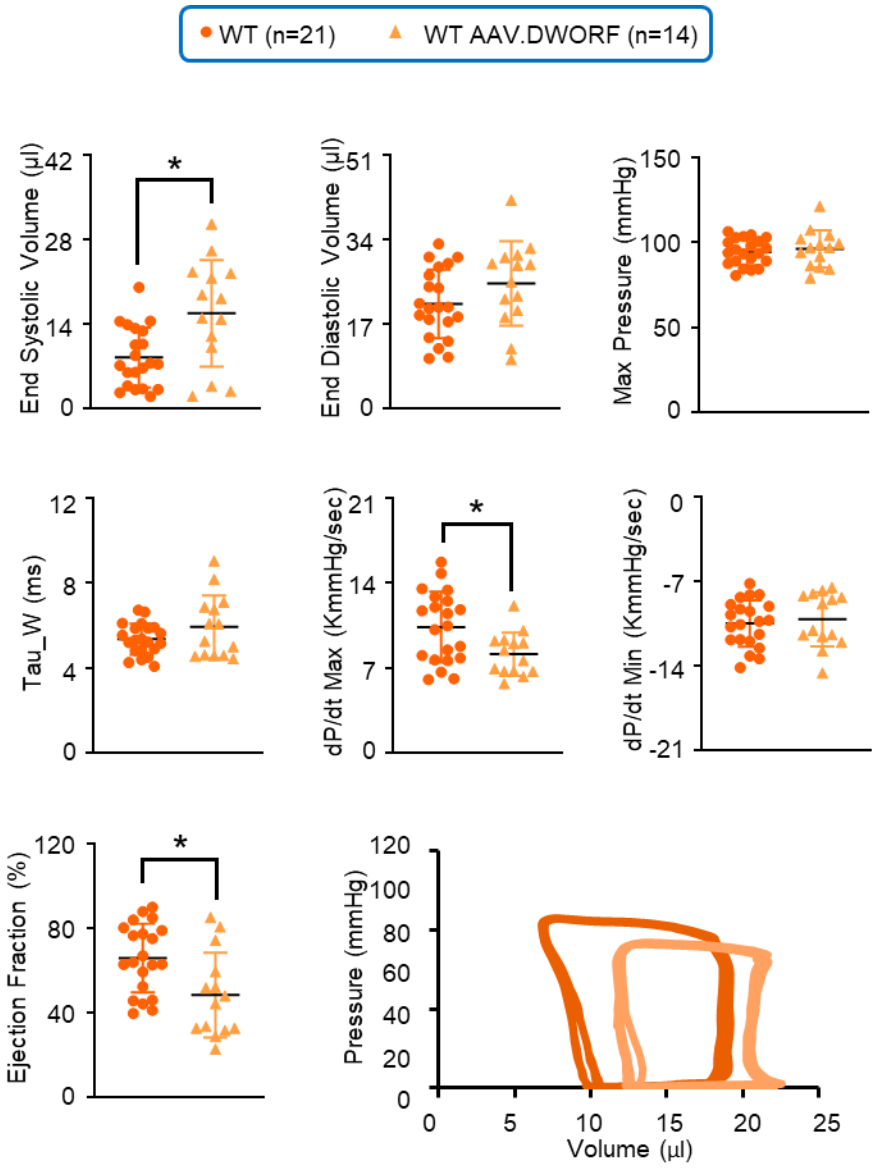

Figure 3.6. AAV.DWORF delivery worsened left ventricular hemodynamics.

Evaluation of left ventricular hemodynamics, including the end-systolic volume, end-diastolic volume, maximum pressure, ejection fraction, time constant of left ventricular relaxation (Tau), dP/dt max, and dP/dt min. Representative pressure-volume loops from WT and AAV.DWORF-treated WT mice (bottom right panel). *$p<0.05$.

Tables

Table 3.1. Weights and weight ratios

	WT	WT AAV.DWORF
Sample Size (N)	15	15
BW (g)	28.24 ± 4.64	27.48 ± 11.08
HW (mg)	98.87 ± 14.43	103.7 ± 23.9
TW (mg)	33.07 ± 5.62	32.46 ± 14.01
HW/BW (mg/g)	3.52 ± 0.74	3.85 ± 1.02[a]
TW/BW (mg/g)	1.18 ± 0.28	1.18 ± 0.37
HW/TW (mg/g)	3.00 ± 0.44	3.00 ± 0.44

[a], significantly different from WT

Abbreviations: ***BW***, *body weight;* ***HW***, *heart weight;* ***TW***, *tibialis muscle weight.*

Chapter 4: Dwarf open reading frame (DWORF) gene therapy did not rescue diaphragm function or histology in a mouse model of Duchenne muscular dystrophy

Emily D. Morales[1], Yongping Yue[1], Thais B. Watkins[1], Xiufang Pan[1], Aaron M. Gibson[2], Gwendolyn Bostick[1], Catherine A. Makarewich[2, 3], Dongsheng Duan[1, 4, 5, 6 *]

[1], Department of Molecular Microbiology and Immunology, School of Medicine, The University of Missouri, Columbia, MO 65212

[2], The Heart Institute, Division of Molecular Cardiovascular Biology, Cincinnati Children's
Hospital Medical Center, Cincinnati, OH, 45229

[3], Department of Pediatrics, The University of Cincinnati College of Medicine, Cincinnati, OH 45229

[4], Department of Cell Biology and Molecular Medicine, Rutgers, New Jersey Medical School, Newark, NJ 07103

[5], Department of Neurology, School of Medicine, The University of Missouri, Columbia, MO 65212

[6], Department of Biomedical Sciences, College of Veterinary Medicine, The University of Missouri, Columbia, MO 65212

Abstract

Duchenne muscular dystrophy (DMD) is the most common form of muscular dystrophy and is caused by an absence of the protein dystrophin in muscle. Without dystrophin, patients experience severe muscle weakness and degeneration. One cause for rapid degeneration is high calcium concentrations within the cytosol of DMD muscle fibers that activate cellular proteases and phospholipases. Dwarf open reading frame (DWORF) is a newly discovered activator of the sarco-endoplasmic reticulum calcium ATPase (SERCA), a pump responsible for moving cytosolic calcium into the sarcoplasmic reticulum (SR) of muscle cells. SERCA function is reduced in DMD. DWORF therapy has been shown to improve cardiomyopathy in several heart failure mouse models. Increasing SERCA activity is one avenue for clearing aberrant cytosolic calcium in DMD as well. Here, we show for the first time that DWORF transcript and protein levels are downregulated in mdx mouse skeletal muscle. Systemic delivery of 6 x 10^{12} vg/mouse of AAV9.DWORF vector to 6-week-old mice via the tail vein had no effect on diaphragm force production, myofiber size, or histology. Surprisingly, AAV DWORF delivery slowed the maximum rates of diaphragm contraction and relaxation and increased central nucleation in treated mdx, but not treated WT, mice. Our results implicate that DWORF downregulation is a contributor to reduced SERCA function in DMD skeletal muscle and that delivery of AAV DWORF gene therapy was unable to rescue muscle function and histology in treated mdx mice.

Introduction

Duchenne muscular dystrophy (DMD) is a rare genetic disorder characterized by severe muscle wasting(D. Duan et al., 2021). Patients with this disease die prematurely from cardiac or respiratory failure caused by the absence of an essential muscle protein called dystrophin. Phenotypes of the disease can be attributed, in part, to a dysregulation of intracellular calcium(Mareedu, Million, et al., 2021). Previous studies have revealed an increased concentration of cytosolic calcium in dystrophic muscle cells(Burr & Molkentin, 2015). It is well-documented that high cytosolic calcium levels contribute to cell death by activating calcium-dependent proteases and phospholipases that digest cellular proteins and membranes(Hopf et al., 1996a; Lindahl, Bäckman, et al., 1995; Spencer & Mellgren, 2002; Turner et al., 1988). Therefore, identifying therapeutic strategies aimed at clearing cytosolic calcium from dystrophic cells will have great impact.

One major source of aberrant cytosolic calcium in DMD is the sarcoplasmic reticulum (SR). This organelle acts as a calcium store and plays a large role in the contraction-relaxation cycle(Rossi & Dirksen, 2006). In healthy muscle cells, contraction begins as calcium exits the SR via the ryanodine receptor (RyR) and enters the cytosol, where it engages with contractile proteins. To initiate relaxation, calcium is pumped back into the SR by the sarco-endoplasmic reticulum calcium ATPase (SERCA). In dystrophic cells, this cycle is altered. Release of calcium to the cytosol is increased, while calcium re-uptake by SERCA is decreased(Bellinger et al., 2009; Fauconnier et al., 2010; Kargacin & Kargacin, 1996; Schneider et al., 2013a).

To reduce cytosolic calcium in dystrophic muscle cells, our lab previously delivered a dwarf open reading frame (DWORF) expression cassette with AAV serotype 9 (AAV9) to the mdx mouse model of DMD **(Chapter 2)**. DWORF is an endogenous micro-peptide SERCA enhancer, which is drastically downregulated in the mdx heart. We found delivery of AAV DWORF gene therapy at 6 weeks of age significantly improved SERCA calcium uptake and led to improvements in heart function and fibrosis. Conversely, delivery of AAV DWORF gene therapy to WT mice induced expression of the SERCA inhibitor sarcolipin (SLN) and reduced cardiac performance **(Chapter 3)**. The role of DWORF in dystrophic skeletal muscle has never been explored. We hypothesize that DWORF is also downregulated in mdx skeletal muscle and that AAV DWORF gene therapy can improve skeletal muscle function and histology.

To test this hypothesis, we first quantified levels of DWORF in the skeletal muscle. We performed all studies in the diaphragm, as this is a highly affected muscle and weakening of the respiratory muscles is a major health concern in DMD. We found DWORF expression was indeed reduced in the diaphragm of mdx mice compared to wildtype (WT) mice at 6 months of age. Next, we delivered 6×10^{12} viral genome (vg) particles/mouse of AAV9 DWORF gene therapy to 6-week-old mice via tail vein injection. Because of the noted differences in the effects of AAV DWORF gene therapy in diseased vs normal mouse hearts, we treated both mdx and WT mice here. Our findings show AAV DWORF gene therapy had no effect on diaphragm force production or histology in treated mdx and WT mice. To our surprise, DWORF therapy decreased the maximum rates of muscle contraction and relaxation and increased central nucleation in treated mdx mice only. These findings suggest decreased DWORF expression

contributes to reduced SERCA function in mdx skeletal muscle, but delivery of AAV DWORF gene therapy was unable to rescue diaphragm function and histology. Additionally, AAV DWORF gene therapy slows maximum rates of contraction and relaxation in dystrophic skeletal muscle by mechanisms yet unknown.

Results

DWORF expression was decreased in the diaphragm of mdx mice. Our previous study shows DWORF expression is decreased in mdx mouse hearts **(Chapter 2)**. To determine whether this is also true in mdx skeletal muscle, we compared DWORF cDNA and protein levels in the diaphragms of 6-month-old mdx and wild-type BL10 (WT) mice **(Figure 4.1)**. DWORF cDNA levels were detected using droplet digital PCR (ddPCR) and showed a nearly-significant (p=0.0597) decrease in DWORF cDNA levels in mdx diaphragms compared to WT **(Figure 4.1A)**. Western blot analysis showed a more drastic decrease (~77%) in DWORF protein expression in mdx diaphragm compared to WT **(Figure 4.1B)**.

AAV.DWORF delivery increased DWORF expression in WT and mdx mouse diaphragm. Before evaluating the effects of DWORF gene therapy on skeletal muscle, we engineered an AAV9.DWORF vector **(Figure 4.2A)**. This AAV9 vector was used in our previous cardiac studies **(Chapters 2-3)** and contains codon-optimized mouse DWORF cDNA expressed from the ubiquitous CAG promoter and enhanced green fluorescence protein (EGFP) cDNA under the control of an internal ribosomal entry site (IRES). We injected the AAV DWORF gene therapy to 6-week-old WT and mdx mice at the dose of 6×10^{12} vector genome particles (vg)/mouse via the tail vein. At 6 months of age, we examined DWORF protein expression in the diaphragm **(Figure 4.2B)**. DWORF expression in injected WT mice was ~ 6-fold higher than in un-injected WT controls. DWORF expression in injected mdx mice was ~ 5-fold higher than in un-

injected WT controls. As discussed previously, and for reasons unknown, we failed to detect GFP expression using this vector.

AAV.DWORF delivery had no effect on diaphragm fibrosis or myofiber size but increased central nucleation in treated mdx mice. After confirming DWORF overexpression following AAV gene therapy, we evaluated its effects on muscle histology and fibrosis **(Figure 4.3)**. We studied the effects of DWORF gene therapy in 6-month-old mice because differences in WT versus mdx diaphragm are clearly observable by this age(Hakim et al., 2019). On histological examination, we performed hematoxylin and eosin (H&E) and Masson trichrome staining. Minimal feret diameter was quantified from laminin immunofluorescent staining. When comparing WT and mdx diaphragms, centronucleation quantification, percent fibrotic area, and myofiber size all showed the expected patterns **(Figure 4.3A-E)**. No differences were observed in percent fibrotic area or myofiber size between treated WT and WT control groups or treated mdx and mdx control groups **(4.3C-E)**. However, centronucleation was significantly increased in treated mdx mice compared to mdx control mice **(Figure 4.3B)**. This difference was not observed in treated WT mice compared to WT control mice.

AAV.DWORF delivery had no effect on diaphragm force production in treated WT and mdx mice. Next, we examined the effects of AAV DWORF gene therapy on skeletal muscle function. As expected, mdx diaphragm muscles showed patterns of reduced specific twitch force, reduced specific tetanic force, and greater drops in force production

following 10 cycles of eccentric contraction compared with WT **(Figure 4.4A-C)**. No differences in force production were observed between treated WT and WT control diaphragms. Likewise, no differences were observed between treated mdx and mdx control diaphragms.

AAV.DWORF delivery slowed the maximum rates of diaphragm contraction and relaxation in treated mdx mice only. To determine whether DWORF gene therapy affects the rate at which skeletal muscle functions, we quantified both the maximum rate of contraction and maximum rate of relaxation **(Figure 4.5)**. No differences were observed between treated WT and WT control groups in either maximum rate of contraction or maximum rate of relaxation **(Figure 4.5A-B)**. Surprisingly, treated mdx diaphragms exhibited a decrease in both the maximum rate of contraction and the maximum rate of relaxation.

Discussion

To improve SERCA function in dystrophic skeletal muscle, we quantified DWORF expression in the diaphragms of mdx mice and evaluated the effects of AAV DWORF gene therapy on diaphragm function and histology. We found DWORF protein expression was reduced by ~77% in mdx diaphragm compared to WT **(Figure 4.1B)**. Following this finding, we systemically injected 6 x 10^{12} vg/mouse of AAV9 DWORF gene therapy to 6-week-old WT and mdx mice by tail vein injection. Delivery of AAV DWORF gene therapy had no effect on diaphragm fibrosis, myofiber size, or overall force production in either of the treated groups **(Figures 4.3 to 4.4)**. To our surprise, AAV DWORF gene therapy increased central nucleation and slowed maximum rates of muscle contraction and relaxation in the treated mdx group only **(Figure 4.3B, Figure 4.5)**. Overall, these results suggest DWORF downregulation contributes to reduced SERCA function in mdx skeletal muscle and show AAV DWORF gene therapy was unable to rescue dystrophic skeletal muscle function and/or histology. Our results showing AAV DWORF gene therapy slowed maximum rates of dystrophic skeletal muscle contraction and relaxation indicate mdx mice have an altered response to DWORF overexpression compared to treated WT mice.

This study was conducted following our previous study examining the role of DWORF in DMD cardiomyopathy **(Chapter 2)**. In this previous study, we found DWORF levels were decreased by ~50% in mdx mouse hearts and AAV DWORF gene therapy significantly improved SR calcium uptake, cardiac function, and fibrosis. Although DWORF levels are decreased to a greater extent in mdx skeletal muscle (~77%

decrease), AAV DWORF gene therapy failed to rescue mdx skeletal function and fibrosis. It is possible that the differences in cardiac vs skeletal muscle outcomes are due to either (1) limited expression of AAV DWORF therapy in the diaphragm due to AAV9 tropism or skeletal muscle degeneration and regeneration, (2) lower levels of SERCA2a (the cardiac and slow-twitch skeletal muscle isoform) expressed in skeletal muscle, or (3) skeletal muscle requires a lower dose of AAV DWORF gene therapy to achieve optimal SERCA activation.

First, AAV DWORF gene therapy may have failed to rescue mdx diaphragms due to limited AAV DWORF expression. AAV9 is known to be a cardiotropic vector(Bostick et al., 2007; Srivastava, 2016). In our previous publication testing the same dose and delivery method of AAV9.DWORF vector in mdx cardiac tissue, we found DWORF expression was increased by ~50-fold in treated mdx mouse hearts compared with mdx controls. In the present study, we found DWORF expression was increased by ~22-fold in treated mdx mouse diaphragms compared with mdx controls. Another possible explanation for this decrease in diaphragm expression is the difference in tissue degeneration and regeneration. Skeletal muscles of murine DMD models undergo profound muscle degeneration and regeneration, a phenomenon that is not observed in the heart. Lower DWORF expression, removal of the AAV9.DWORF from degenerating fibers, or a combination of mechanisms may account for the discrepancies in cardiac vs skeletal muscle outcomes.

A second possibility is the difference in SERCA2a expression between cardiac and diaphragm muscle. SERCA2a is the SERCA isoform found in cardiac and slow-twitch skeletal muscle and is the only isoform endogenously activated by DWORF. It is

possible that delivered DWORF only activates this isoform as well. Due to the mosaic pattern of fiber types found in the diaphragm, not every muscle fiber contains SERCA2a, which may account for the discrepancies in cardiac vs skeletal muscle outcomes. However, a previous study performed by Nelson et al. in COS7 cells transfected with green fluorescent protein (GFP)-tagged DWORF and various SERCA isoforms indicates DWORF is capable of binding to all SERCA isoforms(Nelson et al., 2016). More work needs to be done to elucidate which SERCA isoforms DWORF activates in vivo.

A third possibility is that skeletal muscle requires a much lower dose of AAV DWORF gene therapy than the heart. Our findings indicate a dose of 6 x 10^{12} vg/mouse of AAV DWORF gene therapy improves both cardiac function and fibrosis but has no effect on diaphragm function and fibrosis. These findings are similar to a study conducted by Voit et al, who showed genetic ablation of the SERCA inhibitor SLN in dystrophin mutant and dystrophin/utrophin double mutant mice (mdx:utr −/−:sln −/−) drastically reduced cardiac fibrosis and improved left ventricular function(Voit et al., 2017). However, total ablation of SLN did not statistically improve force production or fibrosis in the diaphragm, despite improvements in SERCA calcium uptake that exceeded uptake by WT samples. On the other hand, SLN haploinsufficient mice (mdx:utr −/− :sln +/−) mice only normalized SERCA calcium uptake in the diaphragm to WT levels but greatly improved diaphragm function and fibrosis. Levels of DWORF expression achieved in the present study may be too high to attain an optimal level of SERCA activation. Future studies evaluating SERCA activity in treated diaphragms and the effects of varying dosages of AAV DWORF gene therapy will address this unknown.

A surprising finding of this study is that AAV DWORF therapy slowed maximum rates of diaphragm contraction and relaxation in treated mdx mice but not in treated WT mice. We expected DWORF overexpression to increase SERCA activation and thus increase the rate of relaxation in skeletal muscle. Our findings suggest mdx mice regulate SERCA activation by mechanisms different than those observed in WT mice. There are likely unexpected changes in SERCA regulation, expression of other calcium handling proteins, and/or fiber type in treated mdx mice. As of yet, these experiments have not been conducted.

In summary, our findings suggest DWORF downregulation contributes to reduced SERCA function in DMD skeletal muscle, but delivery of 6×10^{12} vg/mouse of AAV9 DWORF gene therapy is unable to rescue diaphragm function or histology. These findings are different than those of our previous study showing this same dose significantly improved heart function and fibrosis **(Chapter 2)**. In addition, DWORF gene therapy unexpectedly increased centronucleation and decreased the maximum rates of diaphragm contraction and relaxation in treated mdx mice. Future studies will elucidate why this unexpected finding occurred and how we can optimize AAV DWORF gene therapy for use in dystrophic skeletal muscle.

Materials and Methods

Mice. All animal experiments were approved by the institutional animal care and use committee. Only male mice were used in the study. Mice were housed in a specific pathogen-free animal care facility on a 12-hour light (25 lux):12-hour dark cycle with access to food and water *ad libitum*. All mice were originally purchased from The Jackson Laboratory (Bar Harbor, ME). Dystrophin-deficient mdx mice (C57BL/10ScSn-*Dmd*^{mdx}/J, stock number 001801) and normal control BL10 (C57BL/10ScSnJ, stock number 000476) mice were generated in-house in a barrier facility using breeders purchased from The Jackson Laboratory.

AAV production and administration. The *cis*-plasmid (also called pEM1) used for packaging in AAV9 capsid contained (from 5'-end to 3'-end) the ubiquitous CAG promoter, a codon-optimized mouse DWORF cDNA, the encephalomyocarditis virus IRES (Clontech, Mountain View, CA), the EGFP gene, and an SV40 virus polyadenylation signal. DWORF cDNA was synthesized by GenScript (Piscataway, NJ) and codon-optimized to mouse. Virus was purified through two rounds of isopycnic ultracentrifugation according to our previously published method (J.-H. Shin et al., 2012). AAV DWORF gene therapy was delivered to 6-week-old mice via tail vein injection at a concentration of 6×10^{12} vg/mouse.

Western blot. Freshly isolated diaphragm tissue was snap-frozen in liquid nitrogen and homogenized in radioimmunoprecipitation assay buffer (150 mM NaCl; 1% v/v igepal

CA-630; 50 mM Tris-Cl, pH 8.3; 0.5% w/v sodium deoxycholate; 0.1% w/v sodium dodecyl sulfate) with added protease inhibitors (cOmplete ULTRA mini-tablet, Roche, Indianapolis, IN). Diaphragm lysate was run on 15% bis/acrylamide gels made by standard preparation. Proteins were transferred to PVDF membranes (Millipore, Immoblion-P) by wet transfer technique. Membranes were incubated with custom rabbit polyclonal antibody against mouse DWORF (New England Peptide) at a concentration of 1:1,000(Nelson et al., 2016). Blots were incubated with a goat anti-rabbit IgG-HRP secondary antibody and developed using ClarityTM Western ECL chemiluminescent substrate (Bio-Rad, Hercules, CA) and a digital Bio-Rad ChemiDocTM MP Imaging System.

DWORF transcript quantification. Freshly isolated diaphragm samples were stored in RNAlater stabilization solution (Thermo Fisher Scientific, Waltham, MA; Cat No: AM7021). RNA was extracted using the RNeasy Fibrous Tissue Mini kit (Qiagen, Hilden, Germany; Cat No: 74704). cDNA was generated via reverse transcription using the SuperScript IV VILO Master Mix with ezDNase Enzyme (Thermo Fisher Scientific, Cat No: 11766050). Resulting cDNA concentrations were detected using the Qubit ssDNA assay kit (Thermo Fisher Scientific, Cat No: Q10212). Transcript quantification was completed using ddPCR methods. Results were measured using the QX200 ddPCR system (Bio-Rad) and ddPCR supermix for probes (no dUTP) (Bio-Rad, Cat No: 186-3024). DWORF-specific primer and probe sets were designed as follows: Forward primer: 5'-TTCTTCTCCTGGTTGGATGG-3', Reverse primer: 5'-TCTTCTAAATGGTGTCAGATTGAAGT-3', and Probe 5'-

TTTACATTGTCTTCTTCTAGAAAAGGAAGAAG-3'. Probes were labeled with a 5' 6-carboxyfluorescein, an internal ZEN quencher, and a 3' Iowa Black quencher. Results were recorded as the number of transcript copies per ng of cDNA used in the ddPCR reaction.

Morphological studies. 10 μm cryosections were sectioned from OCT-embedded diaphragm samples. General histology was examined by hematoxylin and eosin (H&E) staining, and fibrosis was examined by Masson trichrome staining. Masson trichrome staining was completed using the Masson Trichrome Stain Kit (Epredia, Kalamazoo, MI). Percent fibrotic area of three random 10x images was quantified and averaged for each diaphragm sample. Percent fibrotic area was calculated by dividing the area of blue staining by the total tissue area using ImageJ/Fiji Software (ImageJ 1.48b). The percentage of centrally nucleated fibers was manually calculated by counting the number of centrally and peripherally nucleated fibers in H&E-stained sections.

Laminin staining was used to calculate myofiber minimal Feret diameter using MyoVision software (Kenneth Campbell group, University of Kentucky). Images were viewed using a Nikon E800 fluorescence microscope. Photomicrographs were taken with a Leica DFC7000 camera.

Skeletal muscle function assay. Diaphragm muscle function was evaluated *ex vivo* using our published protocol(Hakim et al., 2019). Muscle force was measured using a 305B dual-mode servomotor transducer using the Dynamic Muscle Control software (Aurora Scientific, Inc., Aurora, ON, Canada). Data were analyzed using the Dynamic

Muscle Analysis (DMA) software (Aurora Scientific). Specific muscle force was calculated by dividing the absolute muscle force with the muscle cross-sectional area (CSA), which was calculated according to the following equation: CSA = (muscle mass) / [(1.0 × optimal muscle length) × (1.06 g/cm3)]. Muscle density is 1.06 g/cm^3 (Mendez & Keys, 1960). 1.0 represents the ratio of the fiber length to the optimal muscle length (Lf/Lo) for the diaphragm muscle (Burkholder et al., 1994).

Statistical analysis. Data are presented as mean ± stand error of mean. One-way ANOVA with Holm-Sidak's multiple comparisons was performed on more than two group comparisons including one independent variable. Groups compared were pre-selected as follows: WT vs mdx, WT vs treated WT group, and mdx vs treated mdx group. Unpaired t-test was used for two-group comparisons. All statistical analyses were performed using GraphPad PRISM software version 9.1.2 (GraphPad Software, La Jolla, California). A $p < 0.05$ was considered statistically significant.

Acknowledgments

Conceived and designed experiments: EM, XP, and DD. Performed the experiments: EM, YY, TL, XP, AG, GB, and CM. Wrote the paper: EM.

Figures

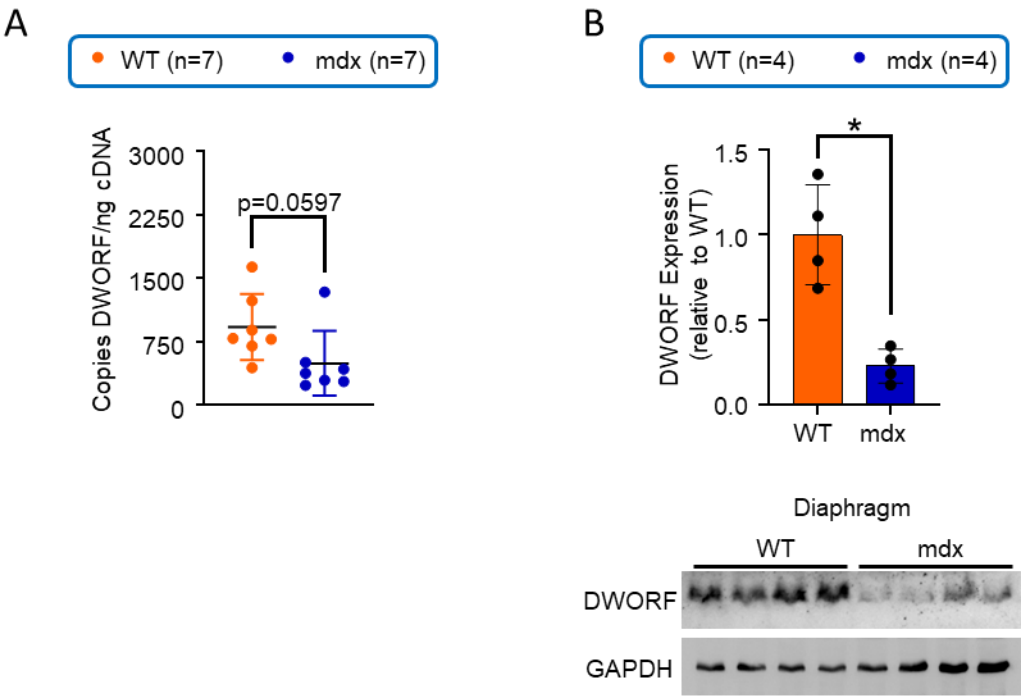

Figure 4.1. DWORF expression was decreased in mdx mouse diaphragms. A, Quantification of DWORF transcript in wild type BL10 (WT) and mdx diaphragms. **B,** Quantification of DWORF protein expression by western blot. The bottom panel shows western blot images, and the top panel shows densitometry results. *p<0.05.

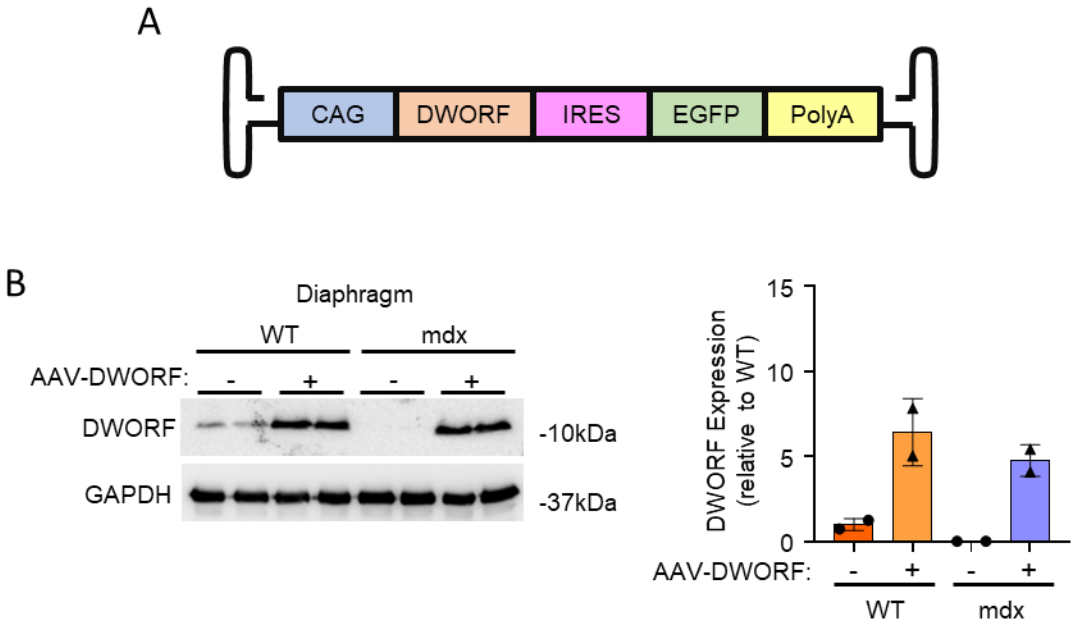

Figure 4.2. AAV.DWORF delivery increased DWORF expression in treated WT and mdx mice. A, Schematic drawing of the AAV.DWORF vector. **B,** Quantification of DWORF protein expression by western blot. The left panel shows western blot images, and the right panel shows densitometry results.

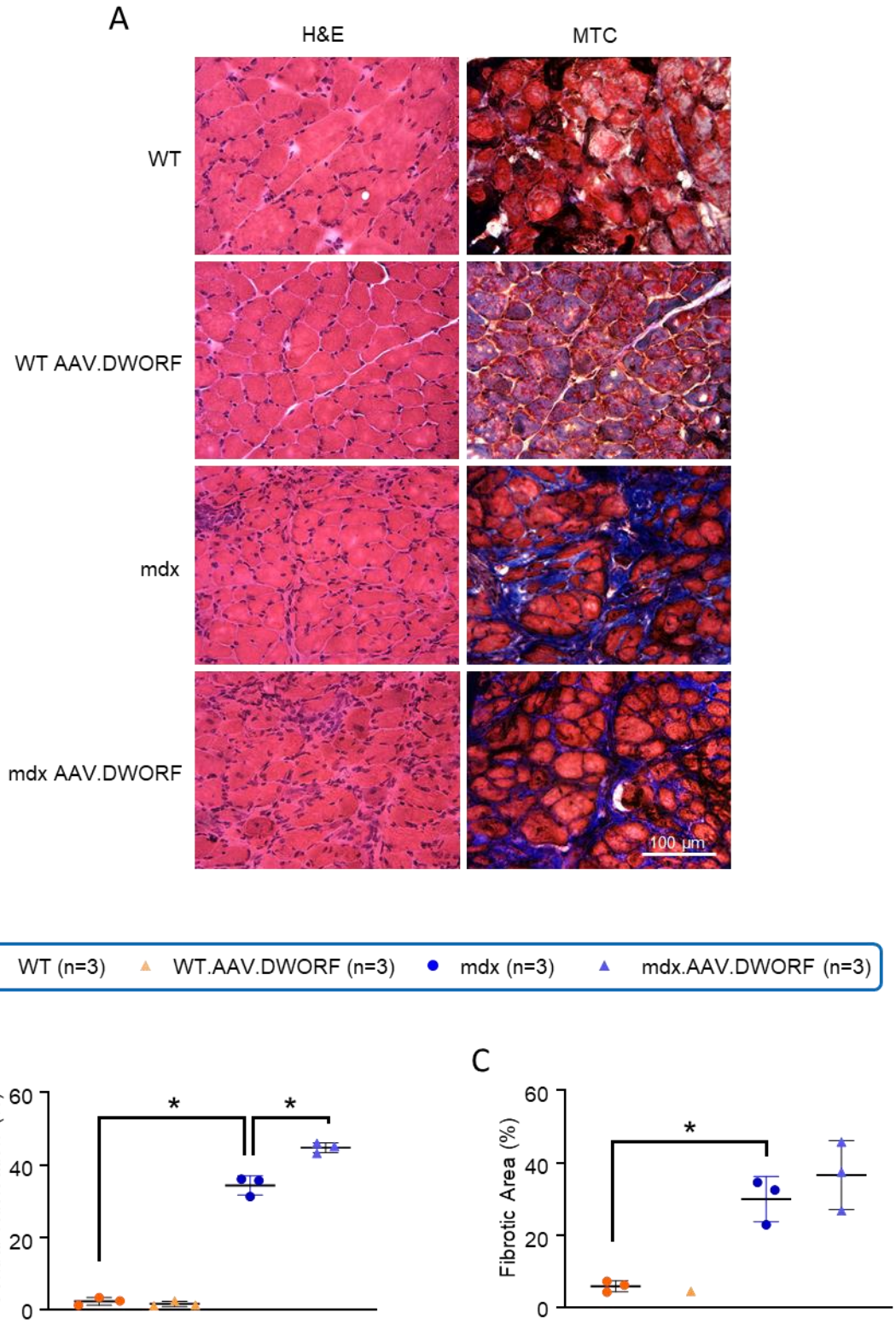
A
H&E
MTC
WT
WT AAV.DWORF
mdx
mdx AAV.DWORF
100 µm
WT (n=3)
WT.AAV.DWORF (n=3)
mdx (n=3)
mdx.AAV.DWORF (n=3)
B
Central Nucleation (%)
60
40
20
0
*
*
C
Fibrotic Area (%)
60
40
20
0
*

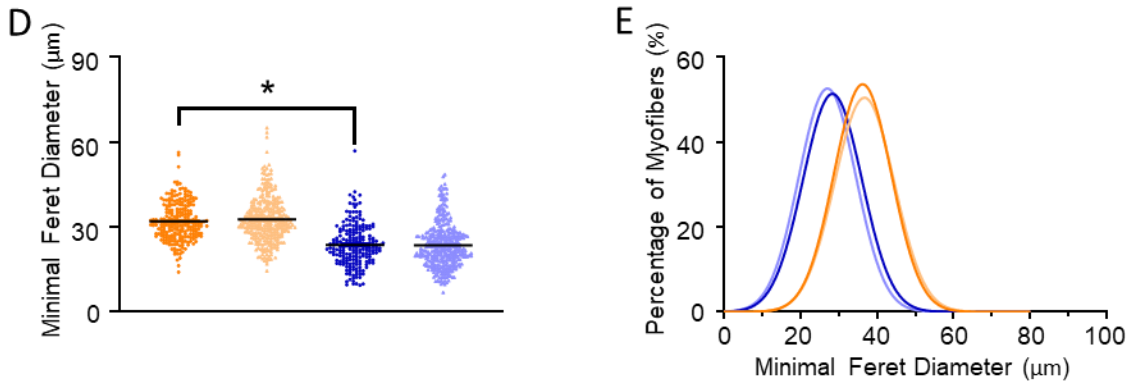

Figure 4.3. AAV.DWORF delivery effects on diaphragm histology. A, Representative photomicrographs of hematoxylin (H&E) and Masson's trichrome (MTC) staining from wild type BL10 (WT), AAV.DWORF-treated WT, mdx, and AAV.DWORF-treated mdx mouse diaphragms. **B,** Percent of centrally nucleated muscle fibers in the diaphragm. **C,** Quantification of the fibrotic area in the diaphragm. **D,** Minimal Feret diameter of diaphragm muscle. **E,** Myofiber size distribution in the diaphragm. *$p<0.05$.

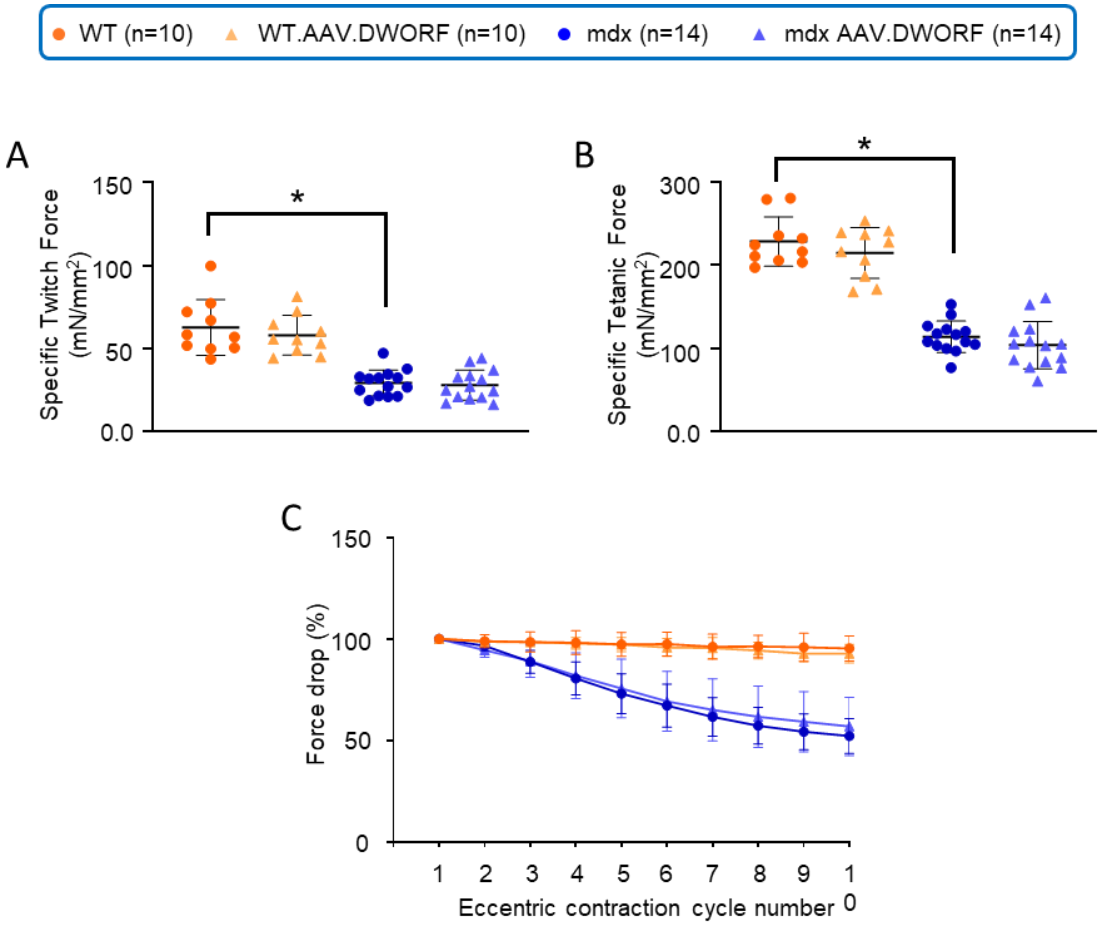

Figure 4.4. AAV.DWORF delivery had no effect on diaphragm force production. **A,** Specific twitch force in diaphragm muscle. **B,** Specific tetanic force in diaphragm muscle. **E,** Overall profiles of 10 cycles of eccentric contraction. *p<0.05.

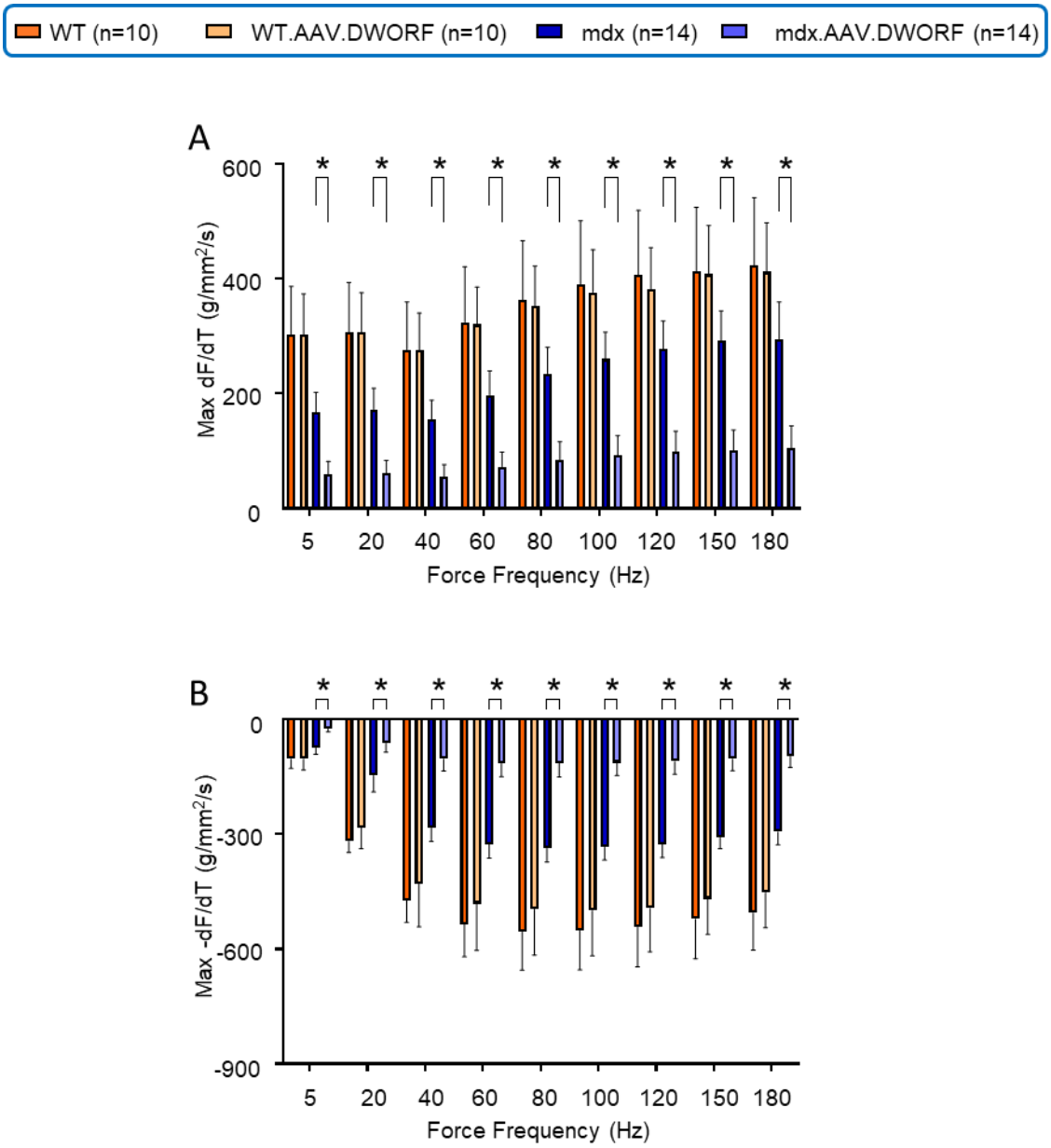

Figure 4.5. AAV.DWORF delivery slowed rates of contraction and relaxation in treated mdx mice only. A, Maximum rate of contraction in diaphragm muscle. **B,** Maximum rate of relaxation in diaphragm muscle. *p<0.05.

Chapter 5. Transcriptional changes of calcium handling proteins in dystrophic canines offers new insight into cytosolic calcium buildup

Emily D. Morales[1], Dongsheng Duan[1, 2, 3, 4 *]

[1], Department of Molecular Microbiology and Immunology, School of Medicine, The University of Missouri, Columbia, MO 65212

[2], Department of Neurology, School of Medicine, The University of Missouri, Columbia, MO 65212

[3], Department of Biomedical, Biological & Chemical Engineering, College of Engineering, The University of Missouri, Columbia, MO 65212

[4], Department of Biomedical Sciences, College of Veterinary Medicine, The University of Missouri, Columbia, MO 65212

Abstract

Muscle degradation experienced by patients with Duchenne Muscular Dystrophy (DMD) can be partly attributed to a buildup of aberrant cytosolic calcium. This excess calcium activates calcium-dependent proteases and phospholipases that degrade cellular proteins and lipids. Previous studies show changes in the expression levels and regulation of calcium handling proteins associated with the sarcoplasmic reticulum (SR) are partly to blame. Calcium exit from the SR is increased in DMD muscle fibers, while calcium re-uptake into the SR is decreased. However, most data collected on SR-associated calcium handling proteins come from studies completed in mouse models of DMD. Little is known about the mechanisms underlying SR calcium leak and reduced uptake in large animal models of DMD, which more closely resemble human patients. In the current study, we analyzed transcript levels of various calcium handling proteins in normal and dystrophic canines, drawing comparisons between different age groups and sex-based differences. The samples analyzed were collected from the left ventricle, diaphragm, and extensor carpi ulnaris. We found differences in transcript levels between normal and affected male canines in skeletal muscle only. No differences were detected in heart samples. The transcriptional differences in skeletal muscle changed over time and disease progression. Additionally, we found several transcriptional differences between male and female canine tissues, primarily in the heart. Our study highlights the importance of considering animal age and sex when conducting studies on dystrophic canines and the need for further research elucidating calcium handling mechanisms in large animal models of DMD.

Introduction

Duchenne muscular dystrophy (DMD) is the most common form of muscular dystrophy(D. Duan et al., 2021). The disease occurs in patients lacking a functional version of dystrophin, a protein important for protecting the integrity of the plasma membrane of muscle fibers. Phenotypes of the disease include severe muscle weakness and degeneration that are exacerbated with age. One cause for muscle degeneration is an increase of cytosolic calcium within the muscle fibers of DMD patients(Burr & Molkentin, 2015; Mareedu, Million, et al., 2021). High levels of cytosolic calcium activate calcium-dependent proteases and phospholipases, which degrade proteins and lipids(Hopf et al., 1996a; Lindahl, Bäckman, et al., 1995; Spencer & Mellgren, 2002; Turner et al., 1988).

A portion of the cytosolic calcium found in DMD muscle fibers comes from the sarcoplasmic reticulum (SR). The SR is important for harboring large concentrations of calcium essential to the contraction-relaxation cycle(Rossi & Dirksen, 2006). In both skeletal and cardiac muscle, calcium from the SR is released to the cytosol upon opening of the ryanodine receptor (RyR), a channel found in the SR membrane. Once in the cytosol, calcium binds to contractile proteins and a contraction ensues. During relaxation, calcium is returned to the SR by the sarco-endoplasmic reticulum ATPase (SERCA). Throughout this cycle, calcium-sequestering proteins within the SR are responsible for isolating calcium ions and regulating their uptake and release. In DMD, an increased amount of calcium is released from the SR while a decreased amount of

calcium re-enters the SR, leading to cytosolic calcium buildup(Mareedu, Million, et al., 2021).

Changes in the expression and regulation of several SR calcium handling proteins are responsible. Studies show RyR in dystrophic muscle is open more often and not solely in response to a contractile stimulus(Bellinger et al., 2009; Fauconnier et al., 2010). In addition, several calcium-sequestering proteins within the SR have reduced expression in dystrophic muscle(Culligan et al., 2002; Dowling et al., 2004; Lohan & Ohlendieck, 2004; Pertille et al., 2010). Both of these factors likely contribute to the increased release of calcium from the SR. Re-uptake of calcium into the SR is also altered due to decreased SERCA function(Bellinger et al., 2009; Fauconnier et al., 2010; Kargacin & Kargacin, 1996; Schneider et al., 2013a). This decrease in function is caused by increased expression of sarcolipin (SLN), a small peptide inhibitor of SERCA, and decreased expression of dwarf open reading frame (DWORF), a small peptide enhancer of SERCA **(Chapter 2, Chapter 4)** (Voit et al., 2017). Collectively, this information paints a picture of the mechanisms behind aberrant cytosolic calcium. However, most of the information acquired about this process comes from studies conducted in mouse models of DMD. There is not enough information on whether this process is similar in large animal models of DMD, whose disease phenotypes more closely resemble those of human patients.

In the present study, we assessed transcript levels of several SR calcium handling proteins in normal and dystrophic canines using droplet digital PCR (ddPCR) methods. The transcripts included those of three calcium-sequestering proteins (calreticulin, calsequestrin 2, sarcalumenin), two SERCA isoforms (SERCA1, SERCA2a), and two

SERCA regulators (sarcolipin, dwarf open reading frame). Tissues were collected from canine left ventricle, diaphragm, and extensor carpi ulnaris (ECU). Male samples were analyzed at three different age groups to illustrate expressional changes during disease progression. In addition, male and female comparisons were made between canines in the middle age group. Our results show transcriptional changes in dystrophic canine skeletal muscle. Differences in male vs female canine tissues were primarily detected in the heart. These findings emphasize the importance of animal age and sex in dystrophic canine studies. They also highlight the need for further elucidation of the mechanisms behind calcium mishandling in large animal models of DMD.

Results

Left ventricle transcript levels showed no changes between normal and affected canines, but several transcripts were altered between male and female ventricles. To assess transcriptional changes in dystrophic canine hearts, we analyzed samples collected from the left ventricle. The left ventricle was chosen because dystrophic hearts exhibit left ventricular dilated cardiomyopathy. ddPCR methods were used to assess the total number of transcript copies/ng of complementary DNA (cDNA) used in the reaction. As expected, SERCA1 (the SERCA isoform found in fast-twitch skeletal muscle fibers) and sarcolipin (a SERCA inhibitor mainly expressed in the atria and skeletal muscle) showed extremely low levels of transcript. No transcriptional changes were observed at any age between normal and affected canines **(Table 5.1)**.

However, female canines from both normal and affected canine groups exhibited reduced transcript levels of all calcium-sequestering proteins (calreticulin, calsequestrin 2, and sarcalumenin) and the SERCA isoform expressed in cardiac and slow-twitch skeletal muscle fibers (SERCA2a) compared to males **(Table 5.2)**.

Diaphragm transcript levels were altered between normal and affected canines, but there were no transcriptional changes between male and female diaphragms. To assess transcriptional changes in skeletal muscle, we first analyzed samples collected from canine diaphragms. The diaphragm was chosen because it is an important muscle used in respiration. Respiratory failure is a main cause of death in DMD. At 0-2 and 8-15

months of age, the SERCA enhancer DWORF was downregulated in affected canine diaphragms compared to normal canine diaphragms **(Table 5.3)**. This downregulation was no longer observed at 30-50 months of age. Both SERCA isoforms (SERCA1 and SERCA2a) were also downregulated in affected canine diaphragms at 8-15 months. This downregulation was no longer observed at 30-50 months of age. Lastly, calsequestrin 2 was upregulated in affected canine diaphragms at 30-50 months of age.

No transcriptional changes were observed between male and female diaphragms **(Table 5.4)**.

ECU transcript levels were altered between normal and affected canines, and several transcripts were altered between male and female ECUs. Next, we analyzed transcript levels of calcium handling proteins in the ECU, a skeletal muscle required for proper movement of the canine forearm. This muscle is weakened and contains high levels of fibrosis in dystrophic canines(Hakim et al., 2021). No transcriptional changes were observed at 0-2 months of age. Transcripts of several calcium handling proteins were downregulated in affected canines at 8-15 months, including sarcalumenin, SERCA1, SERCA2a, and DWORF **(Table 5.5)**. However, no transcripts were downregulated by 30-50 months of age. Instead, SERCA 1 was upregulated in affected canine ECUs at 30-50 months of age.

In addition, transcripts for sarcalumenin, SERCA2a, and DWORF were all downregulated in normal female ECUs compared with normal male ECUs **(Table 5.6)**. No changes were observed between affected female and affected male transcripts.

Discussion

Calcium mishandling in DMD causes a buildup of aberrant cytosolic calcium that activates calcium-dependent proteases and phospholipases(Mareedu, Million, et al., 2021). These enzymes degrade muscle cell proteins and lipids. High levels of cytosolic calcium are partly due to changes in calcium handling proteins residing at the sarcoplasmic reticulum (SR). Most of the information we currently have on changes in calcium handling protein expression comes from studies conducted in mouse models of DMD. However, the canine model of DMD more closely resembles the phenotypes and disease progression observed in humans. Here, we assessed changes in transcript levels of various calcium handling proteins in normal and affected canines using droplet digital PCR (ddPCR) methods. We compared normal and affected male left ventricle, diaphragm, and extensor carpi ulnaris (ECU) tissues at 0-2 months of age, 8-15 months of age, and 30-50 months of age. In addition, we compared transcript levels between normal male and female tissues and affected male and female tissues at 8-15 months. We found transcriptional changes in normal vs affected canine skeletal muscles but found no transcriptional changes in normal vs affected canine heart samples. However, several transcriptional changes were found between male and female hearts. Additionally, differences in transcript levels between normal and affected canines changed with disease progression and canine age. Our findings highlight the importance of selecting the proper age and sex when conducting studies involving dystrophic canines and emphasize the need for more studies elucidating the mechanisms behind calcium mishandling in large animal models of DMD.

Human patients with DMD exhibit delayed motor skill development, which becomes apparent at 2-5 years of age(Duan, 2015; Mercuri et al., 2019). By their early teen years, patents lose ambulation. Patients then die prematurely, around 20 years of age, from cardiac and/or respiratory failure. The most commonly used mouse model of DMD is the mdx mouse. Compared with human patients, this model exhibits very mild disease symptoms. Dystrophic canines more closely resemble the timeline of human disease(Duan, 2015). Dystrophic puppies are often weak at birth and exhibit limb muscle weakness at 2-3 months of age (~3 years in human age). By 6 months of age (~8 years in human age), dystrophic canines develop more pronounced muscle wasting, abnormal gait, and abnormal cardiac function. At 3 years, or 36 months, of age (~20 years in human age), canines die from cardiorespiratory failure or euthanasia due to poor health conditions. Skeletal muscle and cardiac data suggest both male and female dystrophic canines exhibit similar phenotypes of the disease in both skeletal muscle and the heart(Guo et al., 2019).

Calcium-sequestering proteins act as calcium buffers within the SR and help regulate calcium uptake and release. In the present study, we assessed transcript levels of three calcium-sequestering proteins residing within the SR: calsequestrin 2, sarcalumenin, and calreticulin.

Calsequestrin 2 is endogenously expressed in cardiac and slow-twitch skeletal muscles. It binds to the ryanodine receptor and acts as a calcium sensor to help regulate the release of calcium from the SR(Woo et al., 2020). Calsequestrin is downregulated in cardiac and skeletal muscles of mdx mice, the most commonly used mouse model of DMD(Lohan & Ohlendieck, 2004; Pertille et al., 2010). For unknown reasons,

calsequestrin is increased in spared muscle types and fast-twitch muscle fibers from dystrophin and utrophin double-mutant (mdx:utr−/−) mice(Pertille et al., 2010; Schneider et al., 2013a; Voit et al., 2017).

Sarcalumenin is a calcium-sequestering protein expressed in both heart and skeletal muscles that is bound to SERCA and aids in regulation of calcium uptake into the SR(Yoshida et al., 2005). Sarcalumenin-deficient mice exhibit weakened calcium uptake(Yoshida et al., 2005). Sarcalumenin is downregulated in mdx skeletal muscle fibers and heart(Dowling et al., 2004; Lohan & Ohlendieck, 2004).

Calreticulin is expressed in both skeletal and heart muscle. It resides within the SR and binds to calcium, rendering it inactive(Groenendyk et al., 2022). No studies have assessed calreticulin expression in dystrophic mice.

Overall, calcium-sequestering proteins show a trend of downregulation in dystrophic mice. In the present study, we observed an upregulation of calsequestrin 2 transcript in dystrophic canine diaphragm at 30-50 months and a downregulation of sarcalumenin transcript in dystrophic canine ECU at 8-15 months **(Table 5.3, Table 5.5)**. No changes were observed in calreticulin transcript levels. Because calsequestrin is increased in fast-twitch muscle fibers of dystrophic mice, it is possible the increased calsequestrin 2 transcript levels in dystrophic canine diaphragm are due to fiber-type switching. Unlike dystrophic mice, dystrophic canines undergo a fiber-type switch where the ratio of fast-twitch to slow-twitch fibers is increased(Hakim et al., 2021). It is currently unclear why this trend is only observed at 30-50 months. This may be a phenomenon that occurs as the disease progresses. It is also unclear why sarcalumenin is only downregulated in dystrophic canines at 8-15 months. No changes in calcium-

sequestering transcript levels were observed in the heart **(Table 5.1)**. More work needs to be done to assess the levels of calcium-sequestering proteins in dystrophic canines.

In addition to calcium-sequestering proteins, we also assessed transcript levels of two SERCA isoforms and the SERCA regulators sarcolipin and DWORF. SERCA1 is endogenously expressed in fast-twitch skeletal muscle, while SERCA2a is expressed in slow-twitch skeletal muscle and the heart. Sarcolipin is a small peptide inhibitor of SERCA expressed in the atria and skeletal muscle. DWORF is a small peptide enhancer of SERCA2a.

Due to fiber-type switching in dystrophic canines, SERCA1 protein expression is increased in the ECU, while SERCA2a protein is decreased(Voit et al., 2017). In the present study, we found SERCA1 transcript is downregulated in dystrophic canine ECU at 8-15 months and is upregulated at 30-50 months **(Table 5.5)**. Canine samples used to analyze SERCA protein expression were between the ages of 1.73-11.9 months(Voit et al., 2017). At these ages, SERCA1 transcripts are either unchanged or downregulated in dystrophic ECU samples **(Table 5.5)**. This suggests changes in SERCA1 translation are responsible for increased protein expression in dystrophic canine ECU. In line with what is known about fiber-type switching in dystrophic canine skeletal muscle, SERCA2a transcript was downregulated in dystrophic ECU and diaphragm at 8-15 months **(Table 5.5, Table 5.3)**. This finding was not observed by 30-50 months in either tissue. No changes in transcript levels of SERCA isoforms or their regulators were observed in the heart **(Table 5.1)**. It is currently unclear why transcriptional changes are specific to select age groups. More work needs to be done to assess protein expression changes at varying ages.

Previous studies show sarcolipin expression is increased in both dystrophic mouse and canine tissues(Voit et al., 2017). In addition, our previous work shows DWORF expression is decreased in mdx mice **(Chapter 2, Chapter 4)**. Both of these findings contribute to altered SERCA function in DMD. In the present study, we found sarcolipin transcripts were unchanged in dystrophic canines **(Table 5.1, Table 5.3, Table 5.5)**. This suggests sarcolipin upregulation occurs at the translational level. However, DWORF transcript was reduced in dystrophic diaphragm at 0-2 months and 8-15months **(Table 5.3)**. Transcript levels were also reduced in dystrophic ECU at 8-15 months **(Table 5.5)**. No changes were observed in the left ventricle **(Table 5.1)**.

When comparing male and female canines, most transcriptional differences were observed in the left ventricle. Female left ventricles exhibited reduced transcript levels of calreticulin, calsequestrin 2, sarcalumenin, and SERCA2a, regardless of whether the canines were normal or affected **(Table 5.2)**. These findings suggest major differences are present between male and female calcium regulation. Several changes were also observed in canine ECU **(Table 5.6)**. Normal female ECUs exhibited decreased transcript levels of sarcalumenin, SERCA2a, and DWORF compared to normal male ECUs. However, these differences were not observed between affected female and affected male ECUs. This is likely due to the drastic reduction in sarcalumenin, SERCA2a, and DWORF transcripts in affected male tissues. These drastic reductions do not appear in affected female ECUs. No transcriptional changes were observed between male and female diaphragms **(Table 5.4)**. These findings highlight the importance of selecting the proper animal sex in studies involving the use of dystrophic canines. More work needs to be done to determine expression levels of various calcium handling

proteins in male vs female canines and to elucidate why differences in regulation of calcium handling proteins exist in affected male and affected female tissues.

In summary, calcium mishandling in DMD causes degradation of muscle cells. High levels of cytosolic calcium in dystrophic muscles are partly due to increased calcium leak from the SR, reduced expression of SR calcium-sequestering proteins, and reduced calcium uptake into the SR. Most of the work elucidating the involvement of calcium handling proteins in this process has been conducted in mice. Here, we show transcriptional changes in dystrophic canine cardiac and skeletal muscle samples at various ages. Transcriptional changes in dystrophic tissues were only detected in skeletal muscle, but changes in male vs female tissues mainly occurred within the heart. Several of the changes observed fit well within our previous knowledge of calcium mishandling of DMD. However, more work needs to be done to assess changes in canine protein expression. Overall, our findings emphasize the importance of considering animal age and sex in dystrophic canine studies and show there is much left to be explained about calcium mishandling in large animal models of DMD.

Materials and Methods

Animals. All experiments were approved by the University of Missouri's Animal Care and Use Committee and were in-line with National Institutes of Health guidelines. All canines used for normal vs affected comparisons were male. Male vs female comparisons were made using both normal and affected canine groups. All canines were of mixed genetic backgrounds including golden retriever, Labrador retriever, beagle, and Welsh corgi. Animals were generated at the University of Missouri by artificial insemination and were housed in a conventional care facility accredited by the American Association for Accreditation of Laboratory Animal Care. Animals were kept under a 12-hour light/12-hour dark cycle with access to drinking water *ad libitum*. Affected canines were housed in raised platform kennels and were fed wet food as instructed by a veterinarian. Normal canines were housed in regular floor kennels and were fed dry food. Canines were monitored daily by caregivers and were allowed toys in the kennels for activity enrichment. Animals were euthanized according to the American Veterinary Medical Association Guidelines for the Euthanasia of animals.

Transcript quantification. Fresh left ventricle, diaphragm, and ECU samples were snap-frozen in liquid nitrogen prior to use. RNA extraction was performed using the RNeasy Fibrous Tissue Mini kit (Qiagen, Cat No: 74704). Reverse transcription was performed using the SuperScript IV VILO Master Mix with ezDNase Enzyme (Thermo Fisher Scientific, Cat No: 11766050). cDNA concentrations were determined using the

Qubit ssDNA assay kit (Thermo Fisher Scientific, Cat No: Q10212). Droplet digital PCR (ddPCR) was performed using the QX200 ddPCR system (Bio-Rad) using ddPCR supermix for probes (no dUTP) (Bio-Rad, Cat No: 186-3024). Primer and probe sets were designed according to the table below. All probes contained a 5' 6-carboxyfluorescein, an internal ZEN quencher, and a 3' Iowa Black quencher. Results are presented as absolute copies of transcript/ng of cDNA used in the reaction.

Calreticulin	
Forward Primer	5'-GACTGGGATGAAGAGATGGATG-3'
Probe	5'-CTGAGTACAAGGGCGAGTGGAAGC-3'
Reverse Primer	5'-GCCCTTGTAATCTGGGTTGT-3'
Calsequestrin 2	
Forward Primer	5'-CCATCCCTGACAAACCTTACA-3'
Probe	5'-CGTAGGGTGGGTCTTTGGTGTTCC-3'
Reverse Primer	5'-GGATGCCGTTCAAATCATCTTC-3'
Sarcalumenin	
Forward Primer	5'-CTGAATGAGGACAAGCCAGT-3'
Probe	5'-TGCAGCACCACAGAGTAGTCATCC-3'
Reverse Primer	5'-GCTTGATGGAGGAATGGTAGAT-3'
SERCA1	
Forward Primer	5'-CCTCCACTTCCTCATCCTCTA-3'
Probe	5'-ACCCTCTGCCGATGATCTTCAAGC-3'
Reverse Primer	5'-CGAGCCCAATGACTGGAAA-3'

SERCA2a	
Forward Primer	5'-GCTTGGTTTGAAGAAGGTGAAG-3'
Probe	5'-TGGGTGTATGGCAGGAGAGAAATGC-3'
Reverse Primer	5'-CTTAAGTGCTTCGATCGCATTC-3'
Sarcolipin	
Forward Primer	5'-CCTGAGTTGGAGAGAGAGAGAA-3'
Probe	5'-CTACTGCAGCCAGGTGAGGACAAG-3'
Reverse Primer	5'-TGAGGGCACACCCAAGA-3'
DWORF	
Forward Primer	5'-CCTTCTGGTCCCTATTCTTCTC-3'
Probe	5'-TCTTCTCCTAGAAAGGCAAGAAGACT-3'
Reverse Primer	5'-AATCTGTCACGTTCATGCTTT-3'

Statistical analysis. Data are presented as the absolute number of transcript copies/ng of cDNA used in the ddPCR reaction. All analyses performed were unpaired t-tests between two groups. Analyses were calculated using GraphPad PRISM software version 9.1.2 (GraphPad Software, La Jolla, California). A $p < 0.05$ was considered statistically significant.

Acknowledgements

Conceived and designed experiments: EM and DD. Performed the experiments: EM. Wrote the paper: EM.

Tables

Table 5.1. Left Ventricle calcium handling transcript levels in normal vs dystrophic canines.

	0-2 Months		8-15 Months		30-50 Months	
	Normal	Affected	Normal	Affected	Normal	Affected
Calreticulin	1271.3 ± 487.5	1467.6 ± 718.9	1225.4 ± 203.5	1188.0 ± 362.3	753.1 ± 151.0	1134.0 ± 481.8
Calsequestrin 2	1360.7 ± 994.3	1442.9 ± 347.0	7167.9 ± 1123.6	6005.5 ± 1174.3	4416.8 ± 987.6	6000.8 ± 2354.7
Sarcalumenin	1905.6 ± 1479.2	2720.0 ± 1604.3	6201.1 ± 1956.8	5773.4 ± 1256.9	3976.3 ± 849.8	5726.5 ± 1853.5
SERCA 1	3.4 ± 1.0	3.2 ± 1.4	4.0 ± 0.8	4.3 ± 1.4	6.9 ± 12.4	4.3 ± 1.6
SERCA 2a	2996.3 ± 447.5	4828.2 ± 2488.4	24160.0 ± 5543.6	22070.4 ± 5892.3	17556.9 ± 4539.7	30100.8 ± 17342.1
Sarcolipin	0.5 ± 0.4	0.6 ± 0.5	1.8 ± 0.9	1.7 ± 0.5	4.4 ± 9.7	3.7 ± 5.1
Dwarf Open Reading Frame	1.0 ± 1.6	0.4 ± 0.4	4.1 ± 3.4	7.6 ± 18.2	4.9 ± 10.8	2.5 ± 2.2

N=4

All data are represented as mean copies of transcript/ng of cDNA used in the reaction.

***,** significantly different from normal

Table 5.2. Left Ventricle calcium handling transcript levels in male vs female canines.

	Normal		Affected	
	Male	Female	Male	Female
Calreticulin	1225.4 ± 203.5	611.0 ± 42.1*	1188.0 ± 362.3	595.8 ± 126.3*
Calsequestrin 2	7167.9 ± 434.5	2935.1 ± 616.6*	6005.5 ± 1174.3	2482.8 ± 979.0*
Sarcalumenin	6201.1 ± 1956.8	2458.5 ± 88.6*	5773.4 ± 1256.9	1986.4 ± 390.7*
SERCA 1	4.0 ± 0.8	2.5 ± 1.2	4.3 ± 1.4	3.7 ± 3.0
SERCA 2a	24160.0 ± 5543.6	12304.6 ± 313.3*	22070.4 ± 5892.3	7413.3 ± 786.7*
Sarcolipin	1.8 ± 0.9	1.3 ± 1.0	1.7 ± 0.5	732.3 ± 21.1
Dwarf Open Reading Frame	4.1 ± 3.4	1.1 ± 1.1	7.6 ± 18.2	0.9 ± 0.7

N=3-4

All data are represented as mean copies of transcript/ng of cDNA used in the reaction.

***,** significantly different from male

Table 5.3. Diaphragm calcium handling transcript levels in normal vs dystrophic canines.

	0-2 Months		8-15 Months		30-50 Months	
	Normal	Affected	Normal	Affected	Normal	Affected
Calreticulin	685.4 ± 180.7	752.5 ± 142.6	525.5 ± 207.3	693.1 ± 594.7	398.4 ± 61.1	580.4 ± 190.8
Calsequestrin 2	1549.0 ± 1378.9	1453.2 ± 794.7	607.5 ± 434.5	2649.0 ± 2981.0	674.7 ± 102.9	3403.4 ± 732.4*
Sarcalumenin	2277.4 ± 1270.3	3113.2 ± 885.2	2555.4 ± 2008.0	1824.7 ± 1622.8	2160.0 ± 22.4	3117.3 ± 1027.7
SERCA 1	15831.8 ± 10741.1	6998.0 ± 4712.5	15115.7 ± 11597.3	2408.9 ± 4202.6*	19856.2 ± 5151.4	9595.8 ± 5728.5
SERCA 2a	9500.9 ± 8385.2	4307.4 ± 4954.8	21951.6 ± 19302.9	7078.4 ± 7320.0*	15699.3 ± 8398.6	16719.7 ± 3083.7
Sarcolipin	29874.6 ± 17619.1	15036.0 ± 10596.5	14855.3 ± 12117.7	9377.4 ± 8919.1	17728.4 ± 4212.1	17106.9 ± 10567.1
Dwarf Open Reading Frame	24798.9 ± 19250.1	4882.7 ± 7316.4*	25349.1 ± 20111.0	4706.9 ± 4235.2*	16888.2 ± 3480.4	10956.4 ± 5385.7

N=4

All data are represented as mean copies of transcript/ng of cDNA used in the reaction.

***,** significantly different from normal

Table 5.4. Diaphragm calcium handling transcript levels in male vs female canines.

	Normal		Affected	
	Male	Female	Male	Female
Calreticulin	525.5 ± 207.3	312.5 ± 237.4	693.1 ± 594.7	732.3 ± 617.5
Calsequestrin 2	607.5 ± 434.5	475.6 ± 454.5	2649.0 ± 2980.9	1688.5 ± 1627.4
Sarcalumenin	2555.4 ± 2007.9	1303.6 ± 1227.5	1824.7 ± 1622.8	1229.9 ± 1047.0
SERCA 1	15115.7 ± 11597.3	15414.0 ± 12128.8	2408.9 ± 4202.6	1376.4 ± 1286.9
SERCA 2a	21951.6 ± 19302.9	10933.6 ± 9587.7	7078.4 ± 7320.0	5542.3 ± 5457.2
Sarcolipin	14855.3 ± 12117.7	14246.6 ± 10463.4	9377.4 ± 8919.1	7989.8 ± 7926.2
Dwarf Open Reading Frame	25349.1 ± 20111.0	15468.0 ± 13507.5	4706.9 ± 4235.2	3333.8 ± 3284.9

N=3-4

All data are represented as mean copies of transcript/ng of cDNA used in the reaction.

***,** significantly different from male

Table 5.5. ECU calcium handling transcript levels in normal vs dystrophic canines.

	0-2 Months		8-15 Months		30-50 Months	
	Normal	Affected	Normal	Affected	Normal	Affected
Calreticulin	370.8 ± 291.0	842.4 ± 332.9	596.3 ± 157.7	379.0 ± 349.1	370.8 ± 88.4	519.1 ± 85.1
Calsequestrin 2	2280.6 ± 1169.5	3147.9 ± 1926.3	947.5 ± 245.2	892.9 ± 1150.0	693.0 ± 257.5	1467.3 ± 638.6
Sarcalumenin	1709.6 ± 1268.8	1238.6 ± 538.0	4174.8 ± 662.9	1549.0 ± 1270.1*	2030.1 ± 309.9	3277.3 ± 855.2
SERCA 1	19984.5 ± 7324.7	11579.6 ± 6626.1	32123.8 ± 19020.0	11042.4 ± 7014.9*	25990.7 ± 17261.2	46421.1 ± 19482.3*
SERCA 2a	7472.0 ± 11996.6	5177.6 ± 6043.0	42473.4 ± 12206.5	8397.1 ± 1674.9*	25267.3 ± 2920.2	21783.5 ± 11239.8
Sarcolipin	26490.5 ± 7917.4	18677.1 ± 8858.2	17332.2 ± 6295.7	12241.5 ± 12932.8	18477.1 ± 9401.7	20159.1 ± 16002.4
Dwarf Open Reading Frame	19302.6 ± 18542.8	6074.7 ± 10714.8	25521.3 ± 9321.6	7491.2 ± 743.5*	21286.6 ± 9415.8	9508.4 ± 5695.1

N=4

All data are represented as mean copies of transcript/ng of cDNA used in the reaction.

***,** significantly different from normal

Table 5.6. ECU calcium handling transcript levels in male vs female canines.

	Normal		Affected	
	Male	Female	Male	Female
Calreticulin	596.3 ± 157.7	357.3 ± 47.6	379.0 ± 349.1	427.0 ± 220.7
Calsequestrin 2	947.5 ± 245.2	380.4 ± 172.9	892.9 ± 1150.0	685.4 ± 170.2
Sarcalumenin	4174.8 ± 662.9	1955.6 ± 525.4*	1549.0 ± 1270.1	970.1 ± 597.2
SERCA 1	32123.8 ± 19020.0	37722.0 ± 3552.8	11042.4 ± 7014.9	22844.4 ± 13414.9
SERCA 2a	42473.4 ± 12206.5	13238.3 ± 4897.6*	8397.1 ± 1674.9	3816.3 ± 3254.3
Sarcolipin	17332.2 ± 6295.7	18121.8 ± 3644.5	12241.5 ± 12932.8	13958.3 ± 9994.9
Dwarf Open Reading Frame	25521.3 ± 9321.6	10370.1 ± 5031.3*	7491.2 ± 743.5	3667.7 ± 4990.7

N=3-4

All data are represented as mean copies of transcript/ng of cDNA used in the reaction.

***,** significantly different from male

Chapter 6. Discussion

Emily D. Morales[1]

[1], Department of Molecular Microbiology and Immunology, School of Medicine, The University of Missouri, Columbia, MO 65212

Discussion

In the present studies, we evaluated DWORF expression in the mdx mouse model of DMD, explored the effects of a novel AAV9 DWORF gene therapy in both WT and mdx mice, and analyzed the expression levels of various transcripts encoding calcium handling proteins in the canine model of DMD. All treated mice were injected via the tail vein at 6 weeks of age with 6×10^{12} vg/mouse of AAV9.DWORF vector. Collectively, these studies led to the following findings: (1) DWORF is downregulated in mdx cardiac and skeletal muscles, (2) AAV DWORF gene therapy significantly improved SR calcium uptake, cardiac function, and fibrosis in mdx mouse hearts, (3) AAV DWORF gene therapy reduced SR calcium uptake, induced ventricular SLN expression, and worsened cardiac function in WT mouse hearts, (4) AAV DWORF gene therapy did not alter diaphragm force production or histology but slowed maximum rates of contraction and relaxation in treated mdx mice, and (5) several transcriptional differences exist between normal and dystrophic canine muscle samples and between male and female samples from both normal and affected groups. As a whole, the studies presented here suggest DWORF downregulation contributes to SERCA dysfunction in dystrophic tissues and DWORF gene therapy holds promise to treat DMD, especially DMD cardiomyopathy. However, there are apparent differences in the regulation of SERCA regulators between WT and mdx mice and in the ways cardiac and skeletal muscles respond to AAV DWORF gene therapy. Further work needs to be done to optimize SERCA activation/inhibition to best treat DMD. In addition, further studies

need to be conducted to elucidate the mechanisms behind calcium dysregulation in dystrophic canines, as this model more closely resembles DMD in human patients.

DWORF, a small peptide enhancer of SERCA, has received recent attention for playing a role in cardiomyopathy development and treatment. DWORF was downregulated in two independent mouse models of heart failure(Makarewich et al., 2020; Makarewich et al., 2018). DWORF overexpression in these models via a transgenic approach or AAV9.DWORF delivery enhanced SERCA activity and improved cardiac function in these mice.

Our initial study analyzing DWORF's role in DMD cardiomyopathy **(Chapter 2)** was conducted in response to these recent findings. We discovered DWORF expression was also reduced in the hearts of mdx mice by ~50% compared to WT mice **(Figure 2.1)**. We then showed a single dose of AAV DWORF gene therapy at 6 weeks of age significantly improved SR calcium uptake, myocardial histology, uphill treadmill running, ECG, and left ventricular hemodynamics at 18 months of age **(Figures 2.2 to 2.6)**. Our results corroborate the idea that low-level DWORF expression is likely insufficient for proper heart function.

Despite the significant improvements made following AAV gene therapy, SERCA calcium uptake and cardiac function in treated mdx mice were not fully normalized to WT levels **(Figure 2.2, Figures 2.4 to 2.6)**. This suggests DWORF downregulation is not the sole cause of reduced SERCA activity in mdx mice. It is possible that either DWORF has a lower binding affinity for SERCA compared to SLN, and thus cannot fully restore SERCA function, or there are additional yet unknown SERCA inhibition mechanisms that cannot be reversed by DWORF overexpression. No

alterations were found in the expression of other SR calcium-regulating proteins **(Figure 2.2C)**.

As the number of studies assessing the effects of DWORF overexpression in heart failure grows, it is important to consider the potentially negative effects of SERCA over-activation. Several recent studies suggest SERCA over-activation may lead to SR calcium leak, cardiac arrhythmias, and/or worsened muscle function(Fajardo et al., 2017; Law et al., 2018; Sato et al., 2021). Our second study **(Chapter 3)** was conducted in response to these findings.

In this study, we delivered AAV DWORF gene therapy to WT mice, whose endogenous DWORF expression is already at sufficient levels that are higher than those expressed in mdx mice **(Figure 2.1)**. In support of previous findings, AAV DWORF gene therapy worsened multiple ECG and left ventricular hemodynamic parameters in WT mice **(Figures 3.5 to 3.6)**. To our surprise, however, AAV DWORF gene therapy induced SLN expression in the ventricles, despite SLN expression being specific to the atria in un-treated WT mice **(Figure 3.2B)**(Babu et al., 2007; Minamisawa et al., 2003). This increase in SLN expression is likely responsible for the decreased SERCA calcium uptake observed in treated mice in the presence of high calcium concentrations **(Figure 3.1C)**. These results suggest delivery of supraphysiological levels of DWORF may lead to cardiac defects in mouse hearts, and a feedback mechanism exists in WT mice where SLN expression is upregulated in response to increased levels of DWORF. This response appears to be lost in mdx mice, as SLN expression is un-altered in treated mdx mice **(Figure 2.2C)**.

Our third study **(Chapter 4)** is the first to assess the effects of AAV DWORF gene therapy in skeletal muscle. We found DWORF expression was reduced by ~77% in mdx diaphragm compared to WT **(Figure 4.1B)**. Following the discovery that DWORF overexpression in the heart led to negative effects in treated WT mice, we delivered AAV DWORF gene therapy to both WT and mdx mice here. AAV DWORF gene therapy had no effect on diaphragm force production or histology in either treated group **(Figures 4.3 to 4.4)**. However, DWORF gene therapy slowed maximum rates of muscle contraction and relaxation in treated mdx mice only **(Figure 4.3B, Figure 4.5)**. This again shows a difference in the mechanisms behind SERCA regulation between WT and mdx mice. Currently, it is unknown whether this finding is due to altered expression of other calcium handling proteins, fiber type switching, or some other unknown mechanism.

Collectively, these three studies suggest DWORF downregulation contributes to SERCA dysfunction in mdx mice, and AAV DWORF gene therapy holds promise to treat DMD, especially DMD cardiomyopathy. However, several hurdles stand in the way. First, AAV DWORF gene therapy was unable to fully restore SERCA calcium uptake and cardiac function in the mdx heart. Second, DWORF overexpression has the potential to worsen SERCA calcium uptake and cardiac function under WT conditions. Third, AAV DWORF gene therapy was unable to rescue diaphragm function and histology.

In order to improve AAV DWORF gene therapy for use in DMD, several approaches may be explored. One approach is to alter AAV DWORF gene therapy dose. On the surface, increasing the dose of AAV DWORF gene therapy seems promising. Makarewich and colleagues found that ~60-fold DWORF overexpression in a mouse model of dilated cardiomyopathy was more protective than ~17-fold DWORF

overexpression(Makarewich et al., 2020; Makarewich et al., 2018). However, increasing AAV dose may lead to adverse events or death(Srivastava, 2020). In addition, a study performed *ex vivo* in isolated rat hearts shows high-dose DWORF peptide administration may induce coronary vasoconstriction(Mbikou et al., 2020). Our study in WT mice suggests SERCA overactivation may also have a negative impact on the heart, although it is currently unclear whether this will occur in dystrophic hearts treated with a higher dose.

In skeletal muscle, it is possible the level of DWORF expression in treated mice was not enough to impact muscle function or histology. DWORF expression was increased by ~22-fold in treated mdx mouse diaphragms compared with mdx controls, whereas DWORF expression was increased by ~50-fold in treated mdx mouse hearts compared with mdx controls. This may be due to the preference of AAV9 for cardiac tissue or a loss of the AAV9.DWORF vector during profound tissue degeneration and regeneration that occurs in dystrophic skeletal muscle, but not cardiac muscle(Bostick et al., 2007; Srivastava, 2016). An alternative approach to increasing AAV DWORF dosage in skeletal muscle is to determine AAV serotypes or promoters with greater skeletal muscle tropism and expression.

However, it is possible that DWORF expression in treated skeletal muscles was not too low, but rather too high to achieve improved diaphragm function and histology. Previous work done by Voit and colleagues shows genetic ablation of SLN in dystrophin mutant and dystrophin/utrophin double mutant mice (mdx:utr −/−:sln −/−) improved cardiac performance and fibrosis but did not improve diaphragm performance and fibrosis(Voit et al., 2017). SLN haploinsufficient mice (mdx:utr −/− :sln +/−) mice, on

the other hand, exhibited significantly improved diaphragm function and fibrosis. This suggests lower levels of SERCA activation may be beneficial in skeletal muscle.

Another approach to improving AAV DWORF gene therapy is to combine DWORF overexpression with SLN knockdown. This approach will theoretically enhance SERCA activation. Again, we are not in favor of this approach as SERCA over-activation has been shown to have negative consequences on muscle function. In a study conducted by Law and colleagues, ablation of the SERCA inhibitor PLN in mdx mice worsened cardiac function and fibrosis (Law et al., 2018). In skeletal muscle, total ablation of SLN from the mdx mouse model of DMD resulted in worsened skeletal muscle disease(Fajardo et al., 2017).

A third approach to improving AAV DWORF gene therapy is to combine DWORF with micro-dystrophin gene therapy in a single AAV vector. This will combine a re-establishment of the linkage between the cytoskeleton, plasma membrane, and extracellular matrix with improved SERCA activation. DWORF's unique size (102 bp) makes it possible to package into a single vector alongside other therapies. Future studies will need to be conducted to determine which therapy is superior: micro-dystrophin alone, DWORF alone, or a micro-dystrophin/DWORF combination therapy.

In order to administer future calcium pathway-targeting therapies to human patients, more work needs to be done to elucidate calcium handling mechanisms in a large animal model of DMD, such as the dystrophic canine. This is why we conducted our final study assessing transcriptional differences in normal and affected canine tissues **(Chapter 5)**. In this study, we assessed transcript levels of three calcium-sequestering proteins (calreticulin, calsequestrin 2, sarcalumenin), two SERCA isoforms (SERCA 1,

SERCA 2a), and two SERCA regulators (SLN, DWORF). Tissues were collected from canine left ventricle, diaphragm, and extensor carpi ulnaris (ECU). Male samples were analyzed at three different age groups to illustrate expressional changes during disease progression. In addition, male and female comparisons were made from normal and affected canines in the middle age group. Transcriptional changes in dystrophic tissues were detected in skeletal muscle only, but changes in male vs female tissues mainly occurred within the heart. More work needs to be done to assess changes in canine protein expression.

In summary, the studies presented here are the first to show DWORF downregulation plays a role in SERCA dysfunction in dystrophic cardiac and skeletal muscle and that AAV DWORF gene therapy is a promising technique to treat DMD. In addition, they show that transcriptional changes exist between normal and dystrophic canines and between male and female canines. Although AAV DWORF gene therapy appears to be a promising treatment for DMD, several unknowns remain. One unknown is why ventricular SLN is expressed in response to AAV DWORF gene therapy in treated WT hearts but not in treated mdx hearts. It is also unknown why AAV DWORF gene therapy only partially rescued cardiac performance and fibrosis and did not rescue skeletal performance and fibrosis at all. In addition, our findings in dystrophic canines show more work needs to be done to assess changes in dystrophic canine calcium handling protein expression. They also highlight the importance of considering animal age and sex in dystrophic canine studies. In future studies, we plan to include direct cytosolic calcium measurements to better understand our findings following administration of DWORF AAV gene therapy. These studies will shed light on whether

AAV DWORF gene therapy can be improved, translated to canine models, and eventually delivered to human patients.

References

Allen, D. G., & Whitehead, N. P. (2011). Duchenne muscular dystrophy--what causes the increased membrane permeability in skeletal muscle? *Int J Biochem Cell Biol*, *43*(3), 290-294. https://doi.org/10.1016/j.biocel.2010.11.005

Allen, D. G., Whitehead, N. P., & Froehner, S. C. (2016). Absence of Dystrophin Disrupts Skeletal Muscle Signaling: Roles of Ca2+, Reactive Oxygen Species, and Nitric Oxide in the Development of Muscular Dystrophy. *Physiol Rev*, *96*(1), 253-305. https://doi.org/10.1152/physrev.00007.2015

Anderson, D. M., Anderson, K. M., Chang, C. L., Makarewich, C. A., Nelson, B. R., McAnally, J. R., Kasaragod, P., Shelton, J. M., Liou, J., Bassel-Duby, R., & Olson, E. N. (2015). A micropeptide encoded by a putative long noncoding RNA regulates muscle performance. *Cell*, *160*(4), 595-606. https://doi.org/10.1016/j.cell.2015.01.009

Andrews, N. W., Almeida, P. E., & Corrotte, M. (2014). Damage control: cellular mechanisms of plasma membrane repair. *Trends Cell Biol*, *24*(12), 734-742. https://doi.org/10.1016/j.tcb.2014.07.008

Arvanitis, D. A., Vafiadaki, E., Sanoudou, D., & Kranias, E. G. (2011). Histidine-rich calcium binding protein: the new regulator of sarcoplasmic reticulum calcium cycling. *J Mol Cell Cardiol*, *50*(1), 43-49. https://doi.org/10.1016/j.yjmcc.2010.08.021

Babu, G. J., Bhupathy, P., Carnes, C. A., Billman, G. E., & Periasamy, M. (2007). Differential expression of sarcolipin protein during muscle development and

cardiac pathophysiology. *J Mol Cell Cardiol*, *43*(2), 215-222. https://doi.org/10.1016/j.yjmcc.2007.05.009

Balakrishnan, R., Mareedu, S., & Babu, G. J. (2022). Reducing sarcolipin expression improves muscle metabolism in mdx mice. *Am J Physiol Cell Physiol*, *322*(2), C260-C274. https://doi.org/10.1152/ajpcell.00125.2021

Beard, N. A., Laver, D. R., & Dulhunty, A. F. (2004). Calsequestrin and the calcium release channel of skeletal and cardiac muscle. *Prog Biophys Mol Biol*, *85*(1), 33-69. https://doi.org/10.1016/j.pbiomolbio.2003.07.001

Bellinger, A. M., Reiken, S., Carlson, C., Mongillo, M., Liu, X., Rothman, L., Matecki, S., Lacampagne, A., & Marks, A. R. (2009). Hypernitrosylated ryanodine receptor calcium release channels are leaky in dystrophic muscle. *Nat Med*, *15*(3), 325-330. https://doi.org/10.1038/nm.1916

Bernstein, D. (2003). Exercise assessment of transgenic models of human cardiovascular disease. *Physiol Genomics*, *13*(3), 217-226. https://doi.org/10.1152/physiolgenomics.00188.2002

Bhattacharya, S. K., Palmieri, G. M., Bertorini, T. E., & Nutting, D. F. (1982). The effects of diltiazem in dystrophic hamsters. *Muscle Nerve*, *5*(1), 73-78. https://doi.org/10.1002/mus.880050114

Bhupathy, P., Babu, G. J., & Periasamy, M. (2007). Sarcolipin and phospholamban as regulators of cardiac sarcoplasmic reticulum Ca2+ ATPase. *J Mol Cell Cardiol*, *42*(5), 903-911. https://doi.org/10.1016/j.yjmcc.2007.03.738

Boittin, F. X., Shapovalov, G., Hirn, C., & Ruegg, U. T. (2010). Phospholipase A2-derived lysophosphatidylcholine triggers Ca2+ entry in dystrophic skeletal muscle

fibers. *Biochem Biophys Res Commun*, *391*(1), 401-406. https://doi.org/10.1016/j.bbrc.2009.11.070

Bostick, B., Ghosh, A., Yue, Y., Long, C., & Duan, D. (2007). Systemic AAV-9 transduction in mice is influenced by animal age but not by the route of administration. *Gene Ther*, *14*(22), 1605-1609. https://doi.org/10.1038/sj.gt.3303029

Bostick, B., Yue, Y., & Duan, D. (2010). Gender influences cardiac function in the mdx model of Duchenne cardiomyopathy. *Muscle Nerve*, *42*(4), 600-603. https://doi.org/10.1002/mus.21763

Bostick, B., Yue, Y., & Duan, D. (2011). Phenotyping cardiac gene therapy in mice. *Methods Mol Biol*, *709*, 91-104. https://doi.org/10.1007/978-1-61737-982-6_6

Bostick, B., Yue, Y., Long, C., & Duan, D. (2008). Prevention of dystrophin-deficient cardiomyopathy in twenty-one-month-old carrier mice by mosaic dystrophin expression or complementary dystrophin/utrophin expression. *Circ Res*, *102*(1), 121-130. http://www.ncbi.nlm.nih.gov/entrez/query.fcgi?cmd=Retrieve&db=PubMed&dopt=Citation&list_uids=17967782

Bostick, B., Yue, Y., Long, C., Marschalk, N., Fine, D. M., Chen, J., & Duan, D. (2009). Cardiac expression of a mini-dystrophin that normalizes skeletal muscle force only partially restores heart function in aged Mdx mice. *Mol Ther*, *17*(2), 253-261. https://doi.org/10.1038/mt.2008.264

Burkholder, T. J., Fingado, B., Baron, S., & Lieber, R. L. (1994). Relationship between muscle fiber types and sizes and muscle architectural properties in the mouse hindlimb. *J Morphol*, *221*(2), 177-190.

Burr, A. R., Millay, D. P., Goonasekera, S. A., Park, K. H., Sargent, M. A., Collins, J., Altamirano, F., Philipson, K. D., Allen, P. D., Ma, J., López, J. R., & Molkentin, J. D. (2014). Na+ dysregulation coupled with Ca2+ entry through NCX1 promotes muscular dystrophy in mice. *Mol Cell Biol*, *34*(11), 1991-2002. https://doi.org/10.1128/mcb.00339-14

Burr, A. R., & Molkentin, J. D. (2015). Genetic evidence in the mouse solidifies the calcium hypothesis of myofiber death in muscular dystrophy. *Cell Death Differ*, *22*(9), 1402-1412. https://doi.org/10.1038/cdd.2015.65

Cea, L. A., Puebla, C., Cisterna, B. A., Escamilla, R., Vargas, A. A., Frank, M., Martínez-Montero, P., Prior, C., Molano, J., Esteban-Rodríguez, I., Pascual, I., Gallano, P., Lorenzo, G., Pian, H., Barrio, L. C., Willecke, K., & Sáez, J. C. (2016). Fast skeletal myofibers of mdx mouse, model of Duchenne muscular dystrophy, express connexin hemichannels that lead to apoptosis. *Cell Mol Life Sci*, *73*(13), 2583-2599. https://doi.org/10.1007/s00018-016-2132-2

Cea, L. A., Riquelme, M. A., Cisterna, B. A., Puebla, C., Vega, J. L., Rovegno, M., & Sáez, J. C. (2012). Connexin- and pannexin-based channels in normal skeletal muscles and their possible role in muscle atrophy. *J Membr Biol*, *245*(8), 423-436. https://doi.org/10.1007/s00232-012-9485-8

Chakkalakal, J. V., Thompson, J., Parks, R. J., & Jasmin, B. J. (2005). Molecular, cellular, and pharmacological therapies for Duchenne/Becker muscular dystrophies. *Faseb j*, *19*(8), 880-891. https://doi.org/10.1096/fj.04-1956rev

Chambers, P. J., Juracic, E. S., Fajardo, V. A., & Tupling, A. R. (2022). Role of SERCA and sarcolipin in adaptive muscle remodeling. *Am J Physiol Cell Physiol*, *322*(3), C382-c394. https://doi.org/10.1152/ajpcell.00198.2021

Cheng, X., Zhang, X., Gao, Q., Ali Samie, M., Azar, M., Tsang, W. L., Dong, L., Sahoo, N., Li, X., Zhuo, Y., Garrity, A. G., Wang, X., Ferrer, M., Dowling, J., Xu, L., Han, R., & Xu, H. (2014). The intracellular Ca^{2+} channel MCOLN1 is required for sarcolemma repair to prevent muscular dystrophy. *Nat Med*, *20*(10), 1187-1192. https://doi.org/10.1038/nm.3611

Cheung, M. C., Spalding, P. B., Gutierrez, J. C., Balkan, W., Namias, N., Koniaris, L. G., & Zimmers, T. A. (2009). Body surface area prediction in normal, hypermuscular, and obese mice. *J Surg Res*, *153*(2), 326-331. https://doi.org/10.1016/j.jss.2008.05.002

Cho, C. H., Woo, J. S., Perez, C. F., & Lee, E. H. (2017). A focus on extracellular Ca(2+) entry into skeletal muscle. *Exp Mol Med*, *49*(9), e378. https://doi.org/10.1038/emm.2017.208

Cooper, S. T., & Head, S. I. (2015). Membrane Injury and Repair in the Muscular Dystrophies. *Neuroscientist*, *21*(6), 653-668. https://doi.org/10.1177/1073858414558336

Culligan, K., Banville, N., Dowling, P., & Ohlendieck, K. (2002). Drastic reduction of calsequestrin-like proteins and impaired calcium binding in dystrophic mdx

muscle. *J Appl Physiol (1985)*, *92*(2), 435-445. https://doi.org/10.1152/japplphysiol.00903.2001

Danialou, G., Comtois, A. S., Dudley, R., Karpati, G., Vincent, G., Des Rosiers, C., & Petrof, B. J. (2001). Dystrophin-deficient cardiomyocytes are abnormally vulnerable to mechanical stress-induced contractile failure and injury. *Faseb j*, *15*(9), 1655-1657. https://doi.org/10.1096/fj.01-0030fje

Denniss, A. L., Dashwood, A. M., Molenaar, P., & Beard, N. A. (2020). Sarcoplasmic reticulum calcium mishandling: central tenet in heart failure? *Biophys Rev*, *12*(4), 865-878. https://doi.org/10.1007/s12551-020-00736-y

Derler, I., Jardin, I., & Romanin, C. (2016). Molecular mechanisms of STIM/Orai communication. *Am J Physiol Cell Physiol*, *310*(8), C643-662. https://doi.org/10.1152/ajpcell.00007.2016

Deval, E., Levitsky, D. O., Marchand, E., Cantereau, A., Raymond, G., & Cognard, C. (2002). Na(+)/Ca(2+) exchange in human myotubes: intracellular calcium rises in response to external sodium depletion are enhanced in DMD. *Neuromuscul Disord*, *12*(7-8), 665-673. https://doi.org/10.1016/s0960-8966(02)00022-6

Divet, A., & Huchet-Cadiou, C. (2002). Sarcoplasmic reticulum function in slow- and fast-twitch skeletal muscles from mdx mice. *Pflugers Arch*, *444*(5), 634-643. https://doi.org/10.1007/s00424-002-0854-5

Dowling, P., Doran, P., & Ohlendieck, K. (2004). Drastic reduction of sarcalumenin in Dp427 (dystrophin of 427 kDa)-deficient fibres indicates that abnormal calcium handling plays a key role in muscular dystrophy. *Biochem J*, *379*(Pt 2), 479-488. https://doi.org/10.1042/bj20031311

Duan, D. (2006). Challenges and opportunities in dystrophin-deficient cardiomyopathy gene therapy. *Hum Mol Genet, 15 Spec No 2,* R253-261. https://doi.org/15/suppl_2/R253 [pii]

10.1093/hmg/ddl180

Duan, D. (2015). Duchenne muscular dystrophy gene therapy in the canine model. *Hum Gene Ther Clin Dev*, *26*(1), 57-69. https://doi.org/10.1089/humc.2015.006

Duan, D. (2018). Micro-dystrophin gene therapy goes systemic in Duchenne muscular dystrophy patients. *Hum Gene Ther*, *29*(7), 733-736. https://doi.org/10.1089/hum.2018.012

Duan, D., Goemans, N., Takeda, S., Mercuri, E., & Aartsma-Rus, A. (2021). Duchenne muscular dystrophy. *Nat Rev Dis Primers*, *7*(1), 13. https://doi.org/10.1038/s41572-021-00248-3

Duan, D., Goemans, N., Takeda, S., Mercuri, E., & Aartsma-Rus, A. (2021). Duchenne muscular dystrophy. *Nat Rev Dis Primers*, *7*, 13.

Duan, D., Rafael-Fortney, J. A., Blain, A., Kass, D. A., McNally, E. M., Metzger, J. M., Spurney, C. F., & Kinnett, K. (2016). Standard Operating Procedures (SOPs) for Evaluating the Heart in Preclinical Studies of Duchenne Muscular Dystrophy. *J Cardiovasc Transl Res*, *9*(1), 85-86. https://doi.org/10.1007/s12265-015-9669-6

Edwards, J. N., Friedrich, O., Cully, T. R., von Wegner, F., Murphy, R. M., & Launikonis, B. S. (2010). Upregulation of store-operated Ca2+ entry in dystrophic mdx mouse muscle. *Am J Physiol Cell Physiol*, *299*(1), C42-50. https://doi.org/10.1152/ajpcell.00524.2009

Ervasti, J. M., & Campbell, K. P. (1993). A role for the dystrophin-glycoprotein complex as a transmembrane linker between laminin and actin. *J Cell Biol*, *122*(4), 809-823. https://doi.org/10.1083/jcb.122.4.809

Fajardo, V. A., Chambers, P. J., Juracic, E. S., Rietze, B. A., Gamu, D., Bellissimo, C., Kwon, F., Quadrilatero, J., & Russell Tupling, A. (2018). Sarcolipin deletion in mdx mice impairs calcineurin signalling and worsens dystrophic pathology. *Hum Mol Genet*, *27*(23), 4094-4102. https://doi.org/10.1093/hmg/ddy302

Fajardo, V. A., Gamu, D., Mitchell, A., Bloemberg, D., Bombardier, E., Chambers, P. J., Bellissimo, C., Quadrilatero, J., & Tupling, A. R. (2017). Sarcolipin deletion exacerbates soleus muscle atrophy and weakness in phospholamban overexpressing mice. *PLoS One*, *12*(3), e0173708. https://doi.org/10.1371/journal.pone.0173708

Fauconnier, J., Thireau, J., Reiken, S., Cassan, C., Richard, S., Matecki, S., Marks, A. R., & Lacampagne, A. (2010). Leaky RyR2 trigger ventricular arrhythmias in Duchenne muscular dystrophy. *Proc Natl Acad Sci U S A*, *107*(4), 1559-1564. https://doi.org/10.1073/pnas.0908540107

Fisher, M. E., Bovo, E., Aguayo-Ortiz, R., Cho, E. E., Pribadi, M. P., Dalton, M. P., Rathod, N., Lemieux, M. J., Espinoza-Fonseca, L. M., Robia, S. L., Zima, A. V., & Young, H. S. (2021). Dwarf open reading frame (DWORF) is a direct activator of the sarcoplasmic reticulum calcium pump SERCA. *Elife*, *10*. https://doi.org/10.7554/eLife.65545

Franzini-Armstrong, C. (2018). The relationship between form and function throughout the history of excitation-contraction coupling. *J Gen Physiol*, *150*(2), 189-210. https://doi.org/10.1085/jgp.201711889

Friedrich, O., Both, M., Gillis, J. M., Chamberlain, J. S., & Fink, R. H. (2004). Mini-dystrophin restores L-type calcium currents in skeletal muscle of transgenic mdx mice. *J Physiol*, *555*(Pt 1), 251-265. https://doi.org/10.1113/jphysiol.2003.054213

Gao, Q. Q., & McNally, E. M. (2015). The Dystrophin Complex: Structure, Function, and Implications for Therapy. *Compr Physiol*, *5*(3), 1223-1239. https://doi.org/10.1002/cphy.c140048

Gehlert, S., Bloch, W., & Suhr, F. (2015). Ca2+-dependent regulations and signaling in skeletal muscle: from electro-mechanical coupling to adaptation. *Int J Mol Sci*, *16*(1), 1066-1095. https://doi.org/10.3390/ijms16011066

Gervásio, O. L., Whitehead, N. P., Yeung, E. W., Phillips, W. D., & Allen, D. G. (2008). TRPC1 binds to caveolin-3 and is regulated by Src kinase - role in Duchenne muscular dystrophy. *J Cell Sci*, *121*(Pt 13), 2246-2255. https://doi.org/10.1242/jcs.032003

Gonzalez, J. P., Ramachandran, J., Himelman, E., Badr, M. A., Kang, C., Nouet, J., Fefelova, N., Xie, L. H., Shirokova, N., Contreras, J. E., & Fraidenraich, D. (2018). Normalization of connexin 43 protein levels prevents cellular and functional signs of dystrophic cardiomyopathy in mice. *Neuromuscul Disord*, *28*(4), 361-372. https://doi.org/10.1016/j.nmd.2018.01.012

Goonasekera, S. A., Lam, C. K., Millay, D. P., Sargent, M. A., Hajjar, R. J., Kranias, E. G., & Molkentin, J. D. (2011). Mitigation of muscular dystrophy in mice by

SERCA overexpression in skeletal muscle. *J Clin Invest*, *121*(3), 1044-1052. https://doi.org/10.1172/jci43844

Górecki, D. C. (2019). P2X7 purinoceptor as a therapeutic target in muscular dystrophies. *Curr Opin Pharmacol*, *47*, 40-45. https://doi.org/10.1016/j.coph.2019.02.003

Groenendyk, J., Wang, W. A., Robinson, A., & Michalak, M. (2022). Calreticulin and the Heart. *Cells*, *11*(11). https://doi.org/10.3390/cells11111722

Guo, L. J., Soslow, J. H., Bettis, A. K., Nghiem, P. P., Cummings, K. J., Lenox, M. W., Miller, M. W., Kornegay, J. N., & Spurney, C. F. (2019). Natural History of Cardiomyopathy in Adult Dogs With Golden Retriever Muscular Dystrophy. *J Am Heart Assoc*, *8*(16), e012443. https://doi.org/10.1161/jaha.119.012443

Hakim, C. H., Lessa, T. B., Jenkins, G. J., Yang, N. N., Ambrosio, C. E., & Duan, D. (2019). An improved method for studying mouse diaphragm function. *Sci Rep*, *9*(1), 19453. https://doi.org/10.1038/s41598-019-55704-8

Hakim, C. H., Yang, H. T., Burke, M. J., Teixeira, J., Jenkins, G. J., Yang, N. N., Yao, G., & Duan, D. (2021). Extensor carpi ulnaris muscle shows unexpected slow-to-fast fiber-type switch in Duchenne muscular dystrophy dogs. *Dis Model Mech*, *14*(12). https://doi.org/10.1242/dmm.049006

Himelman, E., Lillo, M. A., Nouet, J., Gonzalez, J. P., Zhao, Q., Xie, L. H., Li, H., Liu, T., Wehrens, X. H., Lampe, P. D., Fishman, G. I., Shirokova, N., Contreras, J. E., & Fraidenraich, D. (2020). Prevention of connexin-43 remodeling protects against Duchenne muscular dystrophy cardiomyopathy. *J Clin Invest*, *130*(4), 1713-1727. https://doi.org/10.1172/jci128190

Hirn, C., Shapovalov, G., Petermann, O., Roulet, E., & Ruegg, U. T. (2008). Nav1.4 deregulation in dystrophic skeletal muscle leads to Na+ overload and enhanced cell death. *J Gen Physiol*, *132*(2), 199-208. https://doi.org/10.1085/jgp.200810024

Hopf, F. W., Turner, P. R., Denetclaw, W. F., Jr., Reddy, P., & Steinhardt, R. A. (1996a). A critical evaluation of resting intracellular free calcium regulation in dystrophic mdx muscle. *Am J Physiol*, *271*(4 Pt 1), C1325-1339. https://doi.org/10.1152/ajpcell.1996.271.4.C1325

Hopf, F. W., Turner, P. R., Denetclaw, W. F., Jr., Reddy, P., & Steinhardt, R. A. (1996b). A critical evaluation of resting intracellular free calcium regulation in dystrophic mdx muscle. *Am J Physiol*, *271*(4 Pt 1), C1325-1339.

Hussain, T., Mangath, H., Sundaram, C., & Anandaraj, M. P. J. S. (2000). Expression of the gene for large subunit of m-calpain is elevated in skeletal muscle from Duchenne muscular dystrophy patients. *Journal of Genetics*, *79*(2), 77. https://doi.org/10.1007/BF02728949

Iwata, Y., Katanosaka, Y., Arai, Y., Shigekawa, M., & Wakabayashi, S. (2009). Dominant-negative inhibition of Ca2+ influx via TRPV2 ameliorates muscular dystrophy in animal models. *Hum Mol Genet*, *18*(5), 824-834. https://doi.org/10.1093/hmg/ddn408

Iwata, Y., Katanosaka, Y., Hisamitsu, T., & Wakabayashi, S. (2007). Enhanced Na+/H+ exchange activity contributes to the pathogenesis of muscular dystrophy via involvement of P2 receptors. *Am J Pathol*, *171*(5), 1576-1587. https://doi.org/10.2353/ajpath.2007.070452

Jiao, Q., Takeshima, H., Ishikawa, Y., & Minamisawa, S. (2012). Sarcalumenin plays a critical role in age-related cardiac dysfunction due to decreases in SERCA2a expression and activity. *Cell Calcium*, *51*(1), 31-39. https://doi.org/10.1016/j.ceca.2011.10.003

Kargacin, M. E., & Kargacin, G. J. (1996). The sarcoplasmic reticulum calcium pump is functionally altered in dystrophic muscle. *Biochim Biophys Acta*, *1290*(1), 4-8. https://doi.org/10.1016/0304-4165(95)00180-8

Kim, J. H., Kwak, H. B., Thompson, L. V., & Lawler, J. M. (2013). Contribution of oxidative stress to pathology in diaphragm and limb muscles with Duchenne muscular dystrophy. *J Muscle Res Cell Motil*, *34*(1), 1-13. https://doi.org/10.1007/s10974-012-9330-9

Koenig, M., Monaco, A. P., & Kunkel, L. M. (1988). The complete sequence of dystrophin predicts a rod-shaped cytoskeletal protein. *Cell*, *53*(2), 219-228. https://doi.org/10.1016/0092-8674(88)90383-2

Koenig, X., Rubi, L., Obermair, G. J., Cervenka, R., Dang, X. B., Lukacs, P., Kummer, S., Bittner, R. E., Kubista, H., Todt, H., & Hilber, K. (2014). Enhanced currents through L-type calcium channels in cardiomyocytes disturb the electrophysiology of the dystrophic heart. *Am J Physiol Heart Circ Physiol*, *306*(4), H564-h573. https://doi.org/10.1152/ajpheart.00441.2013

Kuo, I. Y., & Ehrlich, B. E. (2015). Signaling in muscle contraction. *Cold Spring Harb Perspect Biol*, *7*(2), a006023. https://doi.org/10.1101/cshperspect.a006023

Law, M. L., Cohen, H., Martin, A. A., Angulski, A. B. B., & Metzger, J. M. (2020). Dysregulation of Calcium Handling in Duchenne Muscular Dystrophy-Associated

Dilated Cardiomyopathy: Mechanisms and Experimental Therapeutic Strategies. *J Clin Med*, *9*(2). https://doi.org/10.3390/jcm9020520

Law, M. L., Prins, K. W., Olander, M. E., & Metzger, J. M. (2018). Exacerbation of dystrophic cardiomyopathy by phospholamban deficiency mediated chronically increased cardiac Ca(2+) cycling in vivo. *Am J Physiol Heart Circ Physiol*, *315*(6), H1544-h1552. https://doi.org/10.1152/ajpheart.00341.2018

Li, A., Yuen, S. L., Stroik, D. R., Kleinboehl, E., Cornea, R. L., & Thomas, D. D. (2021). The transmembrane peptide DWORF activates SERCA2a via dual mechanisms. *J Biol Chem*, *296*, 100412. https://doi.org/10.1016/j.jbc.2021.100412

Lindahl, M., Backman, E., Henriksson, K. G., Gorospe, J. R., & Hoffman, E. P. (1995). Phospholipase A2 activity in dystrophinopathies. *Neuromuscul Disord*, *5*(3), 193-199.

Lindahl, M., Bäckman, E., Henriksson, K. G., Gorospe, J. R., & Hoffman, E. P. (1995). Phospholipase A2 activity in dystrophinopathies. *Neuromuscul Disord*, *5*(3), 193-199. https://doi.org/10.1016/0960-8966(94)00045-b

Lohan, J., & Ohlendieck, K. (2004). Drastic reduction in the luminal Ca2+ -binding proteins calsequestrin and sarcalumenin in dystrophin-deficient cardiac muscle. *Biochim Biophys Acta*, *1689*(3), 252-258. https://doi.org/10.1016/j.bbadis.2004.04.002

MacLennan, D. H., & Kranias, E. G. (2003). Phospholamban: a crucial regulator of cardiac contractility. *Nat Rev Mol Cell Biol*, *4*(7), 566-577. https://doi.org/10.1038/nrm1151

Makarewich, C. A., Bezprozvannaya, S., Gibson, A. M., Bassel-Duby, R., & Olson, E. N. (2020). Gene Therapy With the DWORF Micropeptide Attenuates Cardiomyopathy in Mice. *Circ Res*, *127*(10), 1340-1342. https://doi.org/10.1161/CIRCRESAHA.120.317156

Makarewich, C. A., Munir, A. Z., Schiattarella, G. G., Bezprozvannaya, S., Raguimova, O. N., Cho, E. E., Vidal, A. H., Robia, S. L., Bassel-Duby, R., & Olson, E. N. (2018). The DWORF micropeptide enhances contractility and prevents heart failure in a mouse model of dilated cardiomyopathy. *Elife*, *7*. https://doi.org/10.7554/eLife.38319

Mareedu, S., Million, E. D., Duan, D., & Babu, G. J. (2021). Abnormal Calcium Handling in Duchenne Muscular Dystrophy: Mechanisms and Potential Therapies. *Front Physiol*, *12*, 647010. https://doi.org/10.3389/fphys.2021.647010

Mareedu, S., Pachon, R., Thilagavathi, J., Fefelova, N., Balakrishnan, R., Niranjan, N., Xie, L. H., & Babu, G. J. (2021). Sarcolipin haploinsufficiency prevents dystrophic cardiomyopathy in mdx mice. *Am J Physiol Heart Circ Physiol*, *320*(1), H200-h210. https://doi.org/10.1152/ajpheart.00601.2020

Matsumura, C. Y., Taniguti, A. P., Pertille, A., Santo Neto, H., & Marques, M. J. (2011). Stretch-activated calcium channel protein TRPC1 is correlated with the different degrees of the dystrophic phenotype in mdx mice. *Am J Physiol Cell Physiol*, *301*(6), C1344-1350. https://doi.org/10.1152/ajpcell.00056.2011

Mbikou, P., Rademaker, M. T., Charles, C. J., Richards, M. A., & Pemberton, C. J. (2020). Cardiovascular effects of DWORF (dwarf open reading frame) peptide in

normal and ischaemia/reperfused isolated rat hearts. *Peptides*, *124*, 170192. https://doi.org/10.1016/j.peptides.2019.170192

Mendell, J. R., & Lloyd-Puryear, M. (2013). Report of MDA muscle disease symposium on newborn screening for Duchenne muscular dystrophy. *Muscle Nerve*, *48*(1), 21-26. https://doi.org/10.1002/mus.23810

Mendez, J., & Keys, A. (1960). Density and composition of mammalian muscle. *Metabolism*, *9*, 184-188.

Mercuri, E., Bönnemann, C. G., & Muntoni, F. (2019). Muscular dystrophies. *Lancet*, *394*(10213), 2025-2038. https://doi.org/10.1016/s0140-6736(19)32910-1

Minamisawa, S., Wang, Y., Chen, J., Ishikawa, Y., Chien, K. R., & Matsuoka, R. (2003). Atrial chamber-specific expression of sarcolipin is regulated during development and hypertrophic remodeling. *J Biol Chem*, *278*(11), 9570-9575. https://doi.org/10.1074/jbc.m213132200

Mitchell, G. F., Jeron, A., & Koren, G. (1998a). Measurement of heart rate and Q-T interval in the conscious mouse. *Am J Physiol*, *274*(3), H747-751. https://doi.org/10.1152/ajpheart.1998.274.3.H747

Mitchell, G. F., Jeron, A., & Koren, G. (1998b). Measurement of heart rate and Q-T interval in the conscious mouse. *Am J Physiol*, *274*(3 Pt 2), H747-751. http://www.ncbi.nlm.nih.gov/entrez/query.fcgi?cmd=Retrieve&db=PubMed&dopt=Citation&list_uids=9530184

Morine, K. J., Sleeper, M. M., Barton, E. R., & Sweeney, H. L. (2010). Overexpression of SERCA1a in the mdx diaphragm reduces susceptibility to contraction-induced

damage. *Hum Gene Ther*, *21*(12), 1735-1739. https://doi.org/10.1089/hum.2010.077

Mullard, A. (2021). Sarepta's DMD gene therapy falls flat. *Nat Rev Drug Discov*, *20*(2), 91. https://doi.org/10.1038/d41573-021-00010-0

Nelson, B. R., Makarewich, C. A., Anderson, D. M., Winders, B. R., Troupes, C. D., Wu, F., Reese, A. L., McAnally, J. R., Chen, X., Kavalali, E. T., Cannon, S. C., Houser, S. R., Bassel-Duby, R., & Olson, E. N. (2016). A peptide encoded by a transcript annotated as long noncoding RNA enhances SERCA activity in muscle. *Science*, *351*(6270), 271-275. https://doi.org/10.1126/science.aad4076

Niranjan, N., Mareedu, S., Tian, Y., Kodippili, K., Fefelova, N., Voit, A., Xie, L. H., Duan, D., & Babu, G. J. (2019). Sarcolipin overexpression impairs myogenic differentiation in Duchenne muscular dystrophy. *Am J Physiol Cell Physiol*, *317*(4), C813-c824. https://doi.org/10.1152/ajpcell.00146.2019

Periasamy, M., & Kalyanasundaram, A. (2007). SERCA pump isoforms: their role in calcium transport and disease. *Muscle Nerve*, *35*(4), 430-442. https://doi.org/10.1002/mus.20745

Pertille, A., de Carvalho, C. L., Matsumura, C. Y., Neto, H. S., & Marques, M. J. (2010). Calcium-binding proteins in skeletal muscles of the mdx mice: potential role in the pathogenesis of Duchenne muscular dystrophy. *Int J Exp Pathol*, *91*(1), 63-71. https://doi.org/10.1111/j.1365-2613.2009.00688.x

Petrof, B. J., Shrager, J. B., Stedman, H. H., Kelly, A. M., & Sweeney, H. L. (1993). Dystrophin protects the sarcolemma from stresses developed during muscle

contraction. *Proc Natl Acad Sci U S A*, *90*(8), 3710-3714. https://doi.org/10.1073/pnas.90.8.3710

Plant, D. R., & Lynch, G. S. (2003). Depolarization-induced contraction and SR function in mechanically skinned muscle fibers from dystrophic mdx mice. *Am J Physiol Cell Physiol*, *285*(3), C522-528. https://doi.org/10.1152/ajpcell.00369.2002

Prosser, B. L., Ward, C. W., & Lederer, W. J. (2011). X-ROS signaling: rapid mechano-chemo transduction in heart. *Science*, *333*(6048), 1440-1445. https://doi.org/10.1126/science.1202768

Protasi, F. (2002). Structural interaction between RYRs and DHPRs in calcium release units of cardiac and skeletal muscle cells. *Front Biosci*, *7*, d650-658. https://doi.org/10.2741/a801

Reddy, U. V., Weber, D. K., Wang, S., Larsen, E. K., Gopinath, T., De Simone, A., Robia, S., & Veglia, G. (2022a). A kink in DWORF helical structure controls the activation of the sarcoplasmic reticulum Ca(2+)-ATPase. *Structure*, *30*(3), 360-370 e366. https://doi.org/10.1016/j.str.2021.11.003

Reddy, U. V., Weber, D. K., Wang, S., Larsen, E. K., Gopinath, T., De Simone, A., Robia, S., & Veglia, G. (2022b). A kink in DWORF helical structure controls the activation of the sarcoplasmic reticulum Ca(2+)-ATPase. *Structure*, *30*(3), 360-370.e366. https://doi.org/10.1016/j.str.2021.11.003

Ríos, E. (2018). Calcium-induced release of calcium in muscle: 50 years of work and the emerging consensus. *J Gen Physiol*, *150*(4), 521-537. https://doi.org/10.1085/jgp.201711959

Robin, G., Berthier, C., & Allard, B. (2012). Sarcoplasmic reticulum Ca2+ permeation explored from the lumen side in mdx muscle fibers under voltage control. *J Gen Physiol*, *139*(3), 209-218. https://doi.org/10.1085/jgp.201110738

Rossi, A. E., & Dirksen, R. T. (2006). Sarcoplasmic reticulum: the dynamic calcium governor of muscle. *Muscle Nerve*, *33*(6), 715-731. https://doi.org/10.1002/mus.20512

Sabourin, J., Lamiche, C., Vandebrouck, A., Magaud, C., Rivet, J., Cognard, C., Bourmeyster, N., & Constantin, B. (2009). Regulation of TRPC1 and TRPC4 cation channels requires an alpha1-syntrophin-dependent complex in skeletal mouse myotubes. *J Biol Chem*, *284*(52), 36248-36261. https://doi.org/10.1074/jbc.M109.012872

Sato, D., Uchinoumi, H., & Bers, D. M. (2021). Increasing SERCA function promotes initiation of calcium sparks and breakup of calcium waves. *J Physiol*, *599*(13), 3267-3278. https://doi.org/10.1113/jp281579

Schneider, J. S., Shanmugam, M., Gonzalez, J. P., Lopez, H., Gordan, R., Fraidenraich, D., & Babu, G. J. (2013a). Increased sarcolipin expression and decreased sarco(endo)plasmic reticulum Ca2+ uptake in skeletal muscles of mouse models of Duchenne muscular dystrophy. *J Muscle Res Cell Motil*, *34*(5-6), 349-356. https://doi.org/10.1007/s10974-013-9350-0

Schneider, J. S., Shanmugam, M., Gonzalez, J. P., Lopez, H., Gordan, R., Fraidenraich, D., & Babu, G. J. (2013b). Increased sarcolipin expression and decreased sarco(endo)plasmic reticulum Ca uptake in skeletal muscles of mouse models of

Duchenne muscular dystrophy. *J Muscle Res Cell Motil*, *34*(5-6), 349-356. https://doi.org/10.1007/s10974-013-9350-0

Shaikh, S. A., Sahoo, S. K., & Periasamy, M. (2016). Phospholamban and sarcolipin: Are they functionally redundant or distinct regulators of the Sarco(Endo)Plasmic Reticulum Calcium ATPase? *J Mol Cell Cardiol*, *91*, 81-91. https://doi.org/10.1016/j.yjmcc.2015.12.030

Shanmuga Sundaram, J., Mohana Rao, V., Meena, A. K., & Anandaraj, M. P. (2006). Altered expression, intracellular distribution and activity of lymphocyte calpain II in Duchenne muscular dystrophy. *Clin Chim Acta*, *373*(1-2), 82-87. https://doi.org/10.1016/j.cca.2006.05.004

Shannon, T. R. (2009). Ryanodine receptor Ca2+ sensitivity and excitation-contraction coupling in muscular dystrophy and heart failure: similar and yet different. *Am J Physiol Heart Circ Physiol*, *297*(6), H1965-1966. https://doi.org/10.1152/ajpheart.00945.2009

Shin, J.-H., Bostick, B., Yue, Y., Hajjar, R., & Duan, D. (2011). SERCA2a gene transfer improves electrocardiographic performance in aged mdx mice. *J Transl Med*, *9*, 132. https://doi.org/1479-5876-9-132 [pii]

10.1186/1479-5876-9-132

Shin, J.-H., Pan, X., Hakim, C. H., Yang, H. T., Yue, Y., Zhang, K., Terjung, R. L., & Duan, D. (2013). Microdystrophin ameliorates muscular dystrophy in the canine model of Duchenne muscular dystrophy. *Mol Ther*, *21*(4), 750-757. https://doi.org/10.1038/mt.2012.283

Shin, J.-H., Yue, Y., & Duan, D. (2012). Recombinant adeno-associated viral vector production and purification. *Methods Mol Biol*, *798*, 267-284. https://doi.org/10.1007/978-1-61779-343-1_15

Shin, J. H., Bostick, B., Yue, Y., Hajjar, R., & Duan, D. (2011). SERCA2a gene transfer improves electrocardiographic performance in aged mdx mice. *J Transl Med*, *9*, 132. https://doi.org/10.1186/1479-5876-9-132

Shin, J. H., Yue, Y., & Duan, D. (2012). Recombinant adeno-associated viral vector production and purification. *Methods Mol Biol*, *798*, 267-284. https://doi.org/10.1007/978-1-61779-343-1_15

Singh, D. R., Dalton, M. P., Cho, E. E., Pribadi, M. P., Zak, T. J., Seflova, J., Makarewich, C. A., Olson, E. N., & Robia, S. L. (2019). Newly Discovered Micropeptide Regulators of SERCA Form Oligomers but Bind to the Pump as Monomers. *J Mol Biol*, *431*(22), 4429-4443. https://doi.org/10.1016/j.jmb.2019.07.037

Singh, D. R., Dalton, M. P., Cho, E. E., Pribadi, M. P., Zak, T. J., Šeflová, J., Makarewich, C. A., Olson, E. N., & Robia, S. L. (2019). Newly Discovered Micropeptide Regulators of SERCA Form Oligomers but Bind to the Pump as Monomers. *J Mol Biol*, *431*(22), 4429-4443. https://doi.org/10.1016/j.jmb.2019.07.037

Smani, T., Zakharov, S. I., Csutora, P., Leno, E., Trepakova, E. S., & Bolotina, V. M. (2004). A novel mechanism for the store-operated calcium influx pathway. *Nat Cell Biol*, *6*(2), 113-120. https://doi.org/10.1038/ncb1089

Smani, T., Zakharov, S. I., Leno, E., Csutora, P., Trepakova, E. S., & Bolotina, V. M. (2003). Ca2+-independent phospholipase A2 is a novel determinant of store-operated Ca2+ entry. *J Biol Chem*, *278*(14), 11909-11915. https://doi.org/10.1074/jbc.M210878200

Spencer, M. J., & Mellgren, R. L. (2002). Overexpression of a calpastatin transgene in mdx muscle reduces dystrophic pathology. *Hum Mol Genet*, *11*(21), 2645-2655. https://doi.org/10.1093/hmg/11.21.2645

Srivastava, A. (2016). In vivo tissue-tropism of adeno-associated viral vectors. *Curr Opin Virol*, *21*, 75-80. https://doi.org/10.1016/j.coviro.2016.08.003

Srivastava, A. (2020). AAV Vectors: Are They Safe? *Hum Gene Ther*, *31*(13-14), 697-699. https://doi.org/10.1089/hum.2020.187

Turner, P. R., Westwood, T., Regen, C. M., & Steinhardt, R. A. (1988). Increased protein degradation results from elevated free calcium levels found in muscle from mdx mice. *Nature*, *335*(6192), 735-738. https://doi.org/10.1038/335735a0

Vandebrouck, A., Sabourin, J., Rivet, J., Balghi, H., Sebille, S., Kitzis, A., Raymond, G., Cognard, C., Bourmeyster, N., & Constantin, B. (2007). Regulation of capacitative calcium entries by alpha1-syntrophin: association of TRPC1 with dystrophin complex and the PDZ domain of alpha1-syntrophin. *Faseb j*, *21*(2), 608-617. https://doi.org/10.1096/fj.06-6683com

Voit, A., Patel, V., Pachon, R., Shah, V., Bakhutma, M., Kohlbrenner, E., McArdle, J. J., Dell'Italia, L. J., Mendell, J. R., Xie, L. H., Hajjar, R. J., Duan, D., Fraidenraich, D., & Babu, G. J. (2017). Reducing sarcolipin expression mitigates Duchenne

muscular dystrophy and associated cardiomyopathy in mice. *Nat Commun*, *8*(1), 1068. https://doi.org/10.1038/s41467-017-01146-7

Wang, Q., Wang, W., Wang, G., Rodney, G. G., & Wehrens, X. H. (2015). Crosstalk between RyR2 oxidation and phosphorylation contributes to cardiac dysfunction in mice with Duchenne muscular dystrophy. *J Mol Cell Cardiol*, *89*(Pt B), 177-184. https://doi.org/10.1016/j.yjmcc.2015.11.009

Wasala, N. B., Yue, Y., Lostal, W., Wasala, L. P., Niranjan, N., Hajjar, R. J., Babu, G. J., & Duan, D. (2020). Single SERCA2a Therapy Ameliorated Dilated Cardiomyopathy for 18 Months in a Mouse Model of Duchenne Muscular Dystrophy. *Mol Ther*, *28*(3), 845-854. https://doi.org/10.1016/j.ymthe.2019.12.011

Weiss, J. L., Frederiksen, J. W., & Weisfeldt, M. L. (1976). Hemodynamic determinants of the time-course of fall in canine left ventricular pressure. *J Clin Invest*, *58*(3), 751-760. https://doi.org/10.1172/JCI108522

Williams, I. A., & Allen, D. G. (2007). The role of reactive oxygen species in the hearts of dystrophin-deficient mdx mice. *Am J Physiol Heart Circ Physiol*, *293*(3), H1969-1977. https://doi.org/10.1152/ajpheart.00489.2007

Woo, J. S., Jeong, S. Y., Park, J. H., Choi, J. H., & Lee, E. H. (2020). Calsequestrin: a well-known but curious protein in skeletal muscle. *Exp Mol Med*, *52*(12), 1908-1925. https://doi.org/10.1038/s12276-020-00535-1

Xu, H., & Van Remmen, H. (2021). The SarcoEndoplasmic Reticulum Calcium ATPase (SERCA) pump: a potential target for intervention in aging and skeletal muscle

pathologies. *Skelet Muscle*, *11*(1), 25. https://doi.org/10.1186/s13395-021-00280-7

Yeung, D., Zablocki, K., Lien, C. F., Jiang, T., Arkle, S., Brutkowski, W., Brown, J., Lochmuller, H., Simon, J., Barnard, E. A., & Górecki, D. C. (2006). Increased susceptibility to ATP via alteration of P2X receptor function in dystrophic mdx mouse muscle cells. *Faseb j*, *20*(6), 610-620. https://doi.org/10.1096/fj.05-4022com

Yeung, E. W., Whitehead, N. P., Suchyna, T. M., Gottlieb, P. A., Sachs, F., & Allen, D. G. (2005). Effects of stretch-activated channel blockers on [Ca2+]i and muscle damage in the mdx mouse. *J Physiol*, *562*(Pt 2), 367-380. https://doi.org/10.1113/jphysiol.2004.075275

Yoshida, M., Minamisawa, S., Shimura, M., Komazaki, S., Kume, H., Zhang, M., Matsumura, K., Nishi, M., Saito, M., Saeki, Y., Ishikawa, Y., Yanagisawa, T., & Takeshima, H. (2005). Impaired Ca2+ store functions in skeletal and cardiac muscle cells from sarcalumenin-deficient mice. *J Biol Chem*, *280*(5), 3500-3506. https://doi.org/10.1074/jbc.M406618200

Young, C. N., Brutkowski, W., Lien, C. F., Arkle, S., Lochmüller, H., Zabłocki, K., & Górecki, D. C. (2012). P2X7 purinoceptor alterations in dystrophic mdx mouse muscles: relationship to pathology and potential target for treatment. *J Cell Mol Med*, *16*(5), 1026-1037. https://doi.org/10.1111/j.1582-4934.2011.01397.x

Young, C. N. J., Chira, N., Róg, J., Al-Khalidi, R., Benard, M., Galas, L., Chan, P., Vaudry, D., Zablocki, K., & Górecki, D. C. (2018). Sustained activation of P2X7

induces MMP-2-evoked cleavage and functional purinoceptor inhibition. *J Mol Cell Biol*, *10*(3), 229-242. https://doi.org/10.1093/jmcb/mjx030

Yu, L., Zhang, X., Yang, Y., Li, D., Tang, K., Zhao, Z., He, W., Wang, C., Sahoo, N., Converso-Baran, K., Davis, C. S., Brooks, S. V., Bigot, A., Calvo, R., Martinez, N. J., Southall, N., Hu, X., Marugan, J., Ferrer, M., & Xu, H. (2020). Small-molecule activation of lysosomal TRP channels ameliorates Duchenne muscular dystrophy in mouse models. *Sci Adv*, *6*(6), eaaz2736. https://doi.org/10.1126/sciadv.aaz2736

Zhihao, L., Jingyu, N., Lan, L., Michael, S., Rui, G., Xiyun, B., Xiaozhi, L., & Guanwei, F. (2020). SERCA2a: a key protein in the Ca(2+) cycle of the heart failure. *Heart Fail Rev*, *25*(3), 523-535. https://doi.org/10.1007/s10741-019-09873-3

VITA

Emily Morales was born June 12th, 1995, in Columbia, Missouri and grew up in the town of Centralia, Missouri. She attended Truman State University in Kirksville, Missouri from 2013-2017, where she obtained her B.S. in Biology and a minor in Chemistry. During that time, she conducted research under the supervision of Dr. Laura Fielden-Rechav in the Department of Biology. In 2016 she was accepted into the Undergraduate Summer Research Program at the University of Missouri, Columbia, where she studied under the supervision of Dr. Xiao Heng in the Department of Biochemistry. After completing her undergraduate degree, Emily returned to the University of Missouri in 2017 to pursue her Ph.D. in Molecular Pathogenesis and Therapeutics under the supervision of Dr. Dongsheng Duan. During her first four years of graduate school, Emily was financially supported by the Life Sciences Fellowship. In July of 2022, Emily obtained her Ph.D. for her work on calcium regulation in Duchenne muscular dystrophy. She also received a minor in College Teaching. In the future, she plans to pursue a career in medical writing.